

# Glutamatergic Supramammillary Nucleus Neurons Respond to Threatening Stressors and Promote Active Coping

## Reviewed Preprint

Revised by authors after peer review.

## About eLife's process

### Reviewed preprint version 2

April 5, 2024 (this version)

### Reviewed preprint version 1

October 3, 2023

### Posted to preprint server

September 25, 2023

### Sent for peer review

July 25, 2023

Abraham Escobedo, Salli-Ann Holloway, Megan Votoupal, Aaron L Cone, Hannah E Skelton, Alex A. Legaria, Imeh Ndiokho, Tasheia Floyd, Alexxai V. Kravitz, Michael R. Bruchas , Aaron J. Norris 

Department of Anesthesiology, Washington University in St. Louis, St. Louis, MO • Department of Medicine, Northwestern University Feinberg School of Medicine, Chicago IL • Department of Neuroscience, Washington University in St. Louis, St. Louis, MO • Department of Psychiatry, Washington University in St. Louis, St. Louis, MO • Medical College of Wisconsin, Milwaukee WI • Department of Obstetrics and Gynecology, Washington University in St. Louis, St. Louis, MO • Center for Neurobiology of Addiction, Pain, and Emotion University of Washington, Seattle, WA • Department of Anesthesiology and Pain Medicine University of Washington, Seattle, WA • Department of Pharmacology University of Washington, Seattle, WA • Department of Bioengineering University of Washington, Seattle, WA

 [https://en.wikipedia.org/wiki/Open\\_access](https://en.wikipedia.org/wiki/Open_access)

 Copyright information

## Abstract

Threat-response neural circuits are conserved across species and play roles in normal behavior and psychiatric diseases. Maladaptive changes in these neural circuits contribute to stress, mood, and anxiety disorders. Active coping in response to stressors is a psychosocial factor associated with resilience against stress-induced mood and anxiety disorders. The neural circuitry underlying active coping is poorly understood, but the functioning of these circuits could be key for overcoming anxiety and related disorders. The supramammillary nucleus (SuM) has been suggested to be engaged by threat. SuM has many projections and contains a poorly understood diversity of populations. We identified a unique population of glutamatergic SuM neurons (SuM<sup>VGLUT2+</sup>::POA) based on projection to the preoptic area of the hypothalamus (POA) and found SuM<sup>VGLUT2+</sup>::POA neurons have extensive arborizations. SuM<sup>VGLUT2+</sup>::POA neurons project to brain areas that mediate various features of the stress and threat responses including the paraventricular nucleus thalamus (PVT), periaqueductal gray (PAG), and the habenula (Hb). Thus, SuM<sup>VGLUT2+</sup>::POA neurons are positioned as a hub, connecting to areas implicated in regulating stress responses. Here we report SuM<sup>VGLUT2+</sup>::POA neurons are recruited by diverse threatening stressors, and recruitment of SuM<sup>VGLUT2+</sup>::POA neurons correlated with active coping behaviors. We found that selective photoactivation of the SuM<sup>VGLUT2+</sup>::POA population drove aversion but not anxiety like behaviors. Activation of SuM<sup>VGLUT2+</sup>::POA neurons in the absence of acute stressors evoked active coping like behaviors and drove instrumental behavior (selective port activations) (Figure 6). Also, activation of SuM<sup>VGLUT2+</sup>::POA neurons was sufficient to convert passive coping strategies to active behaviors during acute stress. In contrast, we found activation of GABAergic (VGAT+) SuM neurons (SuM<sup>VGAT+</sup>) neurons did not alter drive aversion or active coping, but termination of photostimulation was followed by increased mobility in the forced swim test. These findings establish a new node in stress response circuitry that has

projections to many brain areas, evokes flexible active coping behaviors, and offers new opportunities for furthering our neurobiological understanding of stress.

### eLife assessment

This **important** manuscript investigates the role of a subpopulation of glutamatergic neurons in the supramammillary nucleus that projects to the pre-optic hypothalamus area in active coping but not locomotor activity. They provide **solid** evidence from experiments using fibre photometry or photostimulation during threatening tasks that these neurons allow animals to produce flexible behaviours in response to stress. This work will be of interest to behavioural and systems neuroscientists.

## Introduction

Threat-response neural circuits are conserved across species and have roles in normal behaviors and psychiatric diseases[1–4]. Identifying and responding to threatening stressors is critical for survival, but maladaptive changes in underlying neural circuits can contribute to stress, mood, and anxiety disorders[5, 6]. Active coping in response to stressors is a psychosocial factor associated with resilience against stress induced mood and anxiety disorders [7]. Available evidence indicates that active (e.g., escape, fighting) and passive (e.g., freezing, immobility) coping responses to stressors are governed by separable neural circuits[1, 8, 9]. The functioning of circuits underlying active coping could be key for overcoming anxiety and related disorders[10, 11]. The neural circuits, cells, and mechanisms underlying active coping strategies remain unclear[12, 13].

The supramammillary nucleus (SuM) has been suggested to be engaged by threatening stressors and has efferent connections to stress-sensitive brain regions so may be an important regulator of responses to stressors[14–16]. Research on SuM has focused on connections to the hippocampus and septum while SuM projections to other brain areas remain less understood[15, 17, 18]. SuM contains distinct populations with functionally diverse roles including regulation of hippocampal activity during REM, spatial memory, arousal, and environmental interactions[19–23]. In addition to functional diversity, anatomical and molecular-cellular diversity is present in SuM[24–26]. Divergent populations in SuM have been defined by differential to the dentate gyrus and CA2 regions of the hippocampus, and neurochemically based on neurotransmitter expression[27, 28]. Major projections from the SuM, which have yet to be examined, include the preoptic hypothalamus area (POA). We examined if SuM neurons projected to the POA and if this projection could be used to aid in separation of populations in SuM.

We used retrograde adeno associated viral (AAV) and combinatorial genetic tools to identify and characterize a population of glutamatergic SuM neurons with projections to the POA (SuM<sup>VGLUT2+</sup>::POA). We found that SuM<sup>VGLUT2+</sup>::POA neurons represented an anatomical subset of SuM neurons with extensive arborizations to brain regions including those that mediate stress and threat responses including the paraventricular nucleus (PVT), periaqueductal gray (PAG), and the habenula (Hb). Thus, SuM<sup>VGLUT2+</sup>::POA neurons are positioned as hubs with spokes to many areas regulating responses to threatening stressors. We hypothesized this population could respond to and regulate responses to stressors. We found SuM<sup>VGLUT2+</sup>::POA neurons are recruited by multiple types of acute threatening stressors, encode a negative valence, do not promote anxiety-like behaviors, and evoke active coping behaviors. Further, activation of these SuM<sup>VGLUT2+</sup>::POA

neurons was sufficient to convert passive coping strategies to active behaviors. These findings indicate SuM<sup>VGLUT2+</sup>::POA neurons are a central hub linked to multiple stress and threat responsive areas and can drive state transitions between passive and active responses to stress.

## Results

### VGLUT2+ SuM neurons projecting to the POA (SuM<sup>VGLUT2+</sup>::POA) arborize to multiple stress-engaged brain regions

The SuM contains functionally diverse and anatomically distinct populations with efferent projections to many brain regions[16, 24, 29, 30]. The diversity includes glutamatergic, GABAergic, and co-expressing GABAergic/Glutamatergic populations[21, 31]. Using retrograde adeno associated virus (Retro-AAV) (Retro-AAV2-DIO-tdTomato) and anterograde (AAV5-DIO-ChR2eYFP) tracing we identified a population of VGLUT2+ expressing neurons in SuM that project to the POA (SuM<sup>VGLUT2+</sup>::POA) with dense projections in the lateral preoptic area (LPO) within the POA (**Supplemental Figure 1A-F**) in VGLUT2-Cre mice (n=4). Using a viral construct encoding for a nuclear restricted fluorophore that switches from mCherry (red) to eGFP (green) in a Cre- dependent manner (Retro-AAV2-Nuc-flox(mCherry)-eGFP), we found SuM<sup>VGLUT2+</sup>::POA neurons were positive for VGLUT2+ in VGLUT2-Cre mice (n=4) and negative for VGAT expression in VGAT-Cre mice (n=3) (**Supplemental Figure 1G-L**) indicating that SuM<sup>VGLUT2+</sup>::POA neurons do not belong to a GABAergic/Glutamatergic populations.

To examine arborization of SuM<sup>VGLUT2+</sup>::POA neurons we utilized a combinatorial genetic approach. Specifically, we used mice (VGLUT2-Flp) that express Flp recombinase in VGLUT2 expressing cells in a combination with Flp dependent expression (fDIO) of Cre and Cre (DIO) dependent fluorophore expression. We injected Retro-AAV2-DIO-eYFP into POA and AAV-fDIO-Cre in to SuM (**Figure 1A**). We thus expressed Cre in SuM<sup>VGLUT2+</sup> neurons and, of those, only neurons projecting to the POA (SuM<sup>VGLUT2+</sup>::POA neurons) were labeled with eYFP. We found SuM<sup>VGLUT2+</sup>::POA neurons arborize widely, projecting to multiple brain regions including: the nucleus accumbens (Acb), Septum, lateral hypothalamus (LH), ventral medial hypothalamus (VMH), paraventricular nucleus (PVT), lateral habenula (LHb), the ventral lateral periaqueductal gray (VLPAG), dorsal raphe (DRD), lateral parabrachial nucleus (LPBN), laterodorsal tegmental nucleus (LDTg), and medial vestibular nucleus (MVe) (**Figure 1 D-M**). We visualized arborization of SuM<sup>VGLUT2+</sup>::POA neurons in cleared tissue by using optical light sheet imaging. For these experiments we injected VGLUT2-Flp mice (n=3) as in **Figure 1A** and brains were actively cleared using SHIELD for optical light sheet imaging[32]. Compiled three-dimensional images of a brain hemisphere, viewed from the medial to lateral perspective (**Figure 1M**) or viewed from the ventral to dorsal perspective (**Supplemental Figure 2M**), showed projections labeled by eYFP from SuM<sup>VGLUT2+</sup>::POA to POA, areas of hippocampus, septum, Acb, and regions in the pons and midbrain. The results further established projections from SuM<sup>VGLUT2+</sup>::POA neurons to multiple brain areas and illustrate the broad arborization.

We used tracing with Retro-AAV's to further corroborate our findings from anterograde tracing by injecting unilaterally into the Acb, septum, PVT, or PAG in VGLUT2-Cre mice. Cell bodies in SuM were labeled eYFP or tdTomato (**Supplemental Figure 2A-L**). Each area was injected in three or more mice, yielding similar results. We examined the anatomic distribution of SuM::POA neurons in SuM by injecting Retro-AAV2-Cre into the POA and AAV5-Nuc-flox(mCherry)-eGFP into the SuM (**Supplemental Figure 3 A-B**) of wildtype (WT) Cre- mice (n=3) In mice injected with this combination of viruses, we observed neurons labeled by mCherry (Cre negative) or eGFP (Cre expressing) interspersed in the SuM. We verified the combinatorial viral selectively labeled SuM<sup>VGLUT2+</sup>::POA neurons with minimal background[33]. As positive controls, we injected Retro-AAV-Flpo into the POA and AAV-fDIO-Cre into the SuM to label the cells in SuM (**Supplement**

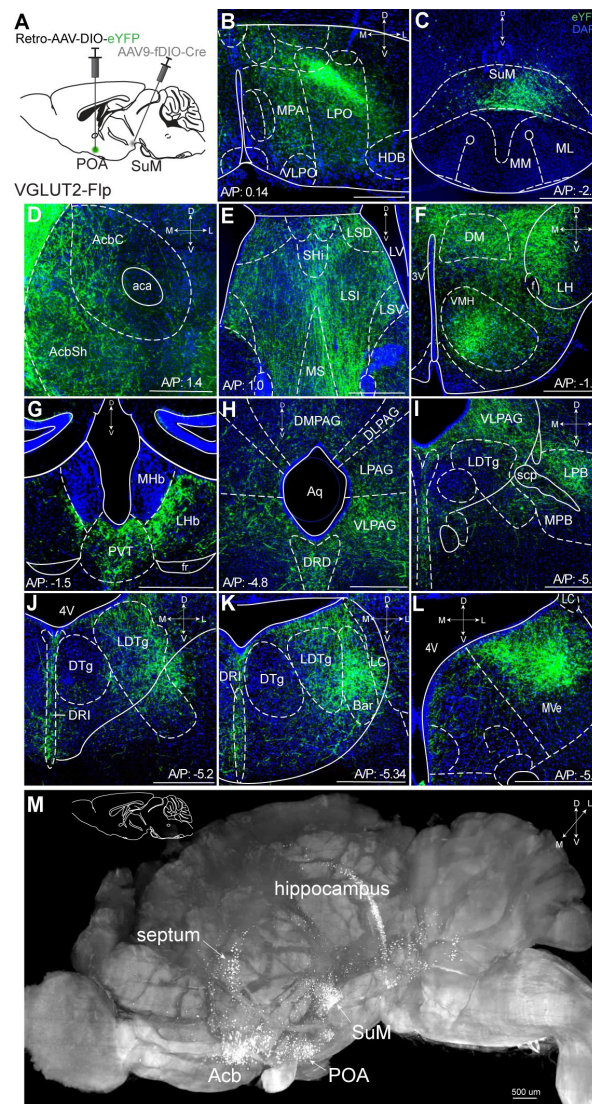


**Figure 1.**

### **$\text{SuM}^{\text{VGLUT2}^+::\text{POA}}$ neurons arborize widely in the brain.**

(A) Schematic of injections of Retro-AAV-DIO-eYFP into the POA and AAV-fDIO-Cre into the SuM of VGLUT2-Flp mice to label only VGLUT+ SuM neurons that project to the POA. (B) Projections of VGLUT2+ SuM neurons labeled with eYFP seen in the POA. (C) Cell bodies labeled with eYFP in the SuM. (D-L) Arborizing processes from the  $\text{SuM}^{\text{VGLUT2}^+::\text{POA}}$  neurons are seen in multiple brain regions including the (D) AcbSh and AcbC; (E) lateral septum; (F) multiple hypothalamic areas; (G) IHB and PVT; (H) the PAG and the DRD; (I) VLPAG and LPB; (J) DRI and LDTg; (K) and DRI, and MVePC. (M) Light sheet microscopy image of a cleared mouse brain hemisphere, viewed from medial to lateral, showing eYFP labeled neurons in  $\text{SuM}^{\text{VGLUT2}^+::\text{POA}}$  with cell bodies in SuM and processes in areas corresponding to septum, hippocampus, Acb, and POA. (500  $\mu\text{m}$  scale bars).

Abbreviations-MPA-medial preoptic, VLPO-ventral lateral preoptic, LPO-lateral preoptic, HDB-nucleus of the horizontal limb of the diagonal band AcbSh-Accumbens shell, AcbC-Accumbens core, Shi-septohypocampal nucleus, LSI-lateral septal nucleus, intermediate part, LSV-lateral septal nucleus, ventral part, LV-lateral ventricle, MS-medial septal nucleus, IHB-lateral habenula, mHB-medial habenula, PVT-paraventricular thalamus, DM-dorsomedial hypothalamic nucleus, LH-lateral hypothalamic area, VMH-



**Figure 3G and H).** As negative controls, we injected only AVV-fDIO-Cre into the SuM in Ai14 mice, which did not yield tdTomato expression (**Supplemental Figure 3C-D**). To confirm that the combination of Retro-AAV2-fDIO-Cres and AAV5-DIO-ChR2eYFP did not lead to labeling of cells with eYFP in the absence of Flp, we injected Retro-AAV2-fDIO-Cre into the POA and AAV-DIO-hChR2eYFP into SuM of WT mice. In these mice we did not observe any expression of eYFP (**Supplemental Figure 3E-F**). The results demonstrate the specificity of our combinatorial viral strategy. All studies were replicated in a minimum of three mice.

## SuM<sup>VGLUT2+</sup>::POA neurons are an anatomical distinct subset of all SuM<sup>VGLUT2+</sup> neurons

Recent studies have highlighted functionally divergent roles of SuM neurons and suggested differential projections, particularly to regions of hippocampus and PVT, may identify functionally distinct populations [19, 20]. To examine if SuM<sup>VGLUT2+</sup>::POA neurons are a subset of SuM<sup>VGLUT2+</sup> neurons, we qualitatively compared the projections of total SuM<sup>VGLUT2+</sup> neurons to SuM<sup>VGLUT2+</sup>::POA neurons. Similar to projections for SuM<sup>VGLUT2+</sup>::POA neurons (**Figure 1**), we observed labeled projections from the total SuM<sup>VGLUT2+</sup> neurons in the POA, PVT, IHB, and the CA2 field of the hippocampus (**Figure 2 A-E**). Importantly, we found areas that received projections from the total SuM<sup>VGLUT2+</sup> and not from SuM<sup>VGLUT2+</sup>::POA neurons. As schematized (**Figure 2K**), projections from the total SuM<sup>VGLUT2+</sup> but not SuM<sup>VGLUT2+</sup>::POA populations were present in dentate gyrus (DG) and medial habenula (mHb) (**Figure 1G and Figure 2 F-J**). Connection of the SuM to the dentate gyrus is well described and seen here for the SuM<sup>VGLUT2+</sup> population [34–38]. The lack of projections from SuM<sup>VGLUT2+</sup>::POA neurons to dentate gyrus, but not to other structures is a notable difference (**Figure 2J**). Thus, the SuM<sup>VGLUT2+</sup>::POA population represents a subset of the total SuM<sup>VGLUT2+</sup> neuronal population with distinct projection targets.

## Threatening stressors but not spontaneous higher velocity movement recruits SuM<sup>VGLUT2+</sup>::POA neurons

Neurons in SuM can be activated by acute stressors, and we sought to examine the recruitment of SuM<sup>VGLUT2+</sup>::POA neurons by threatening stressors [14, 39, 40]. We found that forced swimming induced cFos expression in SuM. Labeling SuM<sup>VGLUT2+</sup>::POA neurons using Retro-AAV-DIO-mCherry revealed an increase in the number of mCherry and cFos labeled cells following forced swim (**Supplemental Figure 4A-G**). To further examine recruitment of SuM<sup>VGLUT2+</sup>::POA neurons by acute stressors, we tested a diverse set of acute threatening stressors using *in vivo* Ca<sup>2+</sup> detection via fiber photometry. We expressed GCaMP7s in SuM<sup>VGLUT2+</sup>::POA neurons (**Figure 3A-B**) using the combinatorial viral genetic approach detailed for anatomic studies. We developed a dunk assay that utilized a moveable platform allowing mice to be placed into and removed from the water while obtaining fiber photometry recordings. Mice were dunked by lowering the platform below the water level forcing mice to swim for a 30-second trial every 2 minutes for a total of 10 trials (n=8 mice). During the 30-second swim time, mice exhibited active swimming and climbing behaviors reflected in the quantification of mean time mobile approaching 100 percent during the swim period without evidence for a shift in the behavioral strategy (**Supplemental Figure 4I**). These data show repeated exposure to an acute stressor, dunk in water, evoked active coping behavior (time mobile). A 95%, 99%, and 99.9% confidence interval (CI) were calculated to analyze the difference in the Ca<sup>2+</sup>-dependent signal preceding and subsequently after the dunk. Analysis of Ca<sup>2+</sup> dependent (470 nm excitation) and isosbestic control (415 nm excitation) signals from fiber photometry recordings revealed a significant (99.9% CI) rapid rise of approximately 5 standard deviations in GCaMP Ca<sup>2+</sup> dependent signal with start of the swim trial that was sustained through the 30-sec swim period. The Ca<sup>2+</sup> dependent signal returned to baseline

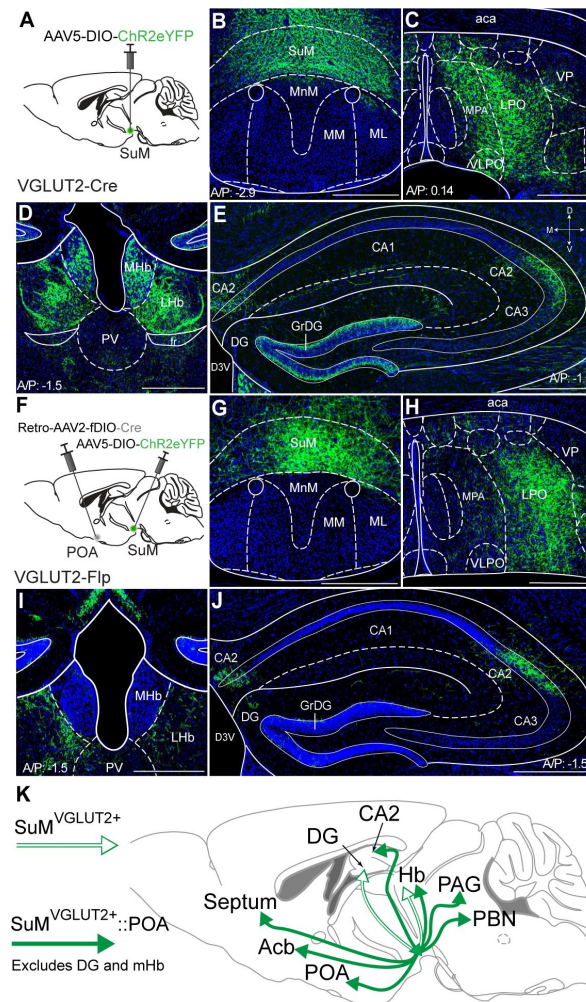


**Figure 2.**

**$\text{SuM}^{\text{VGLUT2}+}::\text{POA}$  neurons project to a subset of brain regions compared to all  $\text{SuM}^{\text{VGLUT2}+}$  neurons.**

(A) Schematic of injections in VGLUT2-Cre mice of AAV-DIO-ChR2eYFP into  $\text{SuM}$ . (B) eYFP (green) labeled neurons present in  $\text{SuM}$  and (C) processes were observed in the  $\text{POA}$ . (D) Processes from  $\text{SuM}^{\text{VGLUT2}+}$  neurons were also present in  $\text{mHb}$ ,  $\text{LHb}$ , and  $\text{PV}$ . (E) In hippocampus, processes were observed in DG and CA2. (F) Schematic of injections in VGLUT2-Flp mice of Retro-AAV-fDIO-Cre and AAV-DIO-ChR2eYFP into  $\text{SuM}$ . (G-H) Cells in  $\text{SuM}$  and processes in  $\text{POA}$  were labeled by ChR2eYFP. (I) Labeled processes in  $\text{LHb}$  were evident but none seen in  $\text{mHb}$ . (J) In hippocampus, labeled processes were present in CA2 but not observed in DG. (500  $\mu\text{m}$  scale bars) (K) Schematic summary showing the projection to DG and  $\text{mHb}$  present in the total  $\text{SuM}^{\text{VGLUT2}+}$  population (outlined arrows) but absent in the  $\text{SuM}^{\text{VGLUT2}+}::\text{POA}$  population (filled arrows).

when the platform was raised, removing the animal from the water (**Figure 3F** and **G**). Repeated exposure to an acute stressor evoking active coping behaviors robustly recruited SuM<sup>VGLUT2+::POA</sup> neurons.

To examine additional stressors, we tested a foot shock paradigm (**Figure 3D**) and a predator ambush assay (**Figure 3E**). In foot shock assays, VGLUT2-Flp mice (n=6), prepared as above (**Figure 3A** and **B**), were subjected to five pseudorandomly spaced trials with a 30 second tone preceding a two-second shock. We observed a significant rapid increase in the Ca<sup>2+</sup> dependent GCaMP7s signal following the foot shock (99.9% CI; **Figure 3H** and **I**). For the predator ambush, we adapted a previously demonstrated paradigm using a mock mechanical spider attack [41]. In this assay a remote-controlled mechanical spider was hidden in a box with a swing door. The box was inside a larger walled arena. Mice were able to freely explore the arena, and at a moment when the mouse was in proximity to the box opening, the spider was moved out towards the mouse. The mice fled, often to a corner, stopped, and turned to face the spider (**Supplemental video 1**). In mice (n=9) subjected to the ambush paradigm, we observed a significant (99.9% CI) increase in Ca<sup>2+</sup> dependent GCaMP signal at the time of the ambush followed by suppression below the initial baseline (**Figure 3J**). Populations of neurons in SuM have previously been found to correlate with future movement velocity [42], so we examined if recruitment of SuM<sup>VGLUT2+::POA</sup> neurons was correlated to periods of spontaneous higher velocity movement. Analyzing data collected prior to the ambush event, we examined if increased velocity, at speeds similar to the fleeing induced by the ambush, was correlated with increased Ca<sup>2+</sup> dependent GCaMP signal in SuM<sup>VGLUT2+::POA</sup> neurons (**Figure 3L**). We found no correlation (**Figure 3K**). We further examined the data for a correlation of increased Ca<sup>2+</sup> dependent signal in SuM<sup>VGLUT2+::POA</sup> neurons to movement velocity during open field exploration in a separate cohort of mice (n=13). Here, we found no evidence for correlation of velocity with Z-score of Ca<sup>2+</sup> dependent signal including a cross correlation analysis to account for a potential temporal offset (**Supplemental Figure 5**). In aggregate, the data support recruitment of SuM<sup>VGLUT2+::POA</sup> neurons by diverse threatening stressors but not during times of higher velocity spontaneous movement.

### SuM<sup>VGLUT2+::POA</sup> neurons evoke active coping-like behaviors

To examine how activation of SuM<sup>VGLUT2+::POA</sup> neurons contributes to responding to threatening stressors, we assessed behavioral changes evoked by photostimulation of SuM<sup>VGLUT2+::POA</sup> neurons. We injected VGLUT2-Cre or WT (Cre-littermates) mice with Retro-AAV5-DIO-ChR2eYFP in the POA, and an optic fiber was placed over SuM (**Figure 4A**). We employed a paradigm with a 15-minute trial divided into three 5-minute periods: pre-stimulation, stimulation at 10 Hz, and post-stimulation. Based on review of videos obtained during the 15-minute trials, we observed behaviors that could be classified into nine distinct categories: grooming, immobile, walking, chewing of bedding, rearing, rapid locomotion (movement was limited by the size of the arena), digging (moving bedding towards the tail), treading (moving bedding forward with front paws), and jumping (**Figure 4B**). A blinded observer scored the behaviors in 10-second intervals for the predominant behavior observed during each interval, and each behavior was assigned a color for visualization. Color coded representation of trials from 16 Cre+ (n=16) and WT (n=16) mice is illustrated (**Figure 4B**). The behavioral pattern in the pre-stimulation period is similar between the Cre+ and WT mice. During the stimulation period, a clear shift in behavior was evident in Cre+ mice. Photostimulation induced rearing, treading, digging, rapid locomotion, and jumping. During the post-stimulation period we observed a new pattern with Cre+ mice spending time immobile and grooming. An example of a Cre+ animal is shown in **Supplemental video 2**.

We analyzed behavior, quantifying specific behaviors during each period. Quantification of jumping revealed that Cre+ mice (n=16) engaged in significantly (p=0.012) more jumps during the stimulation period compared to WT (n=16) mice (**Figure 4C**). During the pre- and post-stimulation periods, there was not a significant difference in the number of jumps (pre-

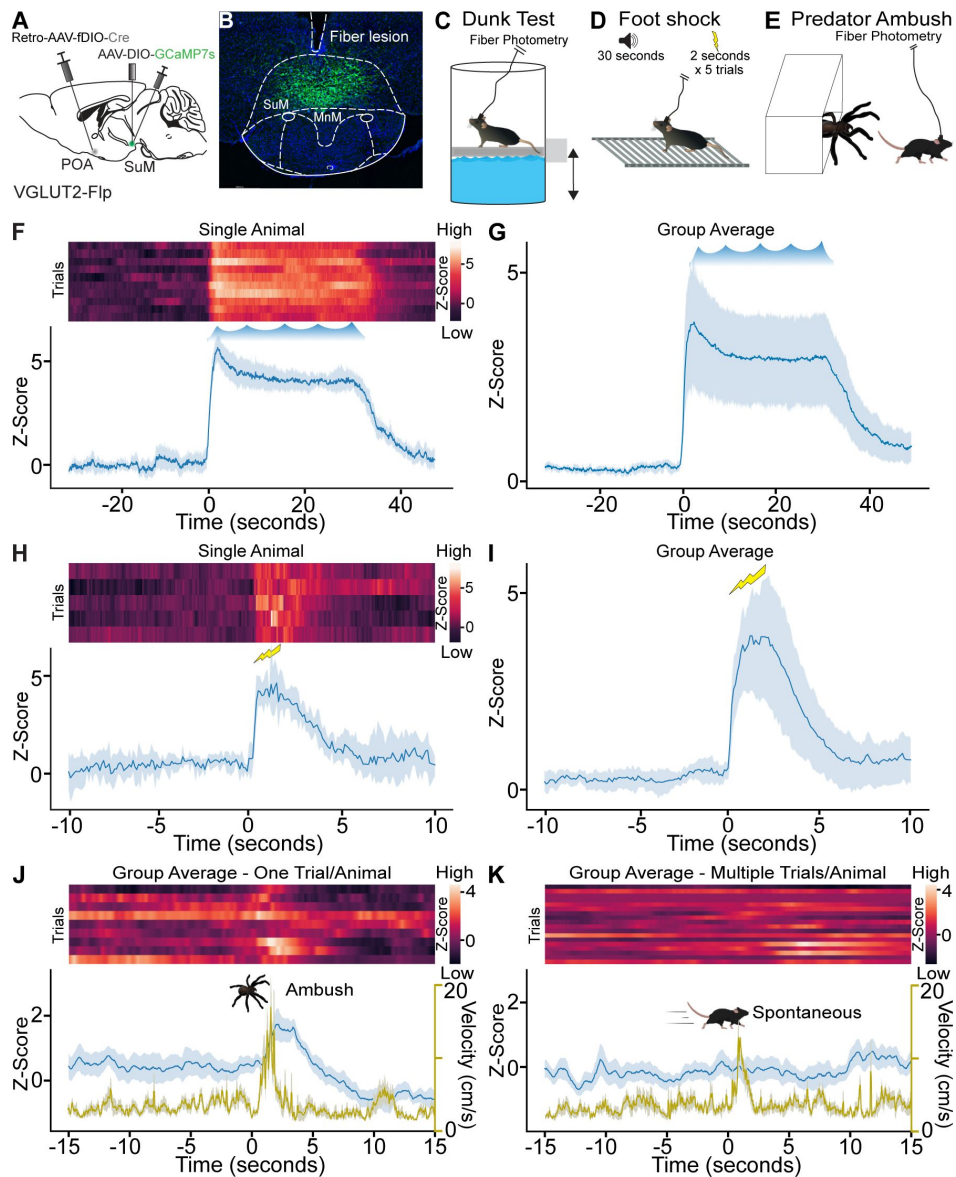


**Figure 3.**

### Acute stressors recruit SuM<sup>VGLUT2+::POA</sup> neurons.

(A) Schematic of VGLUT2-Flp mice injected with AAV-DIO-GCaMP7s in SuM and Retro-AAV-fDIO-Cre in the POA with a (B) fiber placed over SuM for fiber photometry recordings from SuM<sup>VGLUT2+::POA</sup> neurons. (C) While mice were connected for fiber photometry, they were subjected to ten 30-second trials of forced swimming, (D) to a 2-second foot shock following a 30-second tone for five trials, or (E) to ambush by a mock predator via remote-controlled spider. (F) Heat map and mean  $\pm$  95% CI Z-score for recordings obtained from a single animal during the repeated forced swim showing increase  $\text{Ca}^{2+}$  signal during the swim session. (G) The mean  $\pm$  95% CI Z-score of 10 trials for all animals ( $n=8$ ) in the dunk assay. (H) Heat map and mean  $\pm$  95% CI Z-score for recordings from a single animal during the five shock trials showing increase  $\text{Ca}^{2+}$  signal. (I) Mean  $\pm$  95% CI Z-score for recordings of five trials for all animals ( $n=6$ ) in the foot shock assay. (J) Heat map, mean  $\pm$  95% CI Z-score (blue), mean  $\pm$  95% CI velocity (gold), for recordings obtained from animals ( $n=9$ ) during the ambush showing a significant increase ( $***99.9\%$  CI) in  $\text{Ca}^{2+}$  signal as the animals flee from the remote-controlled spider with the mean  $\pm$  95% confidence interval Z-score of 1 trial (ambush) for all 9 animals. (K) Heat map, mean ( $\pm$  95% CI) Z-score (blue), mean ( $\pm$  95% CI) velocity (gold), for the same mice but ambush in the predator assay. Time frame gated for spontaneous locomotion.  $\text{Ca}^{2+}$  signal does not increase significantly during spontaneous locomotion. Mean peak velocity was not significantly different. For  $\text{Ca}^{2+}$  signal differences: \* = 95% CI, \*\* = 99% CI, \*\*\* = 99.9% CI, ns = not significant.



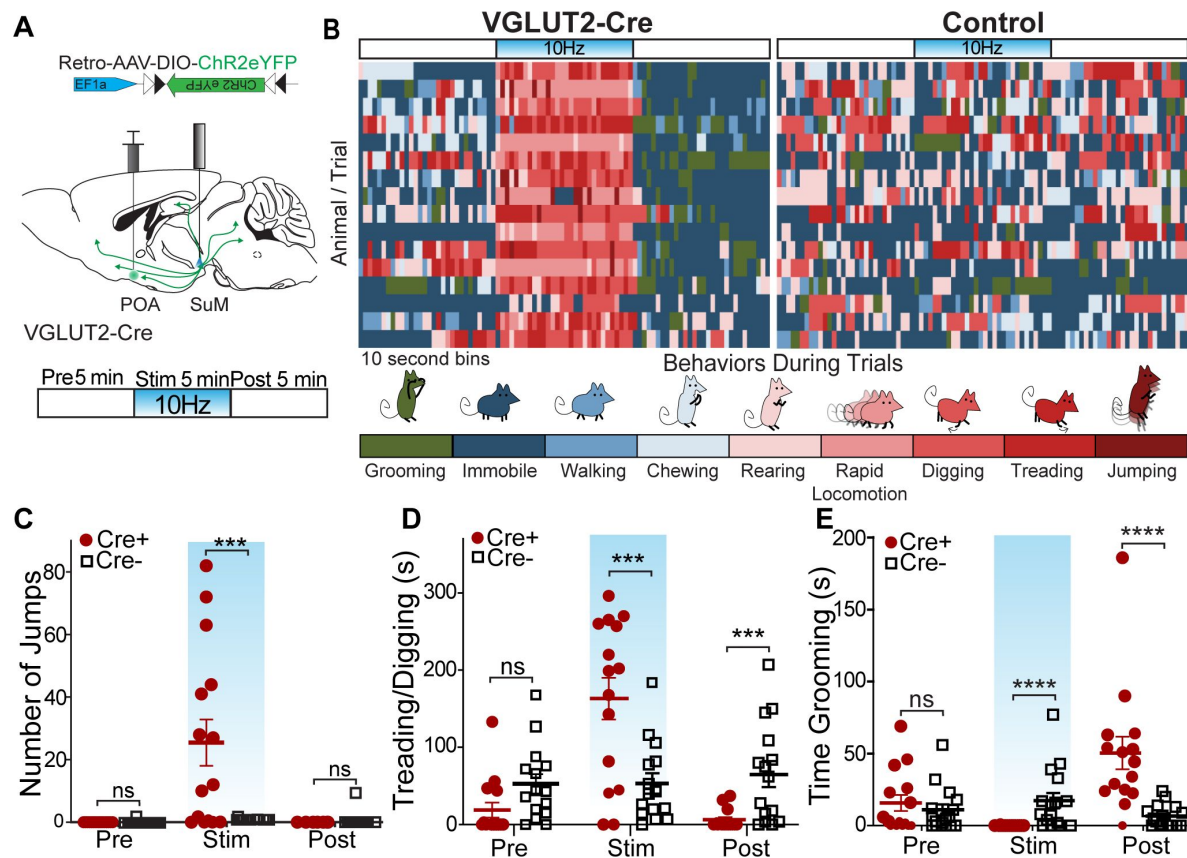


**Figure 4.**

### Photostimulation of SuM<sup>VGLUT2+::POA</sup> neurons evokes active coping behaviors.

(A) Illustration of injections and fiber implant in VGLUT2+ Cre mice and schematic of photostimulation paradigm of 5 min pre, 5 min stimulation, and 5 min post. Behaviors were evaluated during each epoch. (B) For Cre+ (n=16) and Cre- (n=16) mice, the behavior in 10s bins was scored based on the predominant behavior displayed during each 10s period for the 15-minute trial into grooming, stationary, walking, chewing, rearing, rapid locomotion, digging (moving bedding towards the tail), treading (move bedding forward), and jumping. The graphic shows a by-animal scoring of the 15-minute trial color-coded for each of the behavior categories. (C) During the stimulation period, Cre+ (n=15) mice show significantly (\*p=0.012) greater jumps than Cre- (n=16) mice, and jumping behaviors were not significantly different during pre and post stim periods. (D) Behavior was also scored for time spent moving bedding (digging or treading). Cre+ mice showed significantly (\*\*p=0.004) greater time engaging in digging/treading behaviors during the stimulation period, and significantly (\*p=0.014) less time during the post-stimulation period compared to Cre- mice. (E) Behavior was also scored for time spent engaging in grooming behaviors, and Cre+ mice spent significantly (\*p=0.016) less time grooming during the stimulation period and significantly (\*\*p=0.005) more time grooming during the post stimulation period compared to Cre- mice. All data plotted as mean ± SEM.

stimulation =  $p > 0.999$  and post-stimulation =  $p > 0.999$ ). We also observed that during the stimulation period the Cre<sup>+</sup> mice engaged in bouts treading/digging, vigorously moving bedding forwards and backwards, as previously described for defensive burying [43]. Defensive burying, characterized by moving bedding forward or backwards often in alternating pattern, is evoked by threatening and noxious stimuli, and is a described active stress coping strategy in rodents [43–46]. We conservatively quantified together the movement of bedding as treading/digging that may include spontaneous digging (Figure 4D) and found no significant ( $p = 0.95$ ) difference during the pre-stimulation period. In the stimulation period, there was a significant ( $p = 0.004$ ) increase in the time spent treading/digging, and, surprisingly, during the post-stimulation period time treading/digging was significantly ( $p = 0.014$ ) decreased in Cre<sup>+</sup> mice. The variability in behaviors can be attributed to exclusion of one behavior by the other, with individual mice having variability in the predominant behavior displayed during the photostimulation period, but all mice shifted to increased active coping behaviors. The behaviors evoked by photostimulation fit with active coping behaviors seen in the context of stressors. Specifically, escape (jumping, rapid locomotion), defensive burying/treading (digging, pushing bedding forward).

We also quantified grooming behaviors in each of the three periods (Figure 4E). During the pre-stimulation period, there was not a significant difference ( $p > 0.999$ ). During the stimulation period, the Cre<sup>+</sup> mice did not engage in grooming, leading to a significant ( $p = 0.016$ ) decrease in time spent grooming compared to Cre<sup>-</sup> mice. In the post-stimulation period, Cre<sup>+</sup> mice showed a significant ( $p = 0.005$ ) increase in time spent grooming compared to Cre<sup>-</sup> mice. A reasonable interpretation of the rise in grooming post stimulation is that photostimulation evoked a stressed-like state and cessation of photostimulation led to selfcare grooming, as seen following acute stressors [47, 48]. In summary, the analysis of behaviors elicited by photostimulation of SuM<sup>VGLUT2<sup>+</sup>::POA</sup> neurons without conditioned cues or concomitant stressors demonstrates a dramatic shift in behavior to escape oriented (jumping, rapid locomotion) and threat response behavior, including rearing and defensive burying, during the photostimulation period. In contrast to freezing, the behaviors elicited by activation of SuM<sup>VGLUT2<sup>+</sup>::POA</sup> neurons indicate that they may promote active coping strategies.

## Photostimulation of SuM<sup>VGLUT2<sup>+</sup>::POA</sup> neurons drives real-time avoidance

To examine whether activation of SuM<sup>VGLUT2<sup>+</sup>::POA</sup> neurons may contribute to the aversive aspects of threatening stress, we carried out real-time place aversion testing (RTPA) by pairing one side of the chamber with photostimulation of SuM<sup>VGLUT2<sup>+</sup>::POA</sup> (Figure 5A) neurons at multiple frequencies (1, 5, 10, and 20 Hz). Photostimulation of SuM<sup>VGLUT2<sup>+</sup>::POA</sup> neurons produced significant aversion at all frequencies in Cre<sup>+</sup> ( $n = 19$ ) mice compared to Cre<sup>-</sup> ( $n = 21$ ) littermate control mice, and higher stimulation frequencies evoked greater aversion ( $p < 0.001$ ; Figure 5B and C). Example of Cre<sup>+</sup> mice with stimulation at 1, 5, and 10 Hz as well as Cre<sup>-</sup> mice is in Supplemental Video 3. WT and Cre<sup>+</sup> mice explored equivalently, with similar number of entries to the stim side ( $p = 0.41$ ; Figure 5D). Cre<sup>+</sup> mice quickly left the stimulation side, and the average time spent on the stimulation side of the area was significantly lower ( $p < 0.001$ ; Figure 5E). These data indicate, surprisingly, that photostimulation, although aversive, did not generate aversive pairing, as found for other brain areas [49]. To examine the relative aversiveness of SuM<sup>VGLUT2<sup>+</sup>::POA</sup> photostimulation, we carried out RTPA experiments using an arena with a dark side and a bright side (Figure 5F inset). We paired photostimulation with the dark side. As expected, Cre<sup>-</sup> mice show a preference for the dark side of the arena, however, photostimulation of the SuM<sup>VGLUT2<sup>+</sup>::POA</sup> neurons yielded significant aversion of Cre<sup>+</sup> ( $n = 13$ ) compared to Cre<sup>-</sup> ( $n = 12$ ) ( $p < 0.001$ ; Figure 5F). Cre<sup>+</sup> mice spent nearly the entire trial in the brightly lit side, demonstrating photostimulation of SuM<sup>VGLUT2<sup>+</sup>::POA</sup> neurons drove avoidance sufficient to overcome a mildly aversive stimulus (bright light).

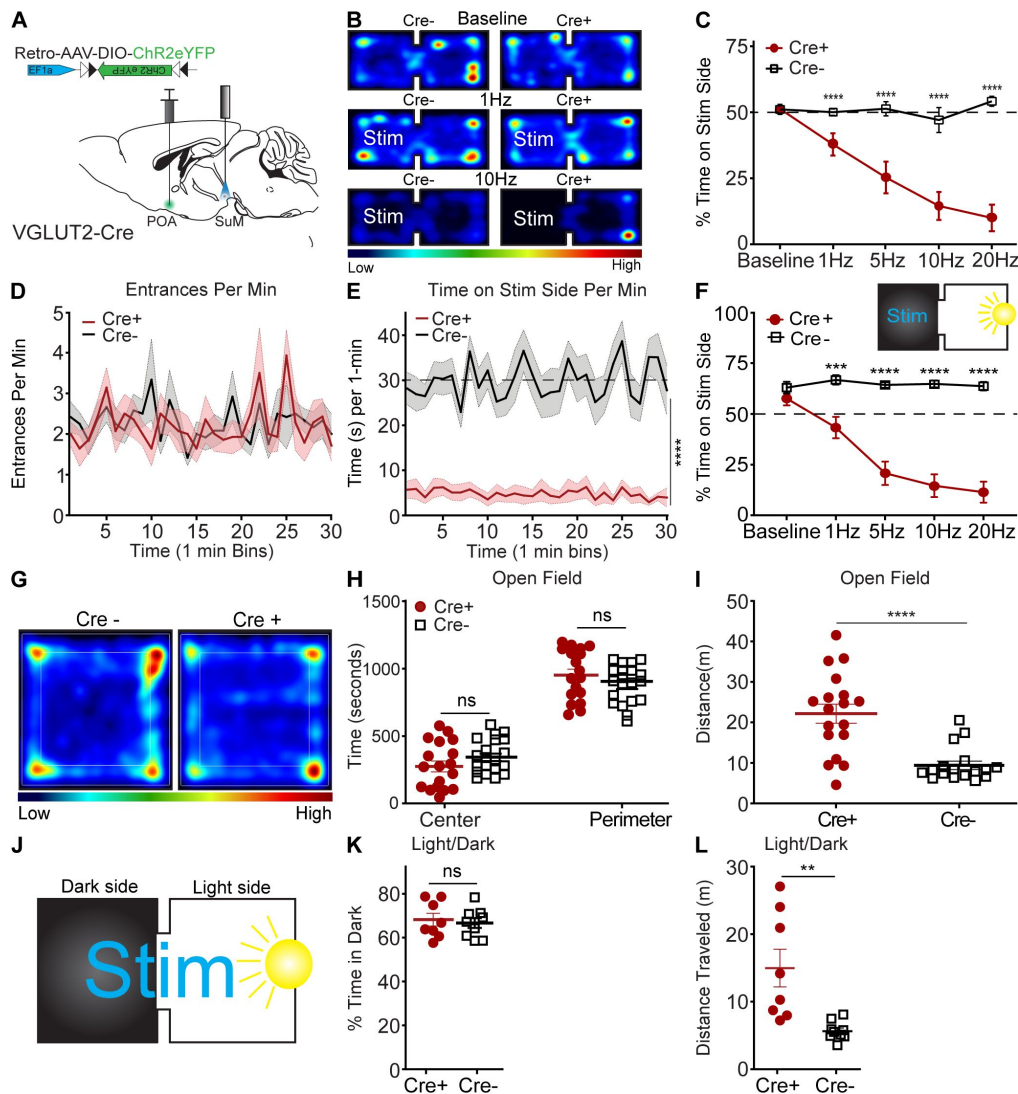


**Figure 5.**

### Activation of SuM<sup>VGLUT2+</sup>::POA neurons drives aversion but does not promote anxiety-like behavior

(A) Schematic of injection of Retro-AAV-ChR2eYFP into the POA and placement of a midline optic fiber over SuM. (B) Representative heat maps for Cre+ and Cre- mice at baseline (no stim) and 10 Hz photostimulation in two-sided arena with photostimulation associated with one side. (C) Quantification of time spent on stimulation side for Cre+ (n = 19) and control Cre- (n = 21) mice showing frequency dependent increase in avoidance of the stimulation side of the area (\*\*\*p < 0.001, \*\*\*\*p < 0.0001). (D) Mean  $\pm$  SEM entrances per min (in 1-min bins) to the during 10 Hz stimulation trials were not significantly (p = 0.87) different between Cre+ (n = 14) and Cre- (n = 13) mice. (E) Mean time spent on the stimulation side for Cre- and Cre+ in 1-minute bins during 10 Hz stimulation trials was significantly (p < 0.0001) lower in Cre+ mice. (F) (Inset) Diagram of light/dark arena with photostimulation provided on the dark side of the arena and quantification of time spent on dark (stimulation) side, demonstrating that Cre- (n = 12) animals show a baseline preference for the dark side of arena that is overcome by photostimulation with Cre+ (n = 13) mice spending significantly (\*\*p = 0.002, \*\*\*p < 0.001, \*\*\*\*p < 0.0001) less time on the stimulation side. (G) Representative heat map of Cre- and Cre+ during 10 Hz photostimulation in open field test. (H) In the open field test, time spent in center and perimeter were not significantly (p = 0.19) between Cre+ (n = 18) and Cre- (n = 17) during 10 Hz photostimulation. (I) Distance traveled during open field testing was significantly (p < 0.001) increased in Cre+ compared to Cre- mice. (J) Schematic of real time light/dark choice testing with stimulation provided at 10 Hz throughout the arena. (K) Both Cre+ (n = 8) and Cre- (n = 9) mice showed a preference for the dark portion of the arena but were not significantly (p = 0.9) different. (L) The total distance traveled by Cre+ mice were significantly (p = 0.003) greater than Cre- mice. All data plotted as mean  $\pm$  SEM.

Reports have described multiple populations of neurons in supramammillary including populations that project to the dentate gyrus of the hippocampus that release both GABA and glutamate. Our anatomic studies indicated that SuM<sup>VGLUT2+</sup>::POA neurons do not project to the dentate gyrus (**Figure 2**) and are not GABAergic (**Supplemental Figure 1G-L**). Thus, SuM<sup>VGLUT2+</sup>::POA neurons are not part of either a GABAergic or dual transmitter population. To examine if GABAergic neurons in SuM (SuM<sup>VGAT+</sup>) can mediate real-time place aversion or preference, we injected VGAT-Cre mice with AAV to express ChR2 (n=26) or control (n=26) in SuM and carried out real-time place aversion testing. Photostimulation at 10 Hz yielded no significant aversion or preference compared to baseline (p=.838) (**Supplemental Figure 6A-D**). This is in contrast to the robust aversion caused by photostimulation of SuM<sup>VGLUT2+</sup>::POA neurons.

## Photoactivation of SuM<sup>VGLUT2+</sup>::POA neurons does not cause anxiogenic-like behavior

Threat can induce anxiety-like, risk aversion behavioral states [50–52]. To test whether activity of SuM<sup>VGLUT2+</sup>::POA neurons contributes to anxiety-like behaviors, we used two established assays for anxiety-like behavior: open field and light-dark exploration [53–56]. During open field testing, 10 Hz photostimulation was applied to SuM<sup>VGLUT2+</sup>::POA neurons. We quantified the time spent in the perimeter (outer 50%) vs. the center (inner 50%) of the arena and found VGLUT2-Cre+ (n=18) and WT (n=17) mice did not significantly differ (center p=0.17 and perimeter p=0.19; **Figure 5G and H**). The total distance traveled was significantly (p<0.001) increased in Cre+ mice compared to WT mice (**Figure 5I**). Increased distance traveled in some mice was not surprising, because prior testing (**Figure 4**) revealed the mice engaged in escape behaviors during photostimulation. We observed behaviors including jumping during open field testing as well. We also carried out open field testing using VGAT-Cre mice to selectively activate SuM<sup>VGAT+</sup> neurons and observed no significant effect on time in center (p=0.254) or perimeter (p=0.287) (**Supplemental Figure 6F**), but mice expressing ChR2eYFP displayed a small but significant (p=0.035) decrease in distance traveled (**Supplemental Figure 6G**). We tested if photostimulation of SuM<sup>VGLUT2+</sup>::POA neurons would increase preference for the dark area, a potential sign of elevated anxiety (**Figures 5J**). We found that photostimulation of SuM<sup>VGLUT2+</sup>::POA neurons did not significantly alter preference (p=0.68; **Figure 5K**) in VGLUT2-Cre+ mice (n=8) compared to WT (n=9). The activation of SuM<sup>VGLUT2+</sup>::POA neurons evoked escape behaviors in open field testing, as seen in **Figure 4**; similarly, a significant increase in total distance was detected during light-dark exploration assay in Cre+ compared to WT (p=0.003; **Figure 5L**). The findings we obtained in open field and light-dark exploration testing do not support a role for SuM<sup>VGLUT2+</sup>::POA neurons in driving anxiety-like behaviors.

## SuM<sup>VGLUT2+</sup>::POA neurons can drive instrumental action-outcome behavior

Current theoretical frameworks for examining threat responses divide behaviors into two broad categories: innate (fixed) and instrumental (action-outcome) [1, 57]. Additionally, stress responses can be divided into active vs passive actions. Behaviors in these separable categories are mediated by distinct neural circuits [1, 58]. For example, areas involved in responding to specific threatening stimuli (looming threat) drive an innate fixed behavior repertoire [10]. Photostimulation of SuM<sup>VGLUT2+</sup>::POA neurons evoked multiple active-like behaviors in response to threatening or noxious stimuli (**Figure 4**). To test if SuM<sup>VGLUT2+</sup>::POA neurons can promote flexible repertoires of behavior including instrumental tasks, as opposed to only innate behaviors (ex. fleeing), we used an operant negative reinforcement paradigm (**Figure 6A-B**). Because our results show photostimulation of SuM<sup>VGLUT2+</sup>::POA neurons is aversive, photostimulation of SuM<sup>VGLUT2+</sup>::POA neurons could be used as a negative reinforcer in a negative reinforcement paradigm. We employed a paradigm using two nose poke ports, one active and one inactive. SuM<sup>VGLUT2+</sup>::POA neurons were photostimulated at 10 Hz during a 10-minute trial. Activation of the active port by a nose poke triggered a 10-second pause in photostimulation of



SuM<sup>VGLUT2+</sup>::POA neurons and turned on a house light for 10 s (**Figure 6A** [↗](#) and **B**). Following this 10-second pause, the house light switched off and photostimulation resumed until the subsequent activation of the active port. We tested animals for four consecutive days with the 10-minute trials without prior training. Importantly, performance of the task had to be completed during photostimulation.

We hypothesized that if stimulation of SuM<sup>VGLUT2+</sup>::POA evokes fixed innate defensive behaviors, or simply promotes high amounts of locomotion, then performance of an operant task (an action-outcome behavior) with active and inactive ports would be impaired because innate defensive behaviors would conflict with performance of the operant task. Importantly, results obtained can help differentiate general elevation in locomotor activity from directed coping behavior. Analyses of port activations during the 10-minute trials revealed that Cre<sup>+</sup> mice (n = 11) paused the photostimulation (reward) significantly more on all four days of testing compared to Cre-littermate (n = 11) mice (Interaction<sub>Genotype x Day</sub> p < 0.001; Day 1 p < 0.001; Day 2 p < 0.001; Day 3 p < 0.001; Day 4 p < 0.001; **Figure 6C** [↗](#)). The number of 10-second pauses approached the maximum, 60 possible in a 10-min period. Cre<sup>+</sup> mice engaged the active port significantly more than Cre- mice (p < 0.001; **Figure 6D** [↗](#)) and this effect was consistent for every training session (Day 1 p < 0.0001; Day 2 p < 0.0001; Day 3 p < 0.0001; Day 4 p = 0.0011). There was a slight difference in baseline performance of the task. The time to the first engagement of the active port was significantly different for Cre<sup>+</sup> compared to Cre- mice during the first test trial (p = 0.046). During the three subsequent tests, Cre<sup>+</sup> mice were significantly faster to engage the active port after the start of the trial compared to Cre- mice (Day 2 p = 0.009; Day 3 p = 0.003; Day 4 p = 0.034; **Figure 6E** [↗](#)). Cre<sup>+</sup> mice engaged the active port significantly more than the inactive port on all test days (p < 0.001; **Supplemental Figure 7A** [↗](#)). There was not a significant difference in Cre<sup>+</sup> and Cre- mice for engagement of the inactive port on any day (Cre<sup>+</sup> p = 0.30; Cre- p = 0.055; **Supplemental Figure 7A-B** [↗](#)). Furthermore, Cre<sup>+</sup> mice were significantly faster in the second through fourth trials at engaging the active port compared the first trial (Day 1 vs Day 2 p = 0.034; vs Day 3 p = 0.021; vs Day 4 p = 0.027; **Figure 6E** [↗](#)). Suggesting that mice became more proficient during subsequent trials.

To examine effort-related motivation, we employed a 30-minute test using a progressive ratio requiring an exponentially increasing number of active port activations to trigger a pause in the photostimulation on the fifth day of operant behavior testing (**Figure 6B** [↗](#)) [59 [↗](#)]. During trials using a progressive ratio, Cre<sup>+</sup> mice activated the active port and paused stimulation significantly (p < 0.001) more times than Cre- mice (**Figure 6F** [↗](#)). Examination of individual cumulative active port activation data showed Cre<sup>+</sup> mice continued to engage the active port throughout progressive ratio trials despite the increasing work required to generate each pause in photostimulation. No breakpoint was observed during the trial (**Figure 6G** [↗](#) and **H**). This finding indicates that activation of SuM<sup>VGLUT2+</sup>::POA neurons remains salient and motivating through the tested period and that photostimulation of SuM<sup>VGLUT2+</sup>::POA does not evoke behaviors precluding completion of the task. Examination of reward behavioral epochs for representative animals shows that for the lowest total number of rewards earned (green dots), the next pause required 20 activations of the active port, and for the highest (red dots), the next pause required 50 activations of the active port. Taken together, results from the instrumental reinforcement tasks demonstrate that activation of SuM<sup>VGLUT2+</sup>::POA neurons does not solely evoke innate stereotyped behaviors and can drive active coping in the form of instrumental behaviors.

## SuM<sup>VGLUT2+</sup>::POA neurons are recruited during active coping behaviors during forced swim

The forced swim test is increasingly established as an assay of coping strategy with passive and active components, and we used forced swim testing in conjunction with fiber photometry to examine if SuM<sup>VGLUT2+</sup>::POA neurons are recruited differentially during active (mobile) or passive (immobile) behaviors [60 [↗](#), 61 [↗](#)]. During a first 15-minute trial of forced swimming, mice shifted from active escape behaviors (wall climbing, robust swimming) to passive (immobile)

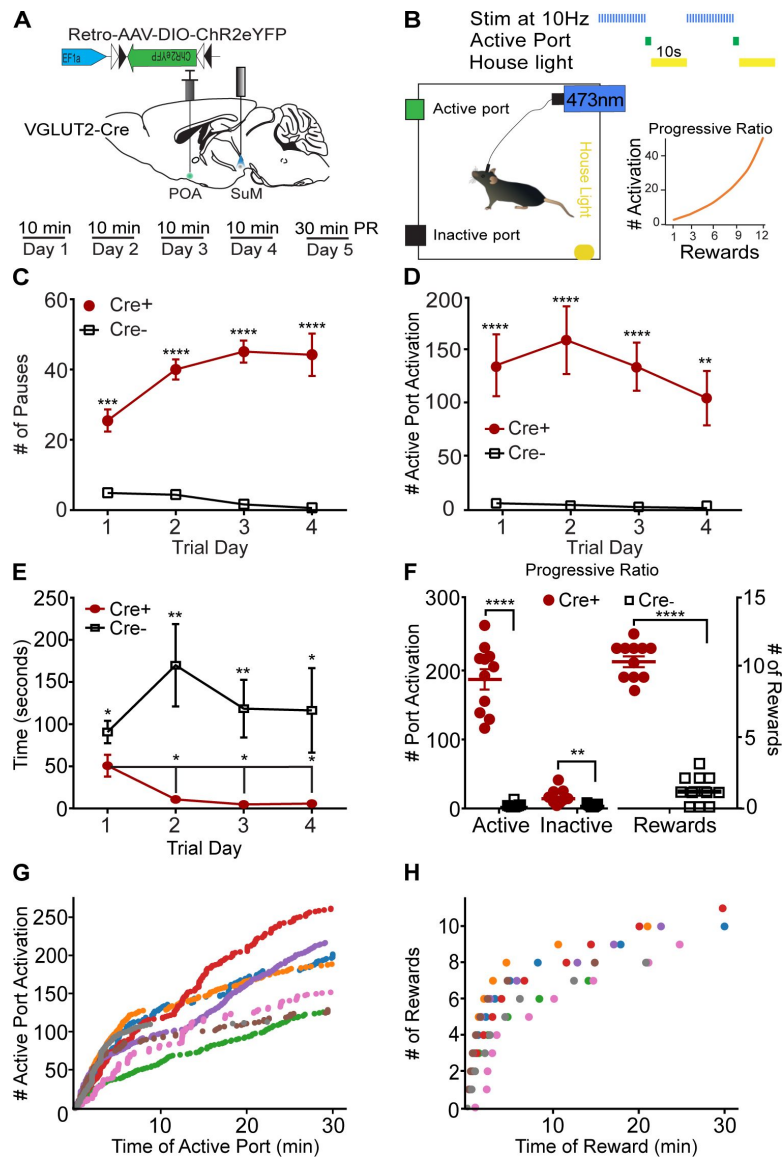


**Figure 6.**

### SuM<sup>VGLUT2+</sup>::POA neurons can drive instrumental action-outcome operant behavior

(A) Schematic of injection and implant in VGLUT2+ Cre mice and paradigm of testing in 10-minute trials with four days before a progressive ratio (PR) trial on day five. (B) Illustration of the testing paradigm and set up. 10 Hz photostimulation was applied during the trials. Activation of the active port triggered the house light and paused stimulation for 10 seconds. Also shown is the progressive ratio used with number of required port activations per reward on vertical axis and reward number on the horizontal. (C) Cre+ mice (n=11) activated the active port triggering significantly (\*\*\*\*p<0.0001) more pauses in stimulation than Cre- mice (n=11) mice on all four days of testing. (D) Cre+ mice activated the port significantly (\*\*\*\*p<0.0001, \*\*\*p<0.001) more than the Cre- mice on all four trials. (E) The time to first activation of the active port was significantly (\*p=0.046) different during the first trial, and Cre+ mice activated the active port significantly (\*\*p<0.01, \*\*p<0.01, \*\*p=0.034) faster on subsequent trials. (F) On the fifth day after four 10-minute trials, mice were tested for 30 minutes using a progressive ratio. Cre+ performed significantly (\*\*\*\*p<0.001) more active port activations than Cre- mice and activated the inactive port significantly (\*\*p=0.001) times. Cre+ mice also triggered significantly (\*\*\*\*p<0.001) more pauses in photostimulation than Cre- mice. (G) Individual data for a representative (n=7) cohort of Cre+ mice showing cumulative active port activations as a function of time during the progressive ratio test show on-going engagement of the active port throughout the 30-minute trial. (H) The cumulative pauses in photostimulation (rewards) earned as a function of time during the progressive ratio trial are shown for individual Cre+ mice. Mice earned between 7 and 11 pause rewards during the trial. All data plotted as means  $\pm$  SEM.

floating) behaviors. We carried out experiments using fiber photometry paired with automated computer-based behavior analysis [62]. The automated behavior scoring enabled high temporal resolution analysis of behaviors (**Supplemental Video 4**) and each frame of the video was coded for the classified behavior and plotted as a color-coded point. We observed four types of behavior during forced swimming: climbing, swimming, hindpaw swimming, and immobile floating, and we trained a model to identify each. Analysis of behavior showed that after the first minutes of the trial, mice shifted from swimming and climbing to immobile floating with intermittent swinging or hindpaw swimming. We analyzed fiber photometry recordings to examine whether recruitment of SuM<sup>VGLUT2+</sup>::POA neurons changed with this shift to more passive behaviors. As shown in the representative trace (**Figure 7A**), the Ca<sup>2+</sup>-dependent signal, but not the isosbestic signal, markedly decreased at the time the shift in behavior was occurring. To combine behavioral data, we assigned numerical values, one through four, to each behavior: climbing (4), swimming (3), hindpaw swimming (2), and immobile floating (1). The mean was plotted as a heat map (red higher values to blue lower values) to be compared to time locked fiber photometry data (**Figure 7B**). Examining the timeframe around the behavioral shift in each animal, we found that as behavior shifted from active coping (climbing, swimming) to more passive strategies and greater immobility, the Ca<sup>2+</sup> signal significantly (95% CI) declined (**Figure 7B**). Examining the data after this initial transition, we observed that many elevations in the Z-score were accompanied by changes in behavior to swimming or hindpaw swimming (**Figure 7A**). To further examine this possible correlation, we examined the time frame around transition to hindpaw swimming for changes in Ca<sup>2+</sup> signal. In a 20-second window centered on the onset of hindpaw swimming, we found that hindpaw swimming was accompanied by a rise in the Ca<sup>2+</sup> dependent signal across multiple events within a trial (**Figure 7C**). A similar analysis across events in multiple animals demonstrated a significant (99.9% CI) rise in the Ca<sup>2+</sup> dependent signal from SuM<sup>VGLUT2+</sup>::POA neurons during the shift from immobility to hindpaw swimming or swimming behaviors (**Figure 7D**). Time series analysis of 20-second epochs centered on random time intervals did not reveal any rise in the Ca<sup>2+</sup> dependent signal (**Figure 7E**). These data indicate that recruitment of SuM<sup>VGLUT2+</sup>::POA neurons fluctuates with changes in coping strategy during a forced swim assay with decreased engagement of this circuit during times of immobility.

## SuM<sup>VGLUT2+</sup>::POA neurons promote active coping during forced swim test

We found that SuM<sup>VGLUT2+</sup>::POA neurons are activated by acute stressors (**Figure 3**) and are recruited during times of greater active coping behaviors (**Figure 7**). To test if SuM<sup>VGLUT2+</sup>::POA neurons can drive a switch in coping strategy in the context of ongoing stressors, we used a two-day forced swim stress test [61, 63]. We tested animals during the second day, when immobile floating is the predominant behavior. As in previous experiments, we used VGLUT2-Cre (Cre+) or WT (Cre-) mice injected in the POA bilaterally with Retro-AVV-DIO-ChR2eYFP. On day one, we subjected mice to 15 mins of forced swim. On the subsequent day, we repeated the forced swim for 6 mins divided into three periods: pre-stimulation, stimulation at 10Hz, and post-stimulation (**Figure 7F**). Trials on the second day were recorded and scored by a blinded observer for time spent immobile in each 2-minute period. An example of a Cre+ mouse with stimulation 10Hz is shown in **Supplemental Video 3**. During the pre-stimulation period, there was not a significantly ( $p > .999$ ) different amount of time immobile between Cre+ ( $n=9$ ) and Cre- ( $n=11$ ) mice. During the stimulation period, Cre+ mice began swimming and attempting to climb the wall of the circular swim arena, reflected by significantly ( $p < 0.001$ ) less time immobile (**Figure 7H**). Interestingly, in the post stimulation phase, the difference in time spent immobile between Cre+ can WT mice decreased but remained significantly ( $p = 0.047$ ) different. These results indicate that in the context of an ongoing stressor, activation of SuM<sup>VGLUT2+</sup>::POA neurons is sufficient to trigger a change in coping strategy from largely passive (floating) to active (swimming, climbing). The persistent effect of the acute activation into the poststimulation phase suggests that activation of SuM<sup>VGLUT2+</sup>::POA neurons may shift how the stressor is processed or approached.

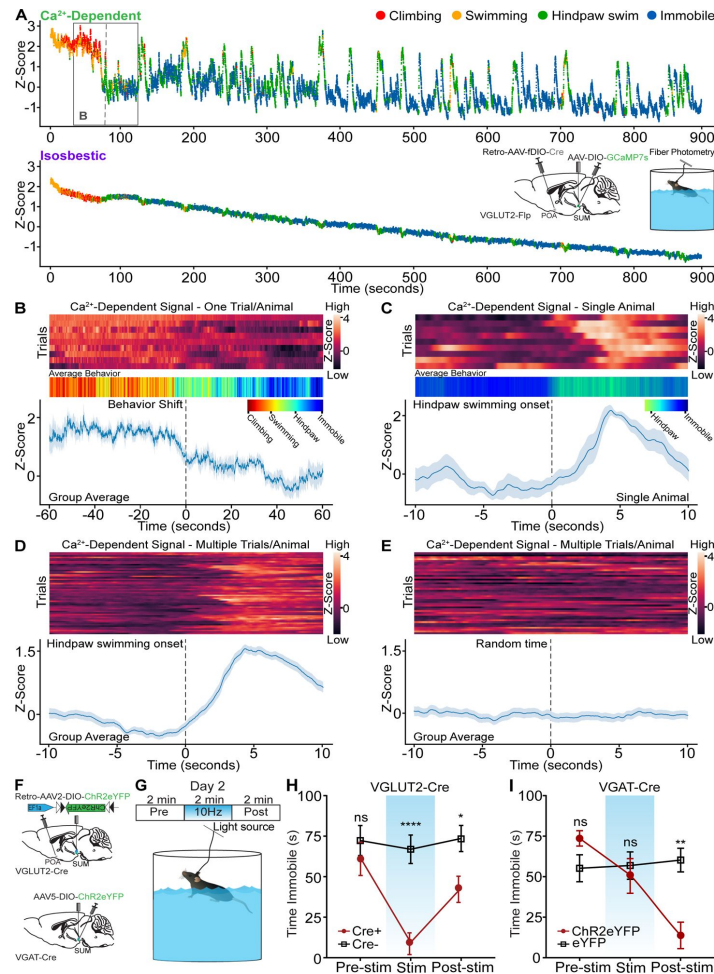


**Figure 7.**

**Sum<sup>VGLUT2+</sup>::POA neurons are recruited during active coping, and activation is sufficient drive a switch to active coping.**

(A) Color-coded per video frame (dot color) behavior combined with normalized  $\text{Ca}^{2+}$  dependent and isosbestic fiber photometry signals. Scoring and analysis of climbing, swimming, hindpaw swimming, and immobility were completed using deep learning-based classification and quantification (LabGym) of recorded behavior. Inset shows injection, implants, and behavioral assay. Box highlights the time frame shown in B. (B) Heat maps for recordings obtained from mice ( $n=9$ ) during forced swim, averaged color-coded behaviors, and mean  $\pm$ SEM Z-score of  $\text{Ca}^{2+}$  dependent signal for 2-min period around behavioral shift from climbing and swimming to hindpaw swimming and immobility, showing significant ( $*95\%$  CI) decline in the  $\text{Ca}^{2+}$  dependent signal. (C) Representative heat map, averaged behavior, and mean  $\pm$ SEM Z-score of  $\text{Ca}^{2+}$  dependent signal for 20-second window around onset of hindpaw swim from a representative animal. (D) Representative heat map and mean  $\pm$ SEM Z-score of  $\text{Ca}^{2+}$  dependent signal for 20-second window around onset of hindpaw swim from events from nine mice. Engaging in hindpaw swim correlates with a brief, significant ( $***99.9\%$  CI) increase in  $\text{Ca}^{2+}$  signal. (E) Representative heat map and mean  $\pm$ SEM Z-score of  $\text{Ca}^{2+}$  dependent signal for 20-second window around random time points. (F) Schematic of injection and implant in VGLUT2-Cre or VGAT-Cre mice. (G) Illustration of testing paradigm on second forced swim test following 15-minute swim on first day. (H) The average time spent immobile during the pre-stimulation period was not significantly ( $p>0.999$ ) different. During 10 Hz photostimulation VGLUT2-Cre+ mice engaged in vigorous swimming and the time spent immobile was significantly ( $****=p<0.001$ ) less than Cre- mice. In the post-stimulation period, the time spent immobile remained significantly ( $*=0.047$ ) lower in Cre+ mice compared to Cre-. (I) In VGAT-Cre+ mice expressing ChR2 ( $n=10$ ), the average time spent immobile during the pre-stimulation period was not significantly ( $p=0.218$ ) different compared to eYFP controls. Photostimulation did not significantly increase time immobile ( $p>0.999$ ). However, there was a significant ( $**p=0.001$ ) decrease in the time spent immobile compared to the post-stimulation period. For  $\text{Ca}^{2+}$  signal differences:  $*$ =95% CI,  $**$ =99% CI,  $***$ =99.9% CI, ns=not significant.



We next examined the effect of 10 Hz photostimulation of SuM<sup>VGAT</sup> neurons on coping strategy using the same two-day swim paradigm. VGAT-Cre mice were injected in the SuM to express ChR2eYFP (n=10) or control (eYFP) (n=11), and a fiber optic was placed over SuM (**Figure 7F**). Quantification of behavior revealed no significant difference in time spent immobile during the pre-stimulation (p=.218) or the stimulation (p>.999) periods. Surprisingly, in the post-stimulation period, we observed a dramatic shift in behavior, marked by a significant (p=0.047) decrease in time spent immobile (**Figure 7I**). The amplitude of change in behavior was similar to what we observed during the stimulation phase of the experiments on SuM<sup>VGLUT2+::POA</sup> neurons (**Figure 7H**). One interpretation of these data is that release of sustained local inhibition leads to rebound activity of output SuM<sup>VGLUT2+::POA</sup> neurons.

## Suppression of SuM<sup>VGLUT2+::POA</sup> neurons is required for feeding

Feeding and responding to threats are conflicting actions, and SuM<sup>VGLUT2+::POA</sup> neurons may play a role in switching between behavioral paradigms (e.g., feeding vs escape). We sought to examine SuM<sup>VGLUT2+::POA</sup> neuron activity in relation to feeding using fiber photometry based GCaMP recordings. To promote differential drive for food, mice were given *ad lib* access to food (fed condition) or food deprivation for 24 hours, and on testing day, were presented with a chow pellet, while Ca<sup>2+</sup> dependent GCaMP fluorescence and isosbestic signals were recorded. In the fed state, mice spent significantly less time interacting with the food (p<0.001; **Figure 8C**) and ate significantly less (p<0.001; **Figure 8D**) compared to food deprived state. We analyzed the Ca<sup>2+</sup> dependent and isosbestic signals around presentation of food to fed and food deprived mice. In the food deprived state, mice spent more time with the food and ate more food (**Figure 8E** and **F**). At the time of food presentation, the Ca<sup>2+</sup> dependent signal decreased significantly (99.9% CI) but not the isosbestic signal. The change in the Ca<sup>2+</sup> dependent signal was larger and more sustained when the animals spent longer interacting with the food (**Figure 8E** and **F**). Together, the data support suppression of SuM<sup>VGLUT2+::POA</sup> neural activity during consummatory behavior with greater consumption associated with enhanced suppression.

To examine whether activation of SuM<sup>VGLUT2+::POA</sup> neurons disrupted consummatory behavior, we tested the impact of photostimulation on feeding behavior in food deprived mice. Using VGLUT2-Cre (Cre+) or WT (Cre- littermates) mice injected with Retro-AAV2-DIO-ChR2eYFP into the POA and implanted with a fiber optic midline over SuM, we examined how feeding behaviors in food deprived mice were altered by 10 Hz photostimulation of SuM<sup>VGLUT2+::POA</sup> neurons (**Figure 8G-I**). We used trials lasting 20 mins with unrestricted access to food added at the start of the trial. Each trial was divided into three periods: a 5-min pre-simulation period, 10-min stimulation period, and a 5-min post-stimulation period. Trials were recorded and scored for time spent interacting with the food pellet. During the pre-stimulation period, Cre+ (n=17) and Cre- (n=16) mice spent interacting with the food was not significantly different (p>0.999). Upon the introduction of photostimulation, the Cre+ mice stopped eating and interacting with the food. During the photostimulation period, Cre+ mice spent significantly less time interacting with the food compared to Cre- mice (p<0.001). Surprisingly, the decrease in time spent interacting with food continued into the post-stimulation phase, where Cre+ mice continued to interact with the food significantly less than Cre- mice (p<0.001; **Figure 8H**). Reflecting the decrease in time spent with the food, Cre+ mice consumed significantly less food during the 20-min trial than Cre- mice (p=0.001; **Figure 8I**). These results indicate that SuM<sup>VGLUT2+::POA</sup> neurons can redirect behavior away from consumption, and suppression of SuM<sup>VGLUT2+::POA</sup> neurons is required for feeding, even in a food deprived state. Ethologically, animals must choose rapidly between responding to threats and feeding when foraging. The findings here implicate this pathway in control of switching between these behaviors.

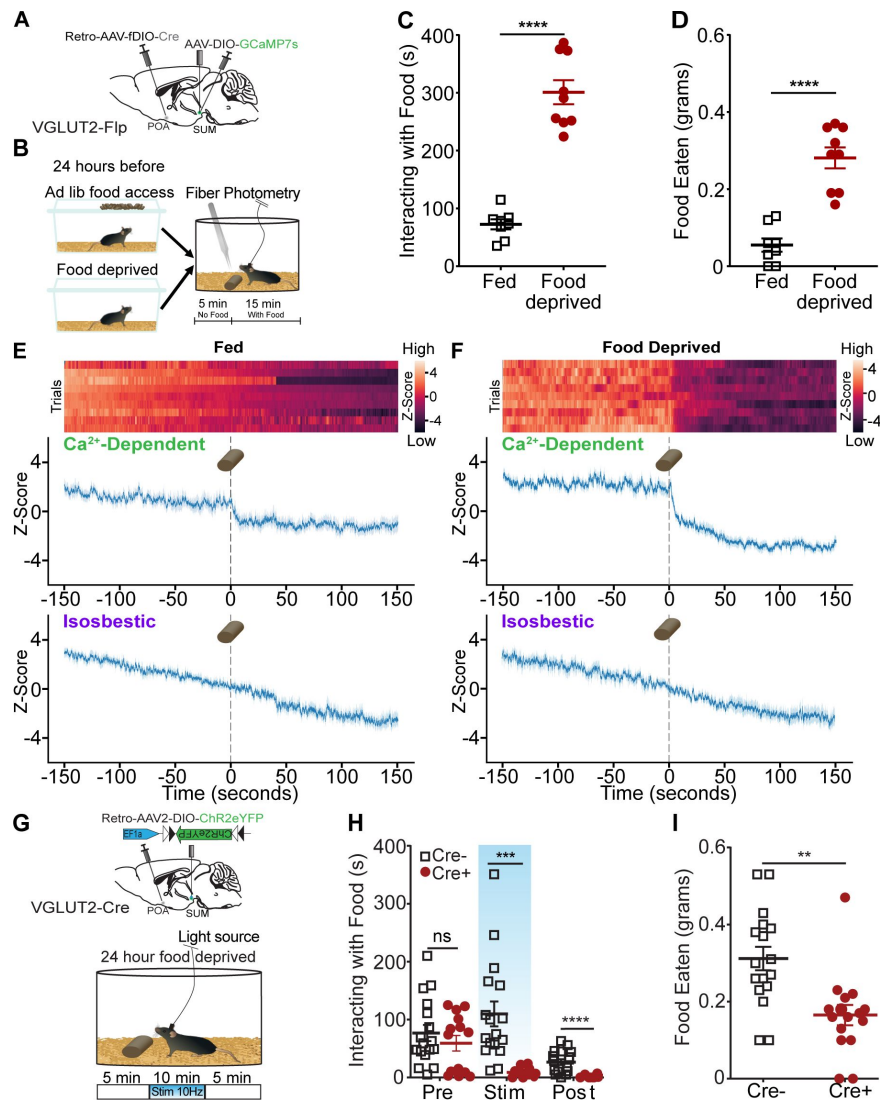


**Figure 8.**

### Consummatory behavior suppresses SuM<sup>VGLUT2+</sup>:POA neuron activity, and SuM<sup>VGLUT2+</sup>:POA neuron blocks food consumption.

(A) Schematic of injections in VGLUT2-Flp mice with AAV-DIO-GCaMP7s in the SuM and Retro-AAV-fDIO-Cre in the POA and a fiber placed over SuM. (B) Mice were given ad lib food access or food deprived for 24 hours prior to testing. After being placed in the arena and allowed to habituate, mice were given a 20-minute trial divided into 5 mins of baseline and 15 mins after a chow pellet was added to the arena. (C) Food deprived mice (n=9) spent significantly (p<0.001) more time interacting with the food pellet and (D) ate significantly (p<0.001) more than in the fed state. (E) Heat map and mean ± SEM Z-scores for Ca<sup>2+</sup> dependent and isosbestic signals for recordings obtained from 9 animals show a small drop in (E) fed mice state (\*95% CI) compared to a sharp decrease in Ca<sup>2+</sup> activity after the introduction of the food pellet following addition in (F) food deprivation (\*\*\*99.9% CI). (G) Mice were fasted for 24 hours prior to testing, and the schematized 20 min paradigm was used. Following food deprivation, animals were given access to a chow pellet. The trial was divided into 5-minute pre- and post-stimulation periods, with a 10-minute period of stimulation. (H) The time spent interacting with the food was quantified for each period. Cre+ (n=16) and Cre- (n=17) mice both rapidly engaged with the food pellet, and the average time spent interacting was not significantly (p=0.37) different. During the stimulation period and the post-stimulation period, the average time interacting with the food was significantly (p=0.0002, p=0.0001) lower in Cre+ mice compared to Cre- mice. (I) The food eaten during the total trial was calculated based on pellet weights, and, on average, Cre+ mice ate significantly (p=0.001) less food during the trial than Cre- mice. (\*\*p=0.001, \*\*\*p<0.001, \*\*\*\*p<0.0001). For Ca<sup>2+</sup> signal differences: \*=95% CI, \*\*=99% CI, \*\*\*=99.9% CI, ns=not significant.

## Discussion

Together, the presented data show SuM<sup>VGLUT2+</sup>::POA neurons function as a hub, with connections to many brain areas, to regulate responses to threatening stressors. We report here that SuM<sup>VGLUT2+</sup>::POA neurons have broad arborizations to multiple brain regions involved in responding to threat and stress (**Figures 1**, **2**, and **Supplemental Figure 2**). We identified diverse threatening stressors (dunk, shock, and predator), which elicit differential behavioral responses, swimming, jumping, and fleeing, recruit SuM<sup>VGLUT2+</sup>::POA neurons. Using a forced swim test, we found that recruitment of SuM<sup>VGLUT2+</sup>::POA neurons is correlated with periods of spontaneous active coping (swimming, climbing) and not with passive (immobile) behaviors. These data collectively indicate that SuM<sup>VGLUT2+</sup>::POA neurons are recruited by threatening stressors, preferentially during active coping. We also examined the roles of SuM<sup>VGLUT2+</sup>::POA neurons in responding to stressors by stimulating SuM<sup>VGLUT2+</sup>::POA neurons, and selective activation of SuM<sup>VGLUT2+</sup>::POA neurons evoked active coping-like behaviors in the absence of a stressor (**Figure 4**). SuM<sup>VGLUT2+</sup>::POA neuron activation drove aversion but did not promote anxiety-like behaviors (**Figure 5**). We also used a negative reinforcement test, requiring selective activation of an active port over the inactive port to show SuM<sup>VGLUT2+</sup>::POA neurons can drive flexible, in contrast to fixed or reflexive, behaviors (**Figure 6**). Activation of SuM<sup>VGLUT2+</sup>::POA neurons increased active coping during ongoing stress in a forced swim assay (**Figure 7H**). Finally, examining the conflicting behaviors required for threat response and feeding, we found SuM<sup>VGLUT2+</sup>::POA neurons were suppressed during feeding and that activation of SuM<sup>VGLUT2+</sup>::POA neurons blocked feeding activity (**Figure 8**). Thus, SuM<sup>VGLUT2+</sup>::POA neurons contribute to affective component of stress, promote active coping behaviors, and shift behavior to shift threat responsivity away from feeding.

The presented results demonstrate SuM<sup>VGLUT2+</sup>::POA neurons act as a distinct subset of neurons projecting to many but not all areas receiving projections from the total SuM<sup>VGLUT2+</sup> population. Notably, mHb and DG projections were present in the SuM<sup>VGLUT2+</sup> population but absent in the SuM<sup>VGLUT2+</sup>::POA projections (**Figure 3K**), consistent with a separation of DG and CA2 projecting SuM neurons [64]. The extensive arborization of SuM<sup>VGLUT2+</sup>::POA neurons challenges the often-employed neural circuit concept that projection from a single area to another area mediates or modifies a behavior. The projections to PVT, Hb, and PAG are of particular interest because these areas regulate stress coping [65–68]. Dopamine receptor 2 expressing neurons in the PVT have been implicated in promoting active coping behaviors and may be a potential target of SuM<sup>VGLUT2+</sup>::POA neurons [8, 9]. The habenula also regulates active vs passive coping behaviors, and the LHb functions in aversive processing, making the selective projections of SuM<sup>VGLUT2+</sup>::POA neurons to the LHb of similar interest [65, 69–72]. In addition, the PAG, which receives projections from SuM<sup>VGLUT2+</sup>::POA neurons, has been implicated in regulating defensive behaviors and coping strategies [66, 67, 73]. The arborization to these and other areas position SuM<sup>VGLUT2+</sup>::POA neurons to be a central hub for regulating behavioral responses to threatening stressors by concurrent recruitment of multiple areas. Understanding the roles of individual projections in contributing to the overall behavioral response will require further studies.

Superficially, the aversiveness of SuM<sup>VGLUT2+</sup>::POA neuron stimulation we report contrasts with a recent study that found photostimulation of SuM neuron projections could be reinforcing. Photostimulation of projections from SuM to the septum drove place preference (septum), but the same report found photostimulation of SuM projections in the PVT was aversive [19]. We report here that SuM<sup>VGLUT2+</sup>::POA neurons also project to the PVT and the septum (**Figure 2**). A plausible interpretation is that SuM contains separable, molecularly defined populations of neurons which gate a host of distinct behavioral strategies through their connectivity and/or co-

transmitter content. Delineating the overarching circuitry will require further in depth studies, but our results together with recent studies establish the SuM as an important and poorly understood node which regulates both appetitive and aversive motivated behavior.

We addressed the challenge of potential confounds from locomotor activity inherent in active coping behaviors, which is of special concern here because a population of SuM neurons have been found to correlate with velocity of movement. To do so we used multiple behavioral assays together with fiber photometry and photostimulation. We found multiple threatening stressors (dunk, shock, ambush) with differing evoked behaviors all recruit SuM<sup>VGLUT2+</sup>::POA neurons (**Figure 3**). We also found increased recruitment of SuM<sup>VGLUT2+</sup>::POA neurons during active coping behaviors (**Figures 3** and **7**). We did not find evidence for recruitment of SuM<sup>VGLUT2+</sup>::POA neurons during elevated locomotion in two cohorts in assays of free movement (**Figure 3K-M** and **Supplemental Figure 5**). These data are in contrast to recent studies that found activity of some neurons in SuM correlated future velocity [42]. We carefully examined the behaviors elicited by activation of SuM<sup>VGLUT2+</sup>::POA neurons both in absence of stressors (**Figure 4**) and during ongoing stressors (**Figure 7**) and found that stimulation of SuM<sup>VGLUT2+</sup>::POA neurons promoted active coping behaviors, which involved increased physical activity. We examined if SuM<sup>VGLUT2+</sup>::POA neurons could also drive performance of an operant task which would be impaired if activation of SuM<sup>VGLUT2+</sup>::POA neurons lead to fixed escape behaviors. We found that the mice effectively performed the operant task, extensively activating the active port, instead of the inactivate port. Taken together, the results from the behavioral tests indicate that SuM<sup>VGLUT2+</sup>::POA promote flexible stressor appropriate coping behaviors and not generalized locomotion.

Although neurons in SuM can release both GABA and glutamate in the dentate gyrus, our anatomic studies indicate that SuM<sup>VGLUT2+</sup>::POA neurons were discrete from GABAergic neurons and do not project the dentate gyrus (**Figure 2** and **Supplemental Figure 2**) [21, 31]. Thus, SuM<sup>VGAT</sup> neurons could be a functionally distinct population. We tested the effects of photostimulation of SuM<sup>VGAT</sup> neuron and, in contrast to SuM<sup>VGLUT2+</sup>::POA neurons, found no effect on place aversion, minor decreases in locomotion, and no significant change in active coping behaviors during stress (FST) during stimulation. Surprisingly, immediately after photostimulation stopped, active coping behavior increased dramatically (**Figure 7I**). These data demonstrate functional separation of SuM<sup>VGAT</sup> and suggest connection between the SuM<sup>VGLUT2+</sup>::POA and SuM<sup>VGAT+</sup> populations that require further investigation to elucidate.

In conclusion, SuM<sup>VGLUT2+</sup>::POA neurons arborize to multiple areas involved in stress and threat response that promote active coping behaviors. Passive coping strategies have been associated with unescapable stress, anhedonia, and depression [7, 74–76]. Targeting neuromodulation of a circuit able to act across many brain areas may represent a therapeutic avenue for common psychiatric conditions, and SuM<sup>VGLUT2+</sup>::POA neurons are a newly identified node in critical approach-avoidance circuitry.

## Acknowledgements

This work was supported by the NIH through 5R01MH112355 to MRB and P30DA048736 (MRB) and 5K08MH119538 to AJN. Support was also provided by the Hope Center Viral Vectors Core and the Genome Technology Resource Center at Washington University in St. Louis (NIH P30CA91842 and UL1TR000448). This work was supported by a Pilot Project Award from the Hope Center for Neurological Disorders and by the Hope Center Viral Vectors Core at Washington University School of Medicine.



## Materials and Methods

### Methods

#### Key Resources Table

Reagent type (species) or resource	Source or reference	Identifiers
<b>Antibodies</b>		
Alexa Fluor 488 Goat anti-Rabbit IgG	Invitrogen	Cat# A11008
Phospho-c-Fos (Ser32) (D82C12) XP®	Cell Signaling Technology	Cat# 5348
<b>Chemicals</b>		
4% paraformaldehyde	J.T. Baker, Avantor	S898-09
Goat Serum	Sigma Aldrich	G9023
Vectashield Hardset Antifade Mounting Medium with DAPI	Vector Laboratories	Cat# NC9029229
<b>Experimental Models: Organisms/Strains</b>		
Slc17a6 <sup>tm2(cre)Lowl/J</sup> (VGLUT2-Cre)	The Jackson Laboratory	RRID:IMSR_JAX:016963
B6;129S-Slc17a6 <sup>tm1.1(flpo)Hze/J</sup> (VGLUT2-Flp)	The Jackson Laboratory	RRID:IMSR_JAX:030212
Mouse: B6.Cg-Gt(ROSA)26Sor <sup>tm14(CAG-tdTomato)Hze/J</sup> (Ai14)	The Jackson Laboratory	RRID:IMSR_JAX:007914
B6J.129S6(FVB)-Slc32a1 <sup>tm2(cre)Lowl/MwarJ</sup> (VGAT-Cre)	The Jackson Laboratory	RRID:IMSR_JAX:028862
C57BL/6J	The Jackson Laboratory	RRID:IMSR_JAX:000664
<b>Bacterial and Virus Strains</b>		
AAV5-EF1a-DIO-hChR2(H134R)-eYFP (2.5 × 10 <sup>13</sup> vg/ml)	Washington University Hope Center Viral Vector Core	N/A
AAV2-Retro-DIO-ChR2-eYFP (2.8 × 10 <sup>12</sup> vg/ml)	Washington University Hope Center Viral Vector Core	N/A
AAV2-retro-FLEX-tdTomato (7 × 10 <sup>12</sup> vg/ml)	Addgene	RRID: Addgene_28306-AAVrg
AAV5-DIO-ChR2-eYFP (1.4 × 10 <sup>13</sup> vg/ml)	Washington University Hope Center Viral Vector Core	N/A
AAV2-Retro-EF1a-fDIO-cre (7 × 10 <sup>12</sup> vg/ml)	Addgene	RRID: Addgene_121675-AAVrg

AAV5-EF1a-Nuc-flox(mCherry)-EGFP ( $5.7 \times 10^{12}$ vg/ml)	Addgene	RRID: Addgene_112677-AAV5
Retro-AAV2-EF1a-Nuc-flox(mCherry)-EGFP ( $7 \times 10^{12}$ vg/mL)	Addgene	RRID: Addgene_112677-AAVrg
AAV2-retro-EF1a-DIO-eYFP ( $3 \times 10^{13}$ vg/ml)	Washington University Hope Center Viral Vector Core	N/A
AAV-retro-EF1a-Flpo ( $1.02 \times 10^{13}$ GC/mL or $7 \times 10^{12}$ vg/ml)	Addgene	RRID: Addgene_55637-AAVrg
AAV9-EF1a-fDIO-cre ( $2.5 \times 10^{13}$ GC/mL or $1 \times 10^{13}$ vg/ml)	Addgene	RRID: Addgene_121675-AAV9
Retro-AAV2-EF1a-Cre ( $2.1 \times 10^{13}$ GC/mL)	Addgene	RRID: Addgene_55636-AAVrg
AAV9-syn-FLEX-GCaMP7s-WPRE ( $1.2 \times 10^{13}$ GC/ml)	Addgene	RRID: Addgene_104487-AAV9
AAV5-EF1a-DIO-eYFP ( $1.8 \times 10^{13}$ vg/ml)	Washington University Hope Center Viral Vector Core	N/A
AAV2 retro-Ef1a-DIO-mCherry ( $4.0 \times 10^{12}$ vg/ml)	University of Carolina Vector Core	N/A
<b>Software</b>		
Bonsai	Bonsai-rx.org	N/A
Ethovision	Noldus	N/A
GraphPad Prism	GraphPad Software	N/A
Labgym	<a href="https://github.com/umyelab/LabGym">https://github.com/umyelab/LabGym</a>	N/A
DeepLabCut	<a href="https://github.com/DeepLabCut/DeepLabCut">https://github.com/DeepLabCut/DeepLabCut</a>	N/A

For further information regarding reagents and resources, contact Aaron Norris, [norrisa@wustl.edu](mailto:norrisa@wustl.edu).

## Experimental model and subject details

Adult (25–35 g, at least 8 weeks of age upon experimental use) male and female VGLUT-Cre (RRID: IMSR\_JAX:016963), VGLUT2-Flp (RRID: IMSR\_JAX: 030212), Ai14 (RRID: IMSR\_JAX: 007908), VGAT-Cre (RRID: IMSR\_JAX: 028862) and C57BL/6J (RRID: IMSR\_JAX: 000664) mice (species *Mus musculus*) were group housed (no more than five littermates per cage) in a 12 hr:12 hr light:dark cycle room with food and water ad libitum[77]. Cre+ and Cre- littermates were used in the experiments unless otherwise noted. The Washington University Animal Care and Use Committee approved all procedures which adhered to NIH guidelines.

## Stereotaxic surgery

Injections and implantations were done as described previously [78, 79]. Briefly, in an induction chamber, mice were anesthetized (4% isoflurane) before being placed in a stereotaxic frame (Kopf Instruments). Anesthesia was maintained with 2% isoflurane. Mice were then injected unilaterally or bilaterally, depending on the combination of virus(es) used and brain regions injected. A blunt needle Neuros Syringe (65457-01, Hamilton Con.) and syringe pump (World Precision Instruments) were used to perform the injection schemes below. After surgery, a warmed recovery chamber housed the animal while it recovered from anesthesia before being returned to its home cage.

Brain Region /Coordinates	Virus Volume	Virus
SuM (AP -2.7-2.85, ML +0.05, DV -4.3-4.5)	50 - 300 nl	AAV5-EF1a-DIO-hChR2(H134R)-EYFP AAV2-retro-DIO-ChR2-eYFP AAV5-EF1a-Nuc-flox(mCherry)-EGFP AAV9-EF1a-fDIO-cre AAV9-syn-FLEX-GCaMP7s-WPRE AAV5-EF1a-DIO-eYFP
POA, bilateral (AP +0.45, ML $\pm$ 0.5, DV -5.35)	50 - 150 nl	AAV2-retro-EF1a-fDIO-cre Retro-AAV2-EF1a-Nuc-flox(mCherry)-EGFP AAV2-retro-EF1a-DIO-eYFP AAV2-retro-EF1a-Flpo AAV2 retro-Ef1a-DIO-mCherry
Septum (AP +0.9, ML +0.3, DV -3.5)	100 nl	AAV2-retro-FLEX-tdTomato
LPAG, unilateral (AP -4.65, ML +0.6, DV -2.85)	100 nl	AAV2-retro-FLEX-tdTomato
Acb, unilateral, (AP +1.4, +0.6 ML, DV -4.75)	100 nl	AAV2-retro-EF1a-DIO-eYFP
PVT, unilateral, (AP -1.5, ML 0.0, DV -2.85)	100 nl	AAV2-retro-EF1a-DIO-eYFP

Injections were made at a rate of 50 nl/min, with the injection needle being withdrawn 5 min after the end of the infusion. Fiber optics for photostimulation or optical fibers for fiber photometry were implanted after injections for all behavioral experiments.

Fiber optic implants for photostimulation were fabricated as previously described using 200 $\mu$ m glass fibers and implanted midline over SuM [78, 80]. For implantation, the skull was cleaned and etched with OptiBond® (Kerr) and the fiber was cemented to the skull with Tetric N-Flow® (Ivoclar Vivadent). Blue light was used to cure and harden cement. Mice were allowed to recover for at least seven days before the start of behavioral experiments. The same process was used for implantation for fiber photometry fibers, which were purchased from Neurophotometrics and trimmed to length.

## Anatomical tracing

For anterograde viral tracing experiments, virus was injected at least six weeks prior to transcardial perfusions with 4% paraformaldehyde to allow for anterograde transport of the fluorophore. AAV5-EF1a-DIO-hChR2eYFP or AAV5-EF1a-DIO-eYFP were used. Alternatively, to label only SuM<sup>VGLUT2+</sup> POA neurons for anterograde tracing, Retro-AAV2-DIO-eYFP or Retro-DIO-ChR21eYFP was injected into the POA with AAV-fDIO-Cre injected in the SuM. A minimum of six weeks was allowed prior to sacrifice, harvesting of brains, and sectioning (30 μM). Serial 30 μM sections approximately 60 μM apart were examined. For retrograde studies, viruses were injected (see figure legends and text for specific viruses) at the targeted site and table for specific viruses [81–83]. Three weeks were allowed to elapse prior to harvesting brains following injections. Images were obtained on a Leica DM6 B upright microscope and processed using Thunder imaging station (Leica).

## Brain clearing and light sheet microscopy

Tissue clearing and imaging was carried out on brains collected and fixed in 4% PFA as described above by LifeCanvas Technologies. Briefly, brains were fixed using SHIELD post fix and cleared for seven days in SmartClear II Pro. Index matched with EASYIndex at room temperature. Samples were mounted ventral side up and imaged at 3.6x with pixel size 1.8 x 1.8 mm, axial resolution < 4 μm, z step 4 μm in 488nm channel. Fos was labeled by Alexa Fluor 488. SuM boundaries were defined by -2.6 to -2.95 rostral to Bregma. The medial mammillary nucleus and the mammillary recess of the 3<sup>rd</sup> ventricle marked the medial and ventral boundaries, while fornix marked the lateral, and fasciculus retroflexus marked the dorsal boundaries. Images were quantified by a trained laboratory member who was blind to the experimental conditions.

## Immunohistochemistry

Mice were intracardially perfused with 4% PFA and then brains were sectioned (30 microns) and placed in 1x PB until immunostaining. Free-floating sections were washed three times in 1x PBS for 10 min intervals. Sections were then placed in blocking buffer (0.5% Triton X-100 and 5% natural goat serum in 1x PBS) for 1 hr at room temperature. After blocking buffer, sections were placed in primary antibody rabbit Phospho-c-Fos (Ser32) antibody (1:500, Cell Signaling Technology) overnight 4 °C temperature. After 3 x 10 min 1x PBS washes, sections were incubated in secondary antibody goat anti-rabbit Alexa Fluor 488 (1:2500, Invitrogen) for 2 hr at room temperature. Sections were washed in 1x PBS (3 x 10 min) followed by 2 x 10 min 1x PB washes. After immunostaining, sections were mounted on Super Frost Plus slides (Fisher) and covered with Vectashield Hard set mounting medium with DAPI (RRID:AB\_2336788, Vector Laboratories) and cover glass prior to being imaged.

## Imaging and cell quantification

‘The Mouse Brain in Stereotaxic Coordinates’ provided the framework to label brain sections relative to bregma [84]. A Leica DM6 B epifluorescent microscope was used to image all sections. For eYFP visualization, a YFP filter cube (Excitation: 490-510, Dichroic: 515, Emission: 520-550) was used and for tdTomato visualization, a Texas Red Filter Cube (Excitation: BP 560/40, Dichroic: LP 585, Emission: BP 630/75) was used. Fos was labeled by Alexa Fluor 488. SuM boundaries were defined by -2.6 to -2.95 rostral to Bregma. The medial mammillary nucleus and the mammillary recess of the 3<sup>rd</sup> ventricle marked the medial and ventral boundaries while fornix marked the lateral, and fasciculus retroflexus the dorsal boundaries. Images were quantified by a trained laboratory member who was blind to the experimental conditions.

## Forced-Swim Test for cFos examination

For stress induction via forced swim (**Figure S4**)[\[61, 85\]](#), mice were individually placed in a cylindrical container (18 cm in diameter) filled with water at 25  $\pm$  1  $^{\circ}$ C for 15 min. Prior to stress force swimming, mice were habituated to the arenas for three days prior to the beginning of FST to minimize stress. 90 mins after forced swim, mice were injected with ketamine and xylazine and were intracardially perfused. Control mice were brought to the behavioral testing area but remained in the home cage until perfusion. Water was replaced after every animal. To examine SuM-POA glutamatergic projections, VGlut2-Cre<sup>+</sup> littermates were injected with AAV2 retro-Ef1a-DIO-mCherry into the POA.

## Fiber Photometry

For all fiber photometry experiments, the same strategy to selectively label SuM<sup>VGLUT2<sup>+</sup></sup>::POA neurons was used. VGLUT2-Flp mice were injected bilaterally in POA with AAV-Retro-EF1a-fDIO-Cre and with AAV-syn-FLEX-GCaMP7s-WPRE in SuM. After two weeks, mice were implanted with fiber-optic cannulas (200 $\mu$ m) in SuM (D/V -4.3-5)[\[86\]](#). Mice recovered a minimum of one week prior to behavioral testing. Recording of Ca<sup>2+</sup> dependent and isosbestic signals were obtained using previously described methods with Bonsai software and FP3002 (Neurophotometrics)[\[59, 87\]](#). 470 and 415 nm LEDs were used to record interleaved isosbestic and Ca<sup>2+</sup> dependent signals following the manufacturer directions.

For repeated forced swim experiments (dunk tank), mice were placed on top of a square wire mesh platform inside a custom-made plastic rectangular enclosure (20 cm x 20 cm x 23 cm) filled with water 30  $\pm$  1  $^{\circ}$ C. The square wire mesh platform could be raised and lowered without touching the animal. Mice were habituated for 2 days before the test day. Each day, mice were tethered to the fiber optic patch cable and placed on top of the platform for 30mins. On test day, mice were tethered and placed on top of the platform for 30mins (habituation) before the beginning of the 1st trial. After 30mins, for each trial the platform was lowered for 30s and raised after 30s with a rest of 2mins between trials for a total of 10 trials (“dunks”). After 10 trials, an additional 2mins were recorded before removing the animal from the enclosure, patted the animals with paper towels, and placed back in its home cage. During testing, mice were tethered to a fiberoptic patch cable that was attached to a counterbalanced arm that prevented downward force on the animal. Water was replaced after each animal. Time mobile was quantified by a trained observer for the ten 30s trials.

For foot shock stress testing, mice were individually placed inside a custom-made clear plastic box (15.24 L x 13.34 W x 14 H cm) inside a sound-attenuated cabinet. A speaker was placed 4 cm above the chamber for the delivery of auditory cues (75dB). A constant current aversive stimulator (ENV-414S) delivered foot shocks through a grid floor (0.7mA). Five shocks of 2s were delivered after a 30s tone. Intertrial interval ranged from 90 to 180s. After the session, the animal was removed from the chamber and placed back in its home cage. The chamber and grid were wiped down with 70% ethanol between animals.

For open field testing velocity measurements, mice were tethered to a fiberoptic patch cable and placed inside a custom-built square arena (50.8 cm x 50.8 cm x 50.8 cm). Mice were allowed to explore the arena for a 20 min session. Velocity was quantified using scripts in Bonsai 2.4. Bedding in the arena was replaced between animals, and the floors and walls of the arena were wiped down with 70% ethanol.

Similar to the repeated forced swim experiments, forced swim mice were placed on top of a square wire mesh platform that could be raised and lowered inside a custom-made plastic rectangular enclosure (20 cm x 20 cm x 23 cm) filled with water at 25  $\pm$  1  $^{\circ}$ C. The platform was lowered at the beginning of the test for 15 min and raised at the conclusion of the test. During



testing, mice were tethered to a fiberoptic patch cable that was attached to a counter balanced arm that prevented downward force on the animal. Water was replaced between animals and the enclosure was wiped down with 70% ethanol and rinsed with water. Time immobile, hindpaw swim, swimming, and climbing were quantified using LabGym (Hu et al., 2022).

To measure the activity of  $\text{SuM}^{\text{VGLUT2}+}::\text{POA}$  neurons in response to a stressor that mice may encounter in their natural habitat [88], a remote-controlled spider was used to simulate an ambush of a potential predator. The remote-controlled spider (17 cm x 16 cm; Amazon) was placed inside a polylactic acid (PLA) enclosure (19 cm x 20 cm x 23 cm) that was then placed inside a custom-built square arena (50.8 cm x 50.8 cm x 50.8 cm). Mice were tethered to a fiberoptic patch cable and placed inside the arena for 10 min. Baseline activity was recorded for 5 min before the ambush. After 5 min, the animal was ambushed once it moved in close proximity to the spider's enclosure (Supplemental video 4). Velocity was measured and analyzed using DeepLabCut (Mathis et al., 2019) within Bonsai. The arena and spider's enclosure were wiped down with 70% ethanol between animals.

For experiments that examined recruitment of  $\text{SuM}^{\text{VGLUT2}+}::\text{POA}$  neurons during consummatory behavior, mice were food deprived or given ad lib access to food for 24 hours prior to testing. On test day, mice were placed inside an 18 cm diameter round arena and allowed to habituate for 30 min before they were tethered to the fiberoptic path cable. Once tethered, mice were placed inside the arena for 20 min. Baseline activity was recorded for 5 min before the introduction of the chow pellet and for 15 min after the chow pellet was introduced. Chow pellets were weighed before and after the 20-min trial. The difference is reported as food eaten. The same procedure was followed for control mice with the only difference being that these animals were not food deprived for 24 hours.

For fiber photometry data analysis, the interleaved isosbestic and  $\text{Ca}^{2+}$  dependent signals were recorded at 60 fps (30 fps each). Deinterleaved signals were analyzed using methods as previously reported [87]. Briefly, raw signals were smoothed using a moving average, fitted with an exponential curve using a non-linear least squares function for baseline correction, signals were standardized using the mean value and standard deviation (Z-Score), the standardized isosbestic and  $\text{Ca}^{2+}$  signals were scaled a non-negative robust linear regression, and normalized  $\text{dF/F}$  was calculated. In experiments shown in **figures 7A** and 8 E-F there was sustained step drop evident in the  $\text{Ca}^{2+}$  dependent signal reflecting change in population activity because it was not seen in the isosbestic signal. The nature and duration of the change of the signal precluded fitting a curve to the  $\text{Ca}^{2+}$  dependent signal. In these cases, we show both the  $\text{Ca}^{2+}$  dependent and isosbestic signals. Z-scores were calculated without baseline correction for both  $\text{Ca}^{2+}$  dependent and isosbestic signals based on the variability in the baseline state.

## Real-time place aversion testing

For real-time place preference testing with optogenetic photostimulation, we used custom-made, unbiased, balanced two-compartment conditioning apparatus (52.5 x 25.5 x 25.5 cm) as described previously [78, 79, 89]. Mice were tethered to a patch cable that allowed free access to the entire arena for 30 min. Entry into one compartment triggered photostimulation, 1 Hz, 5 Hz, 10 Hz, or 20 Hz (473 nm laser, 10 ms pulse width), that persisted while the mouse remained in the light paired side. The side paired with photostimulation was counterbalanced across mice. Ordering was counterbalanced with respect to stimulation frequency and placement. Bedding in the behavior apparatus was replaced between every trial, and the floors and walls of the apparatus were wiped down with 70% ethanol. Time spent in each chamber and total distance traveled for the entire 30-min trial was measured using Ethovision 10 (Noldus Information Technologies). For optogenetic stimulation of VGAT neurons during RTTA,  $\text{Cre}^+$  littermates were injected either with AAV5-EF1a-DIO-hChR2(H134R)-EYFP or with AAV5-EF1a-DIO-eYFP as control, and stimulation was provided at 10 Hz.

## Light/Dark choice

For light/dark choice, the same arenas as used for real-time preference testing were modified and used as previously described [90]. On the light side, a small sport light was placed overhead, and the walls were covered with white laminated paper. Light levels on this side measure 580-590 lux. For the dark side, an infrared spotlight was placed over head, to allow for video tracking of the mice. The walls were covered with matte black plastic. Light levels in the center of the dark side measure 100-110 lux. Animals were recorded using a USB web cam without an infrared filter. For real-time aversion testing, photostimulation was paired with the dark side of the arena as described above. For anxiety-like behavior testing, stimulation was provided uniformly during the trials. Time spent in each chamber and total distance traveled for the entire 30-min trial was measured using Ethovision 10.

## Observational behavioral assay

To observe behaviors evoked by photostimulation of  $\text{SuM}^{\text{VGLUT2+::POA}}$  neurons, mice were habituated for at least three days prior to testing to a round (18 cm diameter), clear arena with counterbalanced optical commutators to minimize the impact of the head tether on movement. Testing occurred after habitation, and approximately 2 cm of bedding material was placed in the arena. Behavior was recorded from the side and scored by a blinded observer.

## Negative reinforcer two nose port operant behavior testing

For operant behavior testing, we used Med Associates mouse operant conditioning chamber with dual nose ports and house light as previously described [59]. Briefly, mice were tethered via cantilevered counterweighted optical commutator to a laser light source. A five-day protocol call was used. Day one through four were 10-min trials. Photostimulation was provided at 10 Hz and activation of the active port resulted in a 10-second pause in the photostimulation and activation of the house light inside the arena. On the first four days, each activation of the active port outside of a 10-second pause resulted in a new pause. On day five was a 30-min trial using a progressive ratio protocol the number activation of the active port to generate a pause increased with each activation based on the *number of activations* ( $j$ ) =  $[5e^{(0.2j)} - 5]$  round to the nearest integer generating the schedule 1, 2, 4, 6, 9, 12, 15, 20, 25, 32, 40, 50.... [91]. The trial was limited to 30-mins due to concern for animal welfare due to the head tether and confined space. Photostimulation terminated at the conclusion of the trial.

## Forced Swim with photostimulation

Forced swim trials with optogenetic stimulation were done as a two-day test. On the first day, all mice were subjected to a 15-min forced swim, dried, and returned to the home cage. On the second day, they were tethered and subjected to a 6-min forced swim, divided into three periods, each two mins in length: pre stimulation, stimulation, and post stimulation. 10 Hz photostimulation was provided during the trial. Mice were closely monitored during each trial of swimming. Trials were recorded and scored by a blinded observer for time spent immobile on the second day of the test. For forced swim trials with optogenetic stimulation of VGAT neurons, Cre+ littermates were injected either with AAV5-EF1a-DIO-hChR2(H134R)-EYFP or with AAV5-EF1a-DIO-eYFP as control.

## Feeding after food deprivation

For tests involving brief access to food after deprivation, the same 18 cm diameter round arenas with counterbalanced optical commutators were used. Mice were habituated to the arenas for a minimum of three days prior to testing. Mice were food deprived by removal of food from the home cage 24 hours prior to testing. Mice were placed in the arena and allowed to habituate prior

to introduction of a chow pellet. The 20-min trial with the foot pellet was recorded and scored by a blinded observer. Chow pellets were weighed before and after the 20-min trial. The difference is reported as food eaten.

## Open Field Test

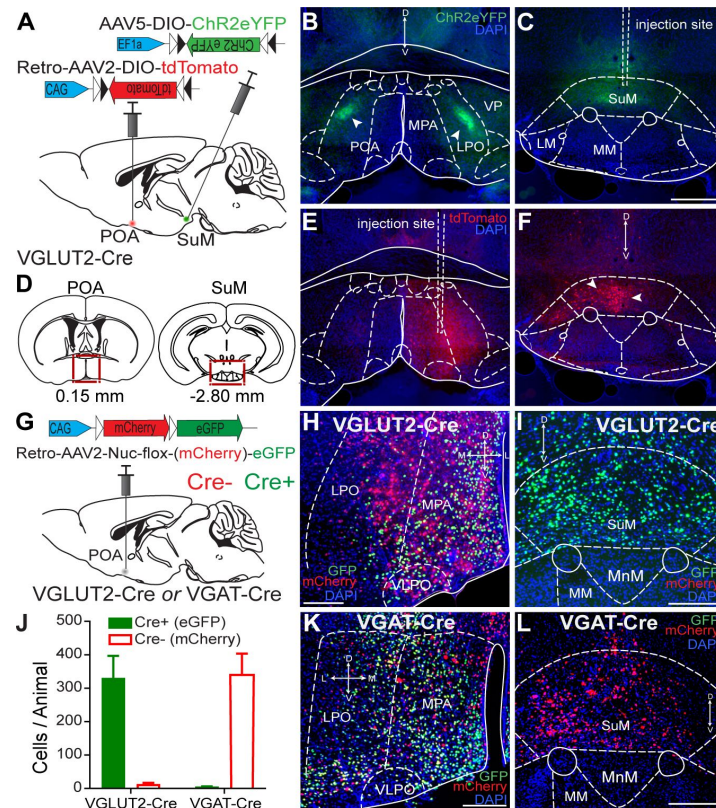
For Open Field testing, we used a purpose-built 20 in square behavior arena. Mice were tethered to a patch cable and placed into the behavioral arena. The laser frequency was set to 10 Hz and was left on for 20 mins. Distance moved for the 20-min trial was quantified using Ethovision 10. Bedding in the arena was replaced between every trial, and the floors and walls of the arena were wiped down with 70% ethanol. Similarly, for optogenetic stimulation of VGAT neurons, Cre+ littermates were injected either with AAV5-EF1a-DIO-hChR2(H134R)-EYFP or with AAV5-EF1a-DIO-eYFP as control.

## Statistical analyses

Statistical analyses were conducted using GraphPad Prism software. Data are shown as mean  $\pm$  SEM, except for Z-scores which are shown as  $\pm$  95% confidence interval, as noted in text. Values for individual p values are given in the text and figure legends. Significance was held at  $\alpha$  less than 0.05. Unless noted in the test, nonparametric Mann-Whitney tests were used for statistical comparisons. In cases of multiple comparisons, Holm-Šidák method was used to correct for multiple comparisons. Paired testing was used with comparing within cohorts with repeated measurements and unpaired between cohorts. All “n” values represent the number of animals in a particular group for an experiment. For fiber photometry statistical analysis, the mean signal of the baseline and stimulus windows was used, and comparisons were made using the Wilcoxon ranked-sum test, with  $\alpha=0.95$ . To analyze the change in the  $\text{Ca}^{2+}$  dependent signal, a t-confidence interval method was used, in which 95%, 99%, and 99.9% confidence intervals were calculated for windows preceding and subsequently following the described point of interest. Differences were considered significant if the null hypothesis (zero) was not included in the CI. Because exact p values are not calculated using this method, the highest confidence level at which the difference is significant (95%, 99%, or 99.9% CI) is reported instead.

## References

1. LeDoux J., Daw N.D. (2018) **Surviving threats: neural circuit and computational implications of a new taxonomy of defensive behaviour** *Nat Rev Neurosci* **19**:269–282
2. LeDoux J.E (2014) **Coming to terms with fear** *Proc Natl Acad Sci U S A* **111**:2871–8
3. Mobbs D., et al. (2015) **The ecology of human fear: survival optimization and the nervous system** *Front Neurosci* **9**
4. Shin L.M., Liberzon I. (2010) **The neurocircuitry of fear, stress, and anxiety disorders** *Neuropsychopharmacology* **35**:169–91
5. Ressler K.J., Mayberg H.S. (2007) **Targeting abnormal neural circuits in mood and anxiety disorders: from the laboratory to the clinic** *Nat Neurosci* **10**:1116–24
6. Kessler R.C., et al. (2007) **Lifetime prevalence and age-of-onset distributions of mental disorders in the World Health Organization’s World Mental Health Survey Initiative** *World Psychiatry* **6**:168–76

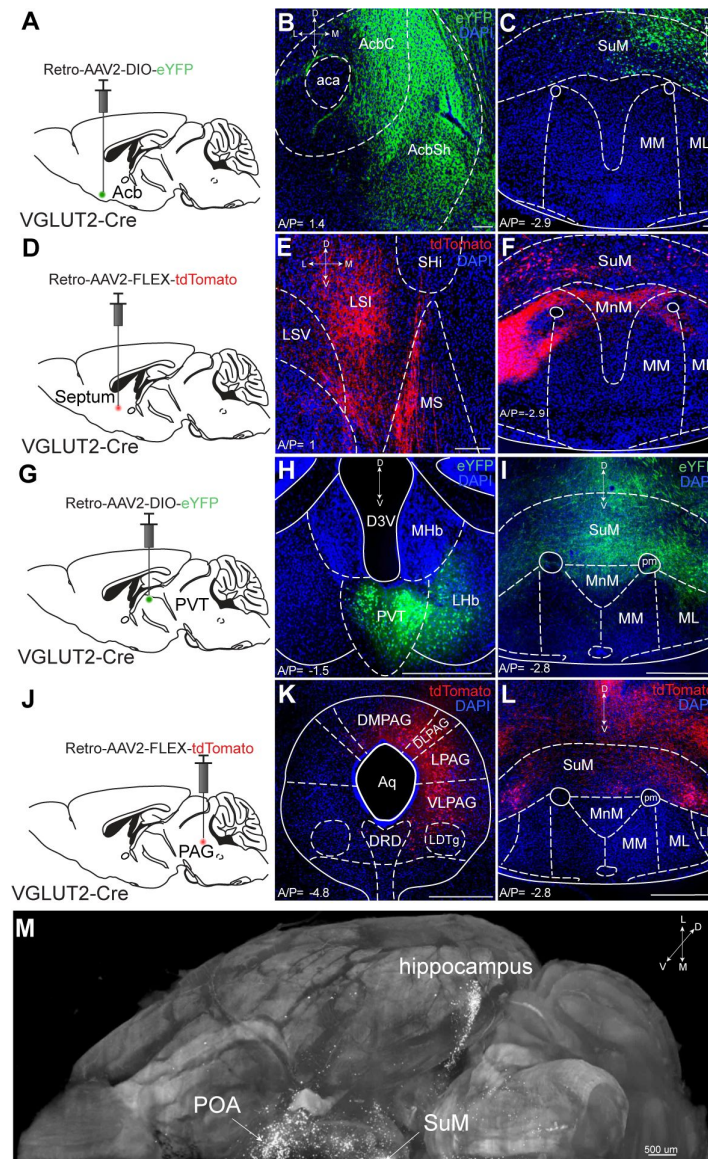


**Supplemental Figure 1.**

### SuMVGLUT2<sup>+</sup> neurons project to the preoptic area of the hypothalamus and are not VGAT<sup>+</sup>.

(A) Schematic of injections into VGLUT2-Cre mice of Retro-AAV-DIO-tdTomato into the POA and AAV-DIO-ChR2eYFP into the SuM. (B and C) Projections of VGLUT2<sup>+</sup> SuM neurons are evident in the POA with dense labeling in LPO and the site of viral injection in SuM (500 μm scale bar). (D) The brain regions, POA and SuM, shown in (B, C, E and F). (E and F) Cell bodies of VGLUT2<sup>+</sup> SuM neurons are evident in SuM with injection of Retro-AAVs in POA. (G) Schematic of injection in POA of fluorophore switching construct in Retro-AAV2 in VGLUT2-Cre or VGAT-Cre mice. (H and I) Labeling of Cre- (red) and Cre+ neurons in POA but only Cre+ seen in SuM of VGLUT2-Cre mice showing all SuM::POA neurons are VGLUT2<sup>+</sup>. (J) Quantification of labeling of Cre+ and Cre- cells in SuM following injections in POA in VGLUT2-Cre and VGAT-Cre mice. (K and L) Labeling of Cre- (red) and Cre+ neurons in POA but only Cre- seen in SuM of VGAT-Cre mice. (100 μm scale bar)

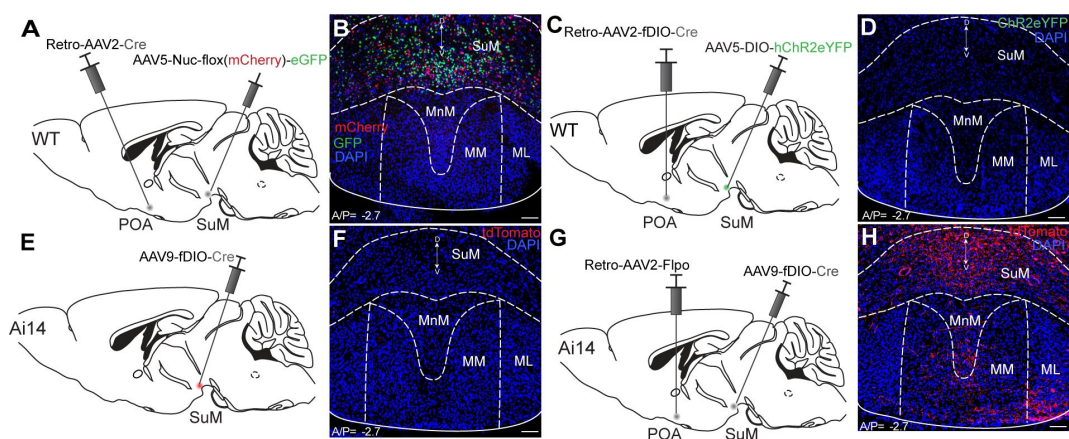




**Supplemental Figure 2.**

### **Retrograde verification of projection targets of SuM<sup>VGLUT2+</sup>::POA.**

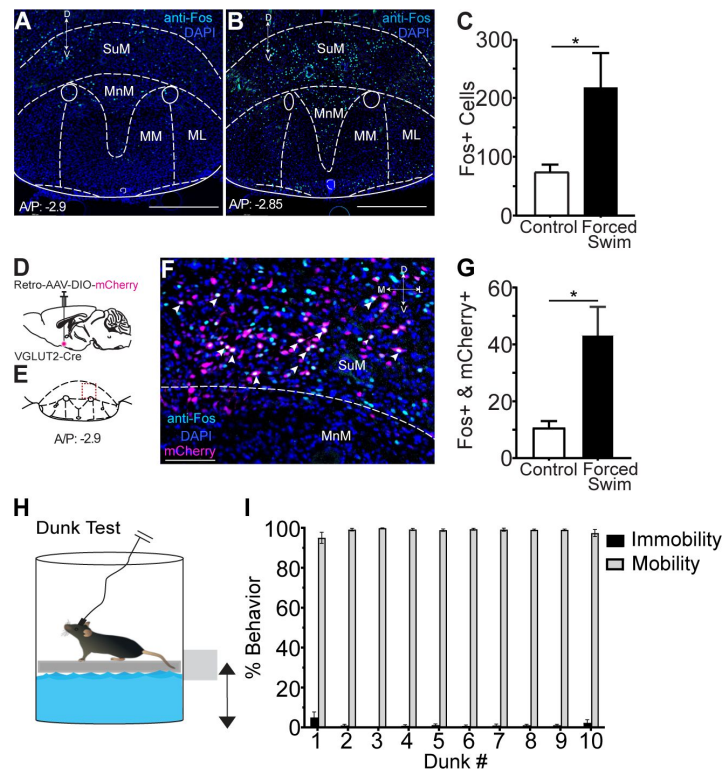
(A, D, G, and J) Schematic showing the injection sites of Retro-AAV's in VGLUT2-Cre mice. (B-C) In VGLUT2-Cre mice, injection of Retro-AAV-DIO-eYFP unilaterally in the (B) accumbens nucleus resulted in labeling of cell bodies in (C) SuM. (E-F) Similarly, injection of Retro-AAV-DIO-tdTomato into (E) septum resulted in labeling of cell bodies in (F) SuM. (H-I) injection of Retro-AAV-DIO-eYFP targeting the (H) PV and LHb resulted in cell bodies in (I) SuM being labeled with eYFP. (K-L) Retro-AAV-DIO-tdTomato injected into (K) PAG labeled cells in (L) SuM. (M) The cleared brain hemisphere from a VGLUT2-Flp mouse injected in the POA with injected Retro-AAV-DIO-eYFP shown in **Figure 2M** displayed from a perspective of ventral to dorsal shows cells labeled in SuM and processes extending widely, including in the hippocampus and POA. (100 and 500 μm scale bars)



**Supplemental Figure 3.**

### **Combinatorial viral and genetic approach is effective with minimal background.**

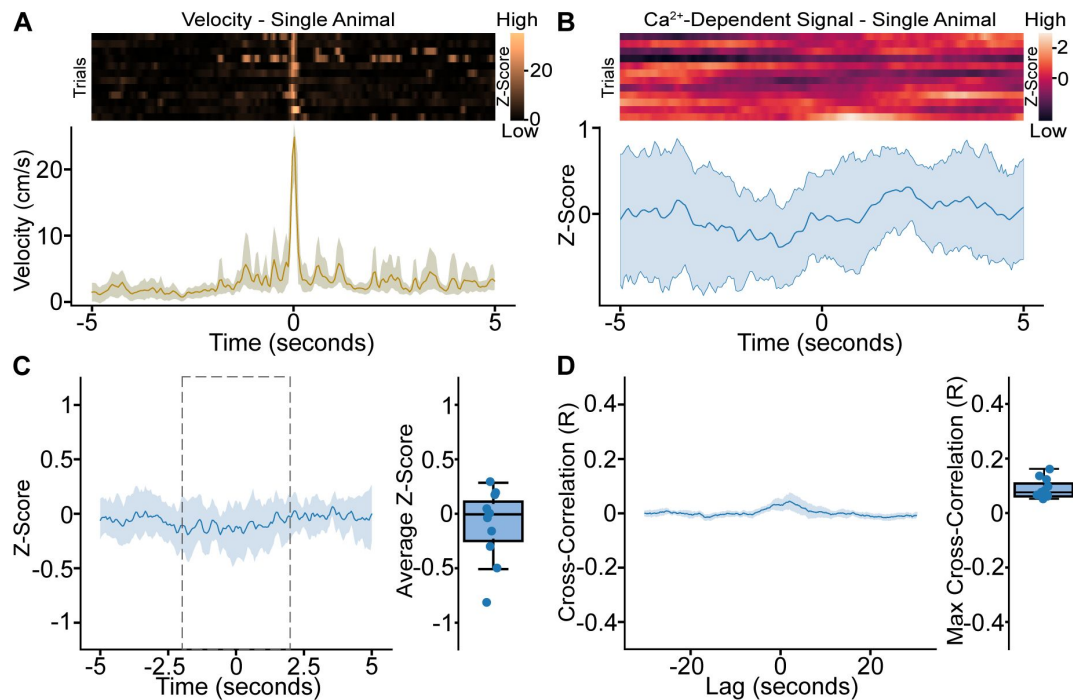
(A) Schematic of injection of Retro-AAV-Cre into the POA and AAV-Nuc-flox(mCherry)-eGFP into the SuM of WT mice. (B) In SuM, eGFP (green) Cre+ and mCherry (red) Cre- labeled neurons are seen based on expression of Cre mediated by POA injected retrograde AAV constructs showing SuM::POA neurons are a subset of all cells in SuM. (C and D) In wildtype mice injected in POA with Retro-AAV-fDIO-Cre and in SuM with AAV-DIO-ChR2eYFP, expression of ChR2eYFP (green) is not seen. (E-H) In Ai14 reporter mice injected with AAV-fDIO-Cre into SuM, tdTomato expression is not observed unless Retro-AAV2-Flp is injected. (100  $\mu$ m scale bars)



**Supplemental Figure 4.**

### **SuMVGLUT2<sup>+</sup>::POA neurons show Fos induction after FST, and dunk test evokes active coping.**

Sections of brains from mice (A) left in the home cage or (B) subjected to 15 minutes of forced swimming 90 min prior to sacrifice were probed with anti-Fos antibodies (cyan) showed (scale bars 500µm) (C) a significant ( $p = 0.029$ ) increase in the mean  $\pm$ SEM number of anti-Fos labeled neurons in brains from mice subjected to force swim ( $n=5$ ) compared to control mice ( $n=4$ ). (D) In VGLUT2-Cre mice, Retro-AAV-DIO-mCherry was injected in the POA of mice ( $n=5$ ) subjected to 15 minutes forced swim. (E) Region of SuM shown with higher magnification in (F) where SuM<sup>VGLUT2<sup>+</sup>::POA</sup> neurons labeled by mCherry show overlap with cells (arrows) labeled by anti-Fos. (Scale bar 100µm) (G) A significant increase ( $p = 0.016$ ) in the number of VGLUT2+ cells labeled with mCherry and anti-Fos is seen in mice subjected to forced swim. (H) Mice subjected to 10 30-second trials of “dunk” forced swimming. (I) Quantitation of average time mobile for every 30-second trial during “dunk” forced swim.

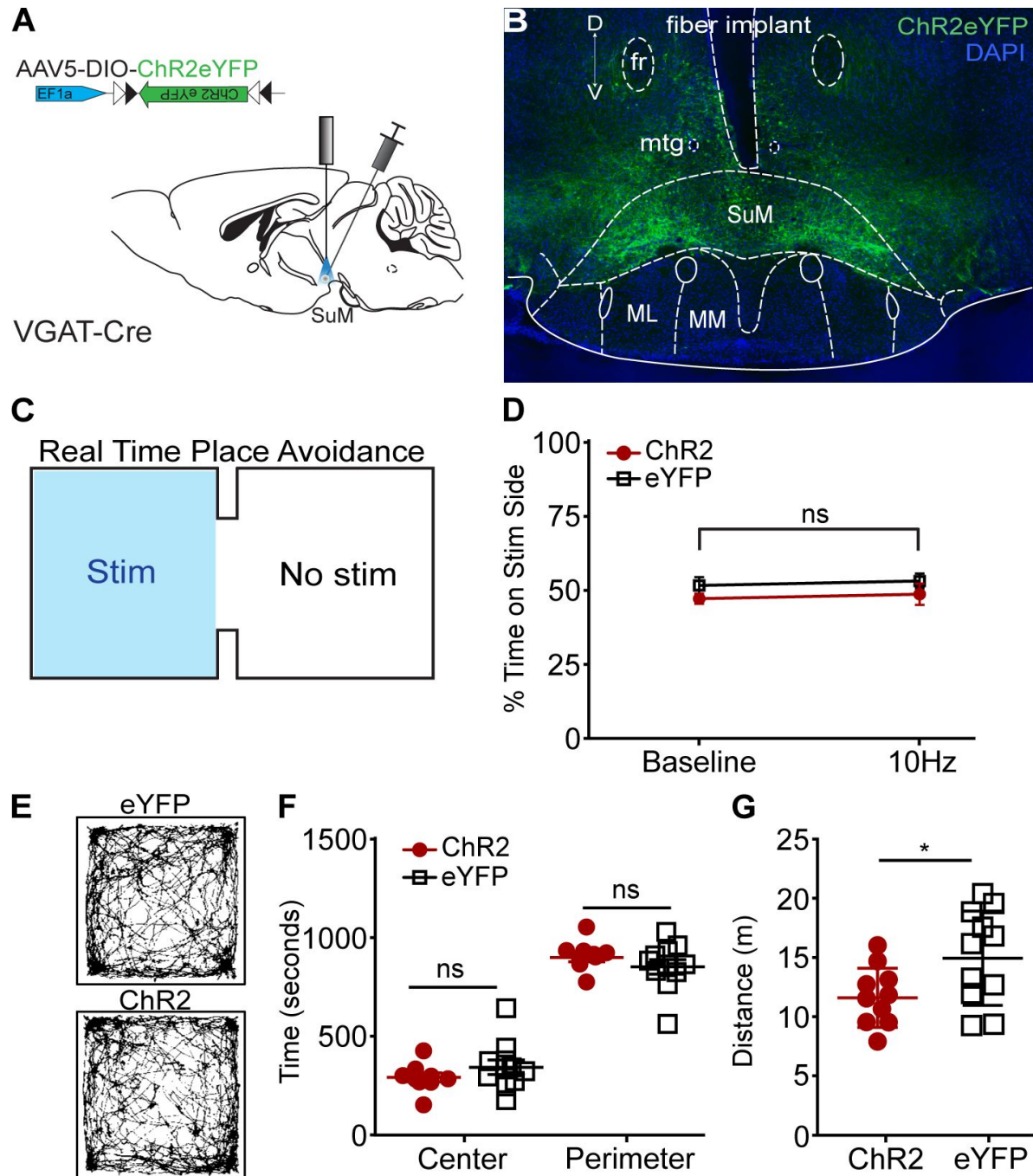


**Supplemental Figure 5.**

**SuMVGLUT2<sup>+</sup>::POA neurons are not recruited during increased locomotor activity in the absence of acute stressor.**

(**A**) Heat maps showing velocity for 12 episodes of rapid locomotion from a representative animal during free movement in open field with mean  $\pm 95\%$  CI for the trials. (**B**) For that same animal, heat maps of  $\text{Ca}^{2+}$ -dependent signal were analyzed during average peak velocity, showing no change in activity during peak velocity. Representative heat map for a single animal with the mean  $\pm 95\%$  confidence interval of the 12 trials for same animal. (**C**) Mean  $\pm 95\%$  confidence interval for Z-score of 12 trials for all 13 animals and Boxplot for average Z-score. (**D**) Cross-correlation analysis shows no correlation between  $\text{Ca}^{2+}$  signal from SuMVGLUT2<sup>+</sup>::POA neurons and spontaneous velocity increases.

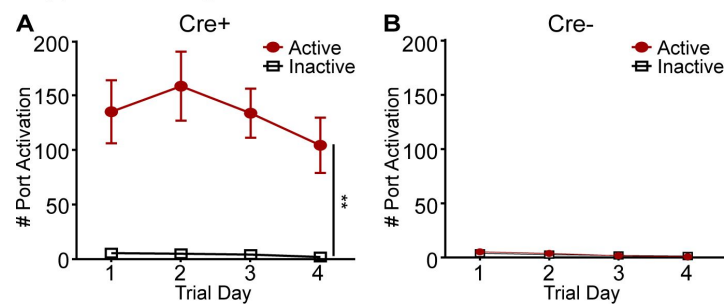




**Supplemental Figure 6.**

**GABAergic neurons in SuM do not drive place preference.**

(A) Schematic of viral injection into VGAT-Cre mice in SuM. (B) VGAT<sup>+</sup> neurons labeled and outline of implanted fiber. (C) Real-time arena showing the pair of photostimulation on one side of the arena. (D) Photostimulation at 10 Hz did not drive a significant place preference ( $p = 0.67$ ). (eYFP (control)  $n=26$  and ChR2=26). All data plotted as mean  $\pm$  SEM. (E) Representative path traces of VGAT-Cre mice with ChR2 or eYFP (control) in open field testing. (F) No significant differences in center ( $p=0.254$ ) or perimeter ( $p=0.287$ ) time when comparing the ChR2eYFP expressing to controls VGAT-Cre mice. (G) Chr2eYFP expressing mice traveled slightly but significantly ( $p=0.034$ ) less distance compared to control.



**Supplemental Figure 7.**

**SuMVGLUT2+::POA stimulations drives active port activation.**

**(A)** Cre+ mice activated the active port significantly more (\*\* $p=0.001$ ) compared to the inactive port. **(B)** In Cre- mice, no significant change in the number of port activations of both the active and inactive ports.

Figure	Panel	Test	Statistic	P value	Bonferroni's Multiple comparisons	Multiple comparisons statistic	Adjusted P value
3	G	T-Confidence Interval	95% CI -30 to 0s [-0.73511383 -0.724353688] 1 to 30s [1.903893784 1.965866945] Difference [2.630811087 2.694498841]	Sig at 95%	N/A	N/A	N/A
			99% CI -30 to 0s [-0.737419984 -0.718129215] 1 to 30s [1.894157095 1.975603635] Difference [2.620805016 2.704550491]	Sig at 99%			
			99.9% CI -30 to 0s [-0.74009622 -0.715452978] 1 to 30s [1.882857892 1.986902837] Difference [2.609193202 2.716116722]	Sig at 99.9%			
	I	T-Confidence Interval	95% CI -3 to -1s [0.213736241 0.298523885] 1 to 3s [5.190328104 6.484427377] Difference [4.932810735 6.22968462]	Sig at 95%	N/A	N/A	N/A
			99% CI -3 to -1s [0.200415137 0.311844989] 1 to 3s [4.987010372 6.687745109] Difference [4.72905708 6.433438275]	Sig at 99%			
			99.9% CI -3 to -1s [0.184956303 0.327303822] 1 to 3s [4.751064858 6.923690623] Difference [4.492605688 6.669889668]	Sig at 99.9%			
	J	T-Confidence Interval	95% CI -3 to -1s [1.116192035 1.439691613] 1 to 3s [0.049420441 0.369842849] Difference [-1.295973579 -0.840646778]	Sig at 95%	N/A	N/A	N/A
			99% CI -3 to -1s [1.065366568 1.49051708] 1 to 3s [-0.000921568 0.420184858] Difference [-1.367510605 -0.769109753]	Sig at 99%			
			99.9% CI -3 to -1s [1.006384792 1.549498856] 1 to 3s [-0.059342302 0.478605592] Difference [-1.450527664 -0.686092694]	Sig at 99.9%			

**Supplemental Table 1.**

**Statistical analyses and values.**

	K	T-Confidence Interval	95% CI -3 to -1s [-0.21380383 0.000116753] 1 to 3s [-0.381118104 -0.039309855] Difference [-0.304985727 0.098244846]  99% CI -3 to -1s [-0.24741319 0.033726113] 1 to 3s [-0.434820072 0.014392113] Difference [-0.368337842 0.16159696]  99.9% CI -3 to -1s [-0.286416073 0.072728995] 1 to 3s [-0.497139961 0.076712002] Difference [-0.441856502 0.235115621]	ns   ns   ns	N/A	N/A	N/A
4	C	Two-Way RM ANOVA	Stimulation Period x Genotype F (2, 58) = 12.82 Stimulation Period F (1.012, 29.36) = 12.27 Genotype F (1, 29) = 11.78	p<0.001****  p=0.0014**  p=0.0018**	Pre-stimulation Stimulation Post-stimulation	t=1 t=3.429 t=1	p=0.9995 p=0.0122* p=0.9995
	D	Two-Way RM ANOVA	Stimulation Period x Genotype F (2, 58) = 21.04 Stimulation Period F (1.794, 52.02) = 18.34 Genotype F (1, 29) = 0.6615	p<0.001****  p<0.001****  p=0.4227	Pre-stimulation Stimulation Post-stimulation	t=1.02 t=3.74 t=3.281	p=0.9495 p=0.0039** p=0.0139*
	E	Two-Way RM ANOVA	Stimulation Period x Genotype F (2, 58) = 14.84 Stimulation Period F (1.667, 48.34) = 6.658 Genotype F (1, 29) = 4.707	p<0.0001****  p=0.0045**  p=0.0384*	Pre-stimulation Stimulation Post-stimulation	t=0.7131 t=3.267 t=3.81	p>0.9999 p=0.0156* p=0.0052**
5	C	Two-Way ANOVA	Frequency x Genotype F (4, 188) = 36.76 Frequency F (4, 188) = 34.61 Genotype F (1, 188) = 352.1	p<0.0001****  p<0.0001****  p<0.0001****	Cre+ vs Cre- 1 Hz 5 Hz 10 Hz 20 Hz	t=4.477 t=10.09 t=12.36 t=15.09	p<0.0001**** p<0.0001**** p<0.0001**** p<0.0001****
	D	Two-Way Mixed Model ANOVA	Time x Genotype F (9.116, 218.1) = 1.418 Time F (1, 24) = 0.02824 Genotype F (29, 694) = 1.038	p=0.1807  p=0.868  p=0.4125	N/A	N/A	N/A
	E	Two-Way Mixed Model ANOVA	Time x Genotype F (29, 694) = 1.035 Time F (7.228, 173.0) = 1.030 Genotype F (1, 25) = 90.74	p=0.4159  p=0.4124  p<0.0001****	N/A	N/A	N/A
	F	Two-Way ANOVA	Frequency x Genotype F (4, 115) = 12.37 Frequency F (4, 115) = 12.38 Genotype F (1, 115) = 187.5	p<0.0001****  p<0.0001****  p<0.0001****	Cre+ vs Cre- 1 Hz 5 Hz 10 Hz 20 Hz	t=4.117 t=7.622 t=8.789 t=9.156	p=0.0004*** p<0.0001**** p<0.0001**** p<0.0001****
	H	Two-Tailed T-Test	Center Cre+ vs Cre- t=1.407, df=36	p=0.1681	N/A	N/A	N/A
		Two-Tailed T-Test	Perimeter t=1.356, df=36	p=0.1837			
	I	Two-Tailed T-Test	Total Distance t=4.857, df=33	p<0.0001****	N/A	N/A	N/A

**Supplemental Table 1.** (continued)







			10 to 150s [0.564052895 1.293569678] Difference [0.248605856 1.107317568]  99% CI -150 to -10s [-0.046808878 0.548508026] 10 to 150s [0.449437502 1.408185071] Difference [0.113692468 1.242230956]  99.9% CI -150 to -10s [-0.129398096 0.631097245] 10 to 150s [0.316428994 1.541193579] Difference [-0.042871391 1.398794816]	ns			
	F	T- Confidence Interval	Isosbestic 95% CI -150 to -10s [0.049394291 0.689096421] 10 to 150s [0.670463682 1.423655887] Difference [0.183719975 1.171908881]  99% CI -150 to -10s [-0.051110197 0.78960091] 10 to 150s [0.55212861 1.541990959] Difference [0.028464246 1.32716461]  99.9% CI -150 to -10s [-0.167743327 0.906234039] 10 to 150s [0.414803502 1.679316067] Difference [-0.151706429 1.507335286]  Ca <sup>2+</sup> -Dependent 95% CI -150 to -10s [-0.875926952 0.142125648] 10 to 150s [1.203199181 1.724507405] Difference [1.258872541 2.402635349]  99% CI -150 to -10s [-1.035874608 0.302073304] 10 to 150s [1.121295723 1.806410863] Difference [1.07917438 2.582333509]  99.9% CI -150 to -10s [-1.221490155 0.487688851] 10 to 150s [1.026248658 1.901457927] Difference [0.87063883 2.79086906]	ns  ns  ns  Sig at 95%  Sig at 99%  Sig at 99.9%	N/A	N/A	N/A
	H	Two-Way RM ANOVA	Stimulation Period x Genotype F (2, 58) = 8.330 Stimulation Period F (1.884, 54.64) = 13.21 Genotype F (1, 29) = 14.81	p=0.0007***  p<0.0001****  p=0.0006***	Cre+ vs Cre- Pre-stimulation Stimulation Post-stimulation  Cre+	t=0.9168 t=4.68 t=5.192	p>0.9999 p=0.0007*** p=0.0002***

**Supplemental Table 1.** (continued)

					Pre stim vs. Stim Pre stim vs. Post stim Stim vs. Post stim	t=3.725 t=4.285 t=3.662	p=0.0153* p=0.0053** p=0.0172*
	I	Two-Tailed T-Test	Cre+ vs Cre- t=3.621, df=31	p=0.001**	N/A	N/A	N/A
<b>Supp Fig 4</b>	C	Mann- Whitney	Control vs FST	p=0.0286*	N/A	N/A	N/A
	G	Mann- Whitney	Control vs FST	p=0.0159*	N/A	N/A	N/A
<b>Supp Fig 6</b>	D	Two-Way RM ANOVA	Stimulation Period x Genotype F (1, 29) = 0.002860 Stimulation Period F (1, 29) = 0.04236 Genotype F (1, 29) = 1.790	p=0.9577 p=0.8384 p=0.1914	Cre+ Baseline vs 10Hz  Cre+ vs Cre- Baseline 10 Hz	t=0.1864  t=0.8956 t=0.9722	p>0.9999  p=0.7483 p=0.67
	F	Two-Tailed T-Test	Center t=1.175, df=19	p=0.254425	N/A	N/A	N/A
		Two-Tailed T-Test	Perimeter t=1.094, df=19	p=0.287443			
	G	Two-Tailed T-Test	Distance t=2.278, df=19	p=0.0345*	N/A	N/A	N/A
<b>Supp Fig 7</b>	A	Two-Way RM ANOVA	Day x Activity State F (3, 60) = 0.99 Day F (2.0, 41) = 1.2 Activity state F (1, 20) = 40	p=0.41 p=0.3 p=0.001**	N/A	N/A	N/A
	B	One-Way RM ANOVA	Day F (2.537, 25.37) = 3.042	p=0.0546	N/A	N/A	N/A

**Supplemental Table 1.** (continued)

7. Southwick S.M., Vythilingam M., Charney D.S.J.A.R.C.P. (2005) **The psychobiology of depression and resilience to stress: implications for prevention and treatment** :255–291
8. Penzo M.A., et al. (2015) **The paraventricular thalamus controls a central amygdala fear circuit** *Nature* **519**:455–9
9. Ma J., et al. (2021) **Divergent projections of the paraventricular nucleus of the thalamus mediate the selection of passive and active defensive behaviors** *Nat Neurosci* **24**:1429–1440
10. Ledoux J.E., Gorman J.M. (2001) **A call to action: Overcoming anxiety through active coping** *American Journal of Psychiatry* **158**:1953–1955
11. Steimer T (2011) **Animal models of anxiety disorders in rats and mice: some conceptual issues** *Dialogues Clin Neurosci* **13**:495–506
12. Gross C.T., Canteras N.S. (2012) **The many paths to fear** *Nat Rev Neurosci* **13**:651–8
13. Amorapanth P., LeDoux J.E., Nader K. (2000) **Different lateral amygdala outputs mediate reactions and actions elicited by a fear-arousing stimulus** *Nature Neuroscience* **3**:74–79
14. Canteras N.S., et al. (1997) **Severe reduction of rat defensive behavior to a predator by discrete hypothalamic chemical lesions** *Brain Res Bull* **44**:297–305
15. Pan W.X., McNaughton N. (2004) **The supramammillary area: its organization, functions and relationship to the hippocampus** *Prog Neurobiol* **74**:127–66
16. Vertes R.P., McKenna J.T. (2000) **Collateral projections from the supramammillary nucleus to the medial septum and hippocampus** *Synapse* **38**:281–293
17. Vertes R.P (1992) **Pha-L Analysis of Projections from the Supramammillary Nucleus in the Rat** *Journal of Comparative Neurology* **326**:595–622
18. Kiss J., et al. (2002) **Possible glutamatergic/aspartatergic projections to the supramammillary nucleus and their origins in the rat studied by selective [(3)H]D-aspartate labelling and immunocytochemistry** *Neuroscience* **111**:671–91
19. Kesner A.J., et al. (2021) **Supramammillary neurons projecting to the septum regulate dopamine and motivation for environmental interaction in mice** *Nat Commun* **12**
20. Li Y., et al. (2020) **Supramammillary nucleus synchronizes with dentate gyrus to regulate spatial memory retrieval through glutamate release** *Elife* **9**
21. Billwiller F., et al. (2020) **GABA-glutamate supramammillary neurons control theta and gamma oscillations in the dentate gyrus during paradoxical (REM) sleep** *Brain Struct Funct* **225**:2643–2668
22. Ito H.T., Moser E.I., Moser M.B. (2018) **Supramammillary Nucleus Modulates Spike-Time Coordination in the Prefrontal-Thalamo-Hippocampal Circuit during Navigation** *Neuron* **99**:576–587
23. Pedersen N.P., et al. (2017) **Supramammillary glutamate neurons are a key node of the arousal system** *Nature Communications* **8**



24. Leranath C., Kiss J. (1996) **A population of supramammillary area calretinin neurons terminating on medial septal area cholinergic and lateral septal area calbindin-containing cells are aspartate/glutamatergic** *J Neurosci* **16**:7699–710
25. Swanson L.J.B.r.b. (1982) **The projections of the ventral tegmental area and adjacent regions: a combined fluorescent retrograde tracer and immunofluorescence study in the rat** :321–353
26. Kocsis K., et al. (2003) **Location of putative glutamatergic neurons projecting to the medial preoptic area of the rat hypothalamus** *Brain Res Bull* **61**:459–68
27. Pan W.-X., McNaughton N.J.P.i.n (2004) **The supramammillary area: its organization, functions and relationship to the hippocampus** :127–166
28. Soussi R., et al. (2010) **Heterogeneity of the supramammillary-hippocampal pathways: Evidence for a unique GABAergic neurotransmitter phenotype and regional differences** :771–785
29. Haglund L., Swanson L.W., Kohler C. (1984) **The Projection of the Supramammillary Nucleus to the Hippocampal-Formation - an Immunohistochemical and Anterograde Transport Study with the Lectin Pha-L in the Rat** *Journal of Comparative Neurology* **229**:171–185
30. Hayakawa T., Ito H., Zyo K. (1993) **Neuroanatomical Study of Afferent-Projections to the Supramammillary Nucleus of the Rat** *Anatomy and Embryology* **188**:139–148
31. Hashimotodani Y., et al. (2018) **Supramammillary Nucleus Afferents to the Dentate Gyrus Co-release Glutamate and GABA and Potentiate Granule Cell Output** *Cell Rep* **25**:2704–2715
32. Park Y.G., et al. (2018) **Protection of tissue physicochemical properties using polyfunctional crosslinkers** *Nat Biotechnol*
33. Madisen L., et al. (2010) **A robust and high-throughput Cre reporting and characterization system for the whole mouse brain** *Nat Neurosci* **13**:133–40
34. Li Y., et al. (2020) **Supramammillary nucleus synchronizes with dentate gyrus to regulate spatial memory retrieval through glutamate release**
35. Wyss J., et al. (1979) **Evidence for an input to the molecular layer and the stratum granulosum of the dentate gyrus from the supramammillary region of the hypothalamus** :165–176
36. Hashimotodani Y., et al. (2018) **Supramammillary nucleus afferents to the dentate gyrus co-release glutamate and GABA and potentiate granule cell output** :2704–2715
37. Nakanishi K., Saito H., Abe K.J.E.J.o.N. (2001) **The supramammillary nucleus contributes to associative EPSP-spike potentiation in the rat dentate gyrus in vivo** :793–800
38. Maglóczy Z., Acsády L., Freund T.F.J.H. (1994) **Principal cells are the postsynaptic targets of supramammillary afferents in the hippocampus of the rat** :322–334
39. Day H.E., Masini C.V., Campeau S. (2004) **The pattern of brain c-fos mRNA induced by a component of fox odor, 2,5-dihydro-2,4,5-trimethylthiazoline (TMT), in rats, suggests both systemic and processive stress characteristics** *Brain Res* **1025**:139–51

40. Santin L.J., et al. (2003) , **c-Fos expression in supramammillary and medial mammillary nuclei following spatial reference and working memory tasks** *Physiol Behav* **78**:733–9
41. Azevedo E.P., et al. (2020) **A limbic circuit selectively links active escape to food suppression** *eLife* **9**
42. Farrell J.S., et al. (2021) **Supramammillary regulation of locomotion and hippocampal activity** *Science* **374**:1492–1496
43. De Boer S.F., Koolhaas J.M. (2003) **Defensive burying in rodents: ethology, neurobiology and psychopharmacology** *Eur J Pharmacol* **463**:145–61
44. Castro D.C., Terry R.A., Berridge K.C. (2016) **Orexin in Rostral Hotspot of Nucleus Accumbens Enhances Sucrose ‘Liking’ and Intake but Scopolamine in Caudal Shell Shifts ‘Liking’ Toward ‘Disgust’ and ‘Fear’** *Neuropsychopharmacology* **41**:2101–11
45. Reynolds S.M., Berridge K.C. (2001) **Fear and feeding in the nucleus accumbens shell: rostrocaudal segregation of GABA-elicited defensive behavior versus eating behavior** *J Neurosci* **21**:3261–70
46. Richard J.M., Berridge K.C. (2011) **Nucleus accumbens dopamine/glutamate interaction switches modes to generate desire versus dread: D(1) alone for appetitive eating but D(1) and D(2) together for fear** *J Neurosci* **31**:12866–79
47. Kalueff A.V., Tuohimaa P.J.B.R.P. (2004) **Grooming analysis algorithm for neurobehavioural stress research** :151–158
48. van Erp A.M., et al. (1994) **Effect of environmental stressors on time course, variability and form of self-grooming in the rat: handling, social contact, defeat, novelty, restraint and fur moistening** *Behav Brain Res* **65**:47–55
49. Kravitz A.V., Tye L.D., Kreitzer A.C. (2012) **Distinct roles for direct and indirect pathway striatal neurons in reinforcement** *Nat Neurosci* **15**:816–8
50. McCall J.G., et al. (2015) **CRH Engagement of the Locus Coeruleus Noradrenergic System Mediates Stress-Induced Anxiety** *Neuron* **87**:605–20
51. Felix-Ortiz A.C., et al. (2013) **BLA to vHPC inputs modulate anxiety-related behaviors** *Neuron* **79**:658–64
52. Jakovcevski M., Schachner M., Morellini F. (2011) **Susceptibility to the long-term anxiogenic effects of an acute stressor is mediated by the activation of the glucocorticoid receptors** *Neuropharmacology* **61**:1297–305
53. Bailey K.R., Crawley J.N., Buccafusco J.J. (2009) **Anxiety-Related Behaviors in Mice** *Methods of Behavior Analysis in Neuroscience*
54. Heredia L., et al. (2014) **Assessing anxiety in C57BL/6J mice: a pharmacological characterization of the open-field and light/dark tests** :108–114
55. Prut L., Belzung C.J.E.j.o.p. (2003) **The open field as a paradigm to measure the effects of drugs on anxiety-like behaviors: a review** :3–33

56. Chaouloff F., Durand M., Mormède P.J.B.b.r. (1997) **Anxiety-and activity-related effects of diazepam and chlordiazepoxide in the rat light/dark and dark/light tests** :27–35
57. Mobbs D., et al. (2015) **The ecology of human fear: survival optimization and the nervous system**
58. Fadok J.P., et al. (2017) **A competitive inhibitory circuit for selection of active and passive fear responses** *Nature* **542**:96–100
59. Parker K.E., et al. (2019) **A Paranigral VTA Nociceptin Circuit that Constrains Motivation for Reward** *Cell* **178**:653–671
60. Costa A.P., et al. (2013) **A proposal for refining the forced swim test in Swiss mice** *Prog Neuropsychopharmacol Biol Psychiatry* **45**:150–5
61. Commons K.G., et al. (2017) **The Rodent Forced Swim Test Measures Stress-Coping Strategy, Not Depression-like Behavior** *ACS Chem Neurosci* **8**:955–960
62. Hu Y., et al. (2022) **LabGym: quantification of user-defined animal behaviors using learning-based holistic assessment**
63. Seo C., et al. (2019) **Intense threat switches dorsal raphe serotonin neurons to a paradoxical operational mode** :538–542
64. Chen S., et al. (2020) **A hypothalamic novelty signal modulates hippocampal memory** *Nature* **586**:270–274
65. Andalman A.S., et al. (2019) **Neuronal Dynamics Regulating Brain and Behavioral State Transitions** *Cell* **177**:970–985
66. Berton O., et al. (2007) **Induction of deltaFosB in the periaqueductal gray by stress promotes active coping responses** *Neuron* **55**:289–300
67. Tovote P., et al. (2016) **Midbrain circuits for defensive behaviour** *Nature* **534**:206–12
68. Keay K.A., Bandler R. (2001) **Parallel circuits mediating distinct emotional coping reactions to different types of stress** *Neurosci Biobehav Rev* **25**:669–78
69. Lee A., et al. (2010) **The habenula prevents helpless behavior in larval zebrafish** *Curr Biol* **20**:2211–6
70. Li B., et al. (2011) **Synaptic potentiation onto habenula neurons in the learned helplessness model of depression** *Nature* **470**:535–9
71. Lazaridis I., et al. (2019) **A hypothalamus-habenula circuit controls aversion** *Molecular Psychiatry* **24**:1351–1368
72. Mondoloni S., Mameli M., Congiu M.J.T.P. (2022) **Reward and aversion encoding in the lateral habenula for innate and learned behaviours** *Translational Psychiatry* **12**
73. Keay K.A., Bandler R. (2001) **Parallel circuits mediating distinct emotional coping reactions to different types of stress** *Neuroscience and Biobehavioral Reviews* **25**:669–678

74. Cryan J.F., Valentino R.J., Lucki I. (2005) **Assessing substrates underlying the behavioral effects of antidepressants using the modified rat forced swimming test** *Neurosci Biobehav Rev* **29**:547–69
75. Knoll A.T., Carlezon W.A.J.B.r. (2010) **Dynorphin, stress, and depression** :56–73
76. Ebner K., Singewald N.J.C.O.i.B.S. (2017) **Individual differences in stress susceptibility and stress inhibitory mechanisms** :54–64
77. Vong L., et al. (2011) **Leptin action on GABAergic neurons prevents obesity and reduces inhibitory tone to POMC neurons** *Neuron* **71**:142–54
78. Norris A.J., et al. (2021) **Parabrachial opioidergic projections to preoptic hypothalamus mediate behavioral and physiological thermal defenses** *Elife* **10**
79. McCall J.G., et al. (2015) **CRH Engagement of the Locus Coeruleus Noradrenergic System Mediates Stress-Induced Anxiety** *Neuron* **87**:605–620
80. Sparta D.R., et al. (2011) **Construction of implantable optical fibers for long-term optogenetic manipulation of neural circuits** *Nat Protoc* **7**:12–23
81. Fenno L.E., et al. (2014) **Targeting cells with single vectors using multiple-feature Boolean logic** *Nat Methods* **11**:763–72
82. Back S., et al. (2019) **Neuron-Specific Genome Modification in the Adult Rat Brain Using CRISPR-Cas9 Transgenic Rats** *Neuron* **102**:105–119
83. Lee J.H., et al. (2010) **Global and local fMRI signals driven by neurons defined optogenetically by type and wiring** *Nature* **465**:788–92
84. Paxinos G., Franklin K.B. (2019) **Paxinos and Franklin's the mouse brain in stereotaxic coordinates**
85. Porsolt R.D., et al. (1979) **Immobility induced by forced swimming in rats: effects of agents which modify central catecholamine and serotonin activity** *Eur J Pharmacol* **57**:201–10
86. Dana H., et al. (2019) **High-performance calcium sensors for imaging activity in neuronal populations and microcompartments** *Nat Methods* **16**:649–657
87. Martianova E., Aronson S., Proulx C.D. (2019) **Multi-Fiber Photometry to Record Neural Activity in Freely-Moving Animals** *J Vis Exp* **152**
88. Nyffeler M., Vetter R.S. (2018) **Black widow spiders, *Latrodectus* spp. (Araneae: Theridiidae), and other spiders feeding on mammals** *The Journal of Arachnology* **46**:541–548
89. Stamatakis A.M., Stuber G.D. (2012) **Activation of lateral habenula inputs to the ventral midbrain promotes behavioral avoidance** *Nat Neurosci* **15**:1105–7
90. Luskin A.T., et al. (2021) **Extended amygdala-parabrachial circuits alter threat assessment and regulate feeding** *Sci Adv* **7**
91. Richardson N.R., Roberts D.C. (1996) **Progressive ratio schedules in drug self-administration studies in rats: a method to evaluate reinforcing efficacy** *J Neurosci Methods* **66**:1–11

## Article and author information

### **Abraham Escobedo**

Department of Anesthesiology, Washington University in St. Louis, St. Louis, MO

### **Salli-Ann Holloway**

Department of Anesthesiology, Washington University in St. Louis, St. Louis, MO

### **Megan Votoupal**

Department of Medicine, Northwestern University Feinberg School of Medicine, Chicago IL

### **Aaron L Cone**

Department of Anesthesiology, Washington University in St. Louis, St. Louis, MO

### **Hannah E Skelton**

Department of Anesthesiology, Washington University in St. Louis, St. Louis, MO

### **Alex A. Legaria**

Department of Neuroscience, Washington University in St. Louis, St. Louis, MO, Department of Psychiatry, Washington University in St. Louis, St. Louis, MO

ORCID iD: [0000-0002-3722-6666](https://orcid.org/0000-0002-3722-6666)

### **Imeh Ndiokho**

Medical College of Wisconsin, Milwaukee WI

### **Tasheia Floyd**

Department of Obstetrics and Gynecology, Washington University in St. Louis, St. Louis, MO

### **Alexxai V. Kravitz**

Department of Anesthesiology, Washington University in St. Louis, St. Louis, MO, Department of Neuroscience, Washington University in St. Louis, St. Louis, MO, Department of Psychiatry, Washington University in St. Louis, St. Louis, MO

ORCID iD: [0000-0001-5983-0218](https://orcid.org/0000-0001-5983-0218)

### **Michael R. Bruchas**

Center for Neurobiology of Addiction, Pain, and Emotion University of Washington, Seattle, WA, Department of Anesthesiology and Pain Medicine University of Washington, Seattle, WA, Department of Pharmacology University of Washington, Seattle, WA, Department of Bioengineering University of Washington, Seattle, WA

**For correspondence:** [mbruchas@uw.edu](mailto:mbruchas@uw.edu)

ORCID iD: [0000-0003-4713-7816](https://orcid.org/0000-0003-4713-7816)

### **Aaron J. Norris**

Department of Anesthesiology, Washington University in St. Louis, St. Louis, MO

**For correspondence:** [norris@wustl.edu](mailto:norris@wustl.edu)

ORCID iD: [0000-0001-7825-1756](https://orcid.org/0000-0001-7825-1756)



## Copyright

© 2023, Escobedo et al.

This article is distributed under the terms of the [Creative Commons Attribution License](#), which permits unrestricted use and redistribution provided that the original author and source are credited.

## Editors

Reviewing Editor

**Laura Bradfield**

University of Technology Sydney, Sydney, Australia

Senior Editor

**Kate Wassum**

University of California, Los Angeles, Los Angeles, United States of America

## Joint Public Review:

Summary:

This important manuscript investigates a subpopulation of glutamatergic neurons in the supramammillary nucleus that projects to the pre-optic hypothalamus area (SuM-VGLUT2+::POA). First, they define the neural circuitry of these neurons, which contact many stress/threat-associated brain regions. Then they employ fibre photometry to measure the activity of these neurons during various threatening tasks and find the responses correlate well with threat stimuli. Finally, they stimulate these neurons and find multiple lines of evidence that mice find this aversive and will act to avoid receiving this stimulation. In sum, they provide solid evidence that this neuronal population represents a new node in stress response circuitry that allows the animal to produce flexible behaviours in response to stress, which will be of interest to neuroscientists across several sub-fields.

Strengths:

Overall this is a solid manuscript tackling an important question. Coping with stress by an animal in danger is essential for survival. This manuscript identifies a novel population of neurons in the murine supramammillary nucleus (SuM) projecting to the pre-optic hypothalamus area among other regions that is involved in this important process. The evidence to support the conclusions is solid.

Specific strengths:

- The topic is novel.
- The manuscript follows a logical structure and neatly moves through the central story. Several potential alternate interpretations are well-controlled for.
- The manuscript employs an array of different tasks to provide converging evidence for their conclusions.
- The authors provide excellent evidence of the specificity of the function of this neuronal population, both from anatomical studies and from behavioural studies (e.g. demonstrating that activity of gabaergic neurons in the same region does not correlate with behaviours in the same way).

- The study is well-powered (sample sizes are good) and the effects are convincing.

#### Weaknesses:

\* Not all of the reviewer comments were addressed in the manuscript itself, although this was acknowledged in the author's responses to reviewers. One key example is as follows:

\* The authors did not entirely address comments related to rigor but they at least acknowledged it. For example, in multiple places they argue that WT, purchased mice are probably not different in baseline behavior compared to Vglut2-IRES-Cre because it is unlikely that adding the IRES-Cre will change behavior. However, they do not acknowledge that transgenic lines are not from the exact same genetic background and generation number, and there is ample evidence in the literature that transgenic mice on a B6J background can differ in basal phenotypes from one another and B6J. In one place they show some basal behavior, at least in heat map form though not quantified. Had the authors decided to apply this more pervasively, it would have made the story even more compelling in terms of a stress/threat-induced phenotype.

#### Comments on revised version from the Reviewing Editor:

The authors have done a thorough job of answering the reviewer queries, and a good job of explaining why they have not answered a particular point. Indeed, there is so much additional information in response to the reviewers that I hope readers of the manuscript will read the reviews and responses as well! I think they add a lot.

<https://doi.org/10.7554/eLife.90972.2.sa0>

### Author Response

The following is the authors' response to the original reviews.

We would like to thank the reviewers for their insightful comments and recommendations. We have extensively revised the manuscript in response to the valuable feedback. We believe the results is a more rigorous and thoughtful analysis of the data. Furthermore, our interpretation and discussion of the findings is more focused and highlights the importance of the circuit and its role in the response to stress. Thank you for helping to improve the presented science.

Key changes made in response to the reviewers comments include:

- Revision of statistical analyses for nearly all figures, with the addition of a new table of summary statistics to include F and/or t values alongside p-values.
- Addition of statistical analyses for all fiber photometry data.
- Examination of data for possible sex dependent effects.
- Clarification of breeding strategies and genotype differences, with added details to methods to improve clarity.
- Addressing concerns about the specificity of virus injections and the spread, with additional details added to methods.
- Modification of terminology related to goal-directed behavior based on reviewer feedback, including removal of the term from the manuscript.

- Clarification and additional data on the use of photostimulation and its effects, including efforts to inactivate neurons for further insight, despite technical challenges.
- Correction of grammatical errors throughout the manuscript.

**Reviewer 1:**

*Despite the manuscript being generally well-written and easy to follow, there are several grammatical errors throughout that need to be addressed.*

Thank you for highlighting this issue. Grammatical errors have been fixed in the revised version of the manuscript.

*Only p values are given in the text to support statistical differences. This is not sufficient. F and/or t values should be given as well.*

In response to this critique and similar comments from Reviewer 2, we re-evaluated our approach to statistical analyses and extensively revised analyses for nearly all figures. We also added a new table of summary statistics (Supplemental Table 1) containing the type of analysis, statistic, comparison, multiple comparisons, and p value(s). For Figures 4C-E, 5C, 6C-E, 7H-I, and 8H we analyzed these data using two-way repeated measures (RM) ANOVA that examined the main effect of time (either number of sessions or stimulation period) in the same animal and compared that to the main effect of genotype of the animal (Cre+ vs Cre-), and if there was an interaction. For Supplemental Figure 7A we also conducted a two-way RM ANOVA with time as a factor and activity state (number of port activations in active vs inactive nose port) as the other in Cre+ mice. For Figures 5D-E we conducted a two-way mixed model ANOVA that accounted and corrected for missing data. In figures that only compared two groups of data (Figures 5F-L, 6F, 8C-D, 8I, and Supp 6F-G) we used two-tailed t-test for the analysis. If our question and/or hypothesis required us to conduct multiple comparisons between or within treatments, we conducted Bonferroni's multiple comparisons test for post hoc analysis (we note which groups we compared in Supplemental Table 1). For figures that did or did not show a change in calcium activity (Figure 3G, 3I-K, 7B, 7D-E, 8E-F), we compared waveform confidence intervals (Jean-Richard-Dit-Bressel, Clifford, McNally, 2020). The time windows we used as comparison are noted in Supplemental Table 1, and if the comparisons were significant at 95%, 99%, and 99.9% thresholds.

None of prior comparisons in prior analyses that were significant were found to have fallen below threshold for significance. Of those found to be not significantly different, only one change was noted. In Figure 6E there was now a significant baseline difference between Cre+ and Cre- mice with Cre- mice taking longer to first engage the port compared to Cre+ mice ( $p=0.045$ ). Although the more rigorous approach the statistical analyses did not change our interpretations we feel the enhanced the paper and thank the reviewer for pushing this improvement.

*Moreover, the fibre photometry data does not appear to have any statistical analyses reported - only confidence intervals represented in the figures without any mention of whether the null hypothesis that the elevations in activity observed are different from the baseline.*

*This is particularly important where there is ambiguity, such as in Figure 3K, where the spontaneous activity of the animal appears to correlate with a spike in activity but the text mentions that there is no such difference. Without statistics, this is difficult to judge.*

Thank you for highlighting this critical point and providing an opportunity to strengthen our manuscript. We added statistical analyses of all fiber photometry data using a recently

described approach based on waveform confidence intervals (Jean-Richard-Dit-Bressel, Clifford, McNally, 2020). In the statistical summary (Supplemental Table 1) we note the time window that we used for comparison in each analysis and if the comparisons were significant at 95%, 99%, and 99.9% thresholds. Thank you from highlighting this and helping make the manuscript stronger.

With respect to Figure 3K, we are not certain we understood the spike in activity the reviewer referred to. Figure 3J and K include both velocity data (gold) and Ca<sup>2+</sup> dependent signal (blue). We used episodes of velocity that were comparable to the avoidance respond during the ambush test and no significant differences in the Ca<sup>2+</sup> signal when gating around changes in velocity in the absence of stressor (Supplemental Table1). This is in contrast to the significant change in Ca<sup>2+</sup> signal following a mock predator ambush (Figure 3J). We interpret these data together to indicate that locomotion does not correlate with an increase in calcium activity in SuMVGLUT2<sup>+</sup>::POA neurons, but that coping to a stressor does. This conclusion is further examined in supplemental Figure 5, including examining cross-correlation to test for temporally offset relationship between velocity and Ca<sup>2+</sup> signal in SUMVGLUT2<sup>+</sup>::POA neurons.

*The use of photostimulation only is unfortunate, it would have been really nice to see some inactivation of these neurons as well. This is because of the well-documented issues with being able to determine whether photostimulation is occurring in a physiological manner, and therefore makes certain data difficult to interpret. For instance, with regards to the 'active coping' behaviours - is this really the correct characterisation of what's going on? I wonder if the mice simply had developed immobile responding as a coping strategy but when they experience stimulation of these neurons that they find aversive, immobility is not sufficient to deal with the summative effects of the aversion from the swimming task as well as from the neuronal activation? An inactivation study would be more convincing.*

We agree with the point of the reviewer, experiments demonstrating necessity of SUMVGLUT2<sup>+</sup>::POA neurons would have added to the story here. We carried out multiple experiments aimed at addressing questions about necessity of SuMVGLUT2<sup>+</sup>::POA neurons in stress coping behaviors, specifically the forced swim assay. Efforts included employing chemogenetic, optogenetic, and tetanus toxin-based methods. We observed no effects on locomotor activity or stress coping. These experiments are both technically difficult and challenging to interpret. Interpretation of negative results, as we obtained, is particularly difficult because of potential technical confounds. Selective targeting of SuMVGLUT2<sup>+</sup>::POA neurons for inhibition requires a process requiring three viral injections and two recombination steps, increasing variability and reducing the number of neurons impacted. Alternatively, photoinhibition targeting SuMVGLUT2<sup>+</sup>::POA cells can be done using Retro-AAV injected into POA and a fiber implant over SuM. We tried both approaches. Data obtained were difficult to interpret because of questions about adequate coverage of SuMVGLUT2<sup>+</sup>::POA population by virally expressed constructs and/or light spread arose. The challenge of adequate coverage to effectively prevent output from the targeted population is further confounded by challenges inherent in neural inhibition, specifically determining if the inhibition created at the cellular level is adequate to block output in the context of excitatory inputs or if neurons must be first engaged in a particular manner for inhibition to be effective. Baseline neural activity, release probability, and post-synaptic effects could all be relevant, which photo-inhibition will potentially not resolve. So, while the trend is to always show “necessary and sufficient” effects, we’ve tried nearly everything, and we simply cannot conclude much from our mixed results. There are also well-established problems with existing photo-inhibition methods, which while people use them and tout them, are often ignored. We have a lot of expertise in photo-inhibition optogenetics, and indeed have used it with some success, developed new methods, yet in this particular case we are unable to draw

conclusions related to inhibition. People have experienced similar challenges in locus coeruleus neurons, which have very low basal activity, and inhibition with chemogenetics is very hard, as well as with optogenetic pump-based approaches, because the neurons fire robust rebound APs. We have spent almost 2.5 years trying to get this to work in this circuit because reviews have been insistent on this result for the paper to be conclusive. Unfortunately, it simply isn't possible in our view until we know more about the cell types involved. This is all in spite of experience using the approach in many other publications.

We also employed less selective approaches, such as injecting AAV-DIO-tetanus toxin light chain (Tettox) constructs directly into SuM VGLUT2-Cre mice but found off target effects impacting animal wellbeing and impeding behavioral testing due viral spread to surrounding areas.

While we are disappointed for being unable to directly address questions about necessity of SuMVGLUT2<sup>+</sup>::POA neurons in active coping with experimental data, we were unable to obtain results allowing for clear interpretation across numerous other domains the reviewers requested. We also feel strongly that until we have a clear picture of the molecular cell type architecture in the SuM, and Cre-drivers to target subsets of neurons, this question will be difficult to resolve for any group. We are working now on RNAseq and related spatial transcriptomics efforts in the SuM and examining additional behavioral paradigm to resolve these issues, so stay tuned for future publications.

Accordingly, we avoid making statements relating to necessity in the manuscript. In spite of having several lines of physiological data with strong robust correlations behavior related to the SuMVGLUT2<sup>+</sup>::POA circuit.

*Nose poke is only nominally instrumental as it cannot be shown to have a unique relationship with the outcome that is independent of the stimuli-outcome relationships (in the same way that a lever press can, for example). Moreover, there is nothing here to show that the behaviours are goal-directed.*

Thank you for highlighting this point. Regarding goal-direct terminology, we removed this terminology from the manuscript. Since the mice perform highly selective (active vs inactive) port activation robustly across multiple days of training the behavior likely transitions to habitual behavior. We only tested the valuation of stimuli termination of the final day of training with time limited progressive ratio test. With respect to lever press versus active port activation, we are unclear how using a lever in this context would offer a different interpretation. Lever pressing may be more sensitive to changes in valuation when compared to nose poke port activation (Atalayer and Rowland 2008); however, in this study the focus of the operant behavior is separating innate behaviors for learned action–outcome instrumental learned behaviors for threat response (LeDoux and Daw 2018). The robust highly selective activation of the active port illustrated in Figure 6 fits as an action–outcome instrumental behavior wherein mice learn to engage the active but not inactive port to terminate photostimulation. The first activation of the port occurs through exploration of the arena but as demonstrated by the number of active port activations and the decline in time of the first active port engagement, mice expressing ChR2eYFP learn to engage the port to terminate the stimulation. To aid in illustrating this point we have added Supplemental Figure 7 showing active and inactive port activations for both Cre<sup>+</sup> and Cre<sup>-</sup> mice. This adds clarity to high rate of selective port activation driven by stimulation of SUMVGLUT2<sup>+</sup>::POA neurons compared to controls. The elimination of goal directed and providing additional data narrows and supports one of the key points of the operant experiment.

*With regards to Figure 1: This is a nice figure, but I wonder if some quantification of the pathways and their density might be helpful, perhaps by measuring the intensity of fluorescence in image J (as these are processes, not cell bodies that can be counted)?*



*Mind you, they all look pretty dense so perhaps this is not necessary! However, because the authors are looking at projections in so-called 'stress-engaged regions', the amygdala seems conspicuous by its absence. Did the authors look in the amygdala and find no projections? If so it seems that this would be worth noting.*

This is an interesting question but has proven to be a very technically challenging question. We consulted with several leaders who routinely use complimentary viral tracing methods in the field. We were unable to devise a method to provide a satisfactorily meaningful quantitative (as opposed to qualitative) approach to compare SUMVGLUT2+::POA to SuMVGLUT2+ projections. A few limitations are present that hinder a meaningful quantitative approach. One limitation was the need for different viral strategies to label the two populations. Labeling SuMVGLUT2+::POA neurons requires using VGLUT2-Flp mice with two injections into the POA and one into SuM. Two recombinase steps were required, reducing efficiency of overlap. This combination of viral injections, particularly the injections of RetroAAVs in the POA, can induce significant quantitative variability due to tropism, efficacy, and variability of retro-viral methods, and viral infection generally. These issues are often totally ignored in similar studies across the “neural circuit” landscape, but it doesn’t make them less relevant here.

Although people do this in the field, and show quantification, we actually believe that it can be a quite misleading read-out of functionally relevant circuitry, given that neurotransmitter release ultimately is amplified by receptors post-synaptically, and many examples of robust behavioral effects have been observed with low fiber tracing complimentary methods (McCall, Siuda et al. 2017). In contrast, the broader SuMVGLUT2+ population was labeled using a single injection into the SuM. This means there like more efficient expression of the fluorophore. Additionally, in areas that contain terminals and passing fibers understanding and interpreting fluorescent signal is challenging. Together, these factors limit a meaningful quantitative comparison and make an interpretation difficult to make. In this context, we focused on a conservative qualitative presentation to demonstrate two central points. That 1) SuMVGLUT2+::POA neurons are subset of SuMVGLUT2+ neurons that project to specific areas and that exclude dentate gyrus, and they 2) arborize extensively to multiple areas which have be linked to threat responses. We agree that there is much to be learned about how different populations in SuM connect to targets in different regions of the brain and to continue to examine this question with different techniques. A meaningful quantitative study comparing projections is technically complex and, we feel, beyond our ability for this study.

Also, for the reasons above we do not believe that quantification provides exceptional clarity with respect to the putative function of the circuit, glutamate released, or other cotransmitters given known amplification at the post-synaptic side of the circuit.

With regard to the amygdala, other studies on SuM projections have found efferent projections to amygdala (Ottersen, 1980; Vertes, 1992). In our study we were unable to definitively determine projections from SuMVGLUT2+::POA neurons to amygdala, which if present are not particularly dense. For this reason we were conservative and do not comment on this particular structure.

*I would suggest removing the term goal-directed from the manuscript and just focusing on the active vs. passive distinction.*

We removed the use of goal-directed. Thank you for helping us clarify our terminology.

*The effect observed in Figure 7I is interesting, and I'm wondering if a rebound effect is the most likely explanation for this. Did the authors inhibit the VGAT neurons in this region at any other times and observe a similar rebound? If such a rebound was not*

*observed it would suggest that it is something specific about this task that is producing the behaviour. I would like it if the authors could comment on this.*

We agree that results showing the change in coping strategy (passive to active) in forced swim after but not during stimulation of SuMVGAT+ neurons is quite interesting (Figure 7I). This experiment activated SuMVGAT+ neurons during a section of the forced swim assay and mice showed a robust shift to mobility after the stimulation of SuMVGAT+ neurons stopped. We did not carry out inhibition of SuMVGAT+ neurons in this manuscript. As the reviewer suggested, strong inhibition of local SuM neurons, including SUMVGLUT2+::POA neurons, could lead to rebound activity that may shift coping behaviors in confusing ways. We agree this is an interesting idea but do not have data to support the hypothesis further at this time.

## **Reviewer 2**

*(1) These are very difficult, small brain regions to hit, and it is commendable to take on the circuit under investigation here. However, there is no evidence throughout the manuscript that the authors are reliably hitting the targets and the spread is comparable across experiments, groups, etc., decreasing the significance of the current findings. There are no hit/virus spread maps presented for any data, and the representative images are cropped to avoid showing the brain regions lateral and dorsal to the target regions. In images where you can see the adjacent regions, there appears expression of cell bodies (such as Supp 6B), suggesting a lack of SuM specificity to the injections.*

We agree with the reviewer that the areas studied are small and technically challenging to hit. This was one of driving motivations for using multiple tools in tandem to restrict the area targeted for stimulation. Approaches included using a retrograde AAVs to express ChR2eYFP in SUMVGLUT2+::POA neurons; thereby, restricting expression to VGLUT2+ neurons that project to the POA. Targeting was further limited by placement of the optic fiber over cell bodies on SuM. Thus, only neurons that are VGLUT2+, project to the POA, and were close enough to the fiber were active by photostimulation. Regrettably, we were not able to compile images from mice where the fiber was misplaced leading to loss of behavioral effects. We would have liked to provide that here to address this comment. Unfortunately, generating heat maps for injections is not possible for anatomic studies that use unlabeled recombinase as part of an intersectional approach. Also determining the point of injection of a retroAAV can be difficult to accurately determine its location because neurons remote to injection site and their processes are labeled.

Experiments described in Supplemental Figure 6B on VGAT neurons in SuM were designed and interpreted to support the point that SUMVGLUT2+::POA neurons are a distinct population that does not overlap with GABAergic neurons. For this point it is important that we targeted SuM, but highly confined targeting is not needed to support the central interpretation of the data. We do see labeling in SuM in VGAT-Cre mice but photo stimulation of SuMVGAT+ neurons does not generate the behavioral changes seen with activation of SUMVGLUT2+::POA neurons. As the reviewer points out, SuM is small target and viral injection is likely to spread beyond the anatomic boundaries to other VGAT+ neurons in the region, which are not the focus here. The activation would be restricted by the spread of light from the fiber over SuM (estimated to be about a 200um sphere in all directions). We did not further examine projections or localization of VGAT+ neurons in this study but focused on the differential behavioral effects of SUMVGLUT2+::POA neurons.

*(2) In addition, the whole brain tracing is very valuable, but there is very little quantification of the tracing. As the tracing is the first several figures and supp figure and the basis for the interpretation of the behavior results, it is important to understand things including how robust the POA projection is compared to the collateral regions,*

*etc. Just a rep image for each of the first two figures is insufficient, especially given the above issue raised. The combination of validation of the restricted expression of viruses, rep images, and quantified tracing would add rigor that made the behavioral effects have more significance.*

*For example, in Fig 2, how can one be sure that the nature of the difference between the nonspecific anterograde glutamate neuron tracing and the Sum-POA glutamate neuron tracing is real when there is no quantification or validation of the hits and expression, nor any quantification showing the effects replicate across mice? It could be due to many factors, such as the spread up the tract of the injection in the nonspecific experiment resulting in the labeling of additional regions, etc.*

*Relatedly, in Supp 4, why isn't C normalized to DAPI, which they show, or area? Similar for G what is the mcherry coverage/expression, and why isn't Fos normalized to that?*

Thank you for highlighting the importance of anatomy and the value of anatomy. Two points based on the anatomic studies are central to our interpretation of the experimental data. First, SUMVGLUT2<sup>+</sup>::POA are a distinct population within the SuM. We show this by demonstrating they are not GABAergic and that they do not project to dentate gyrus. Projections from SuM to dentate gyrus have been described in multiple studies (Boulland et al., 2009; Haglund et al., 1987; Hashimoto et al., 2018; Vertes, 1992) and we demonstrate them here for SUMVGLUT2<sup>+</sup> cells. Using an intersectional approach in VGLUT2-Flp mice we show SUMVGLUT2<sup>+</sup>::POA neurons do not project to dentate gyrus. We show cell bodies of SUMVGLUT2<sup>+</sup>::POA neurons located in SuM across multiple figures including clear brain images. Thus, SUMVGLUT2<sup>+</sup>::POA neurons are SuM neurons that do not project to dentate gyrus, are not GABAergic, send projections to a distinct subset of targets, most notably excluding dentate gyrus. Second, SUMVGLUT2<sup>+</sup>::POA neurons arborize sending projections to multiple regions. We show this using a combinatorial genetic and viral approach to restrict expression of eYFP to only neurons that are in SuM (based on viral injection), project to the POA (based on retrograde AAV injection in POA), and VGLUT2<sup>+</sup> (VGLUT2-Flp mice). Thus, any eYFP labeled projection comes from SUMVGLUT2<sup>+</sup>::POA neurons. We further confirmed projections using retroAAV injection into areas identified using anterograde approaches (Supplemental Figure 2). As discussed above in replies to Reviewer 1, we feel limitations are present that preclude meaningful quantitative analysis. We thus opted for a conservative interpretation as outlined.

Prior studies have shown efferent projections from SuM to many areas, and projections to dentate gyrus have received substantial attention (Boulland et al., 2009; Haglund, Swanson, and Kohler, 1984; Hashimoto et al., 2018; Soussi et al., 2010; Vertes, 1992; Pan and McNaughton, 2004). We saw many of the same projections from SUMVGLUT2<sup>+</sup> neurons. We found no projections from SUMVGLUT2<sup>+</sup>::POA neurons to dentate gyrus (Figure 2). Our description of SuM projection to dentate gyrus is not new but finding a population of neurons in SuM that does not project to dentate gyrus but does project to other regions in hippocampus is new. This finding cannot be explained by spread of the virus in the tract or non-selective labeling.

*(3) The authors state that they use male and female mice, but they do not describe the n's for each experiment or address sex as a biological variable in the design here. As there are baseline sex differences in locomotion, stress responses, etc., these could easily factor into behavioral effects observed here.*

Sex specific effects are possible; however, the studies presented here were not designed or powered to directly examine them. A point about experimental design that helps mitigate against strong sex dependent effect is that often the paradigm we used examined baseline (pre-stimulation) behavior, how behavior changed during stimulation, and how behavior

returned (or not) to baseline after stimulation. Thus, we test changes in individual behaviors. Although we had limited statistical power, we conducted analyses to examine the effects of sex as variable in the experiments and found no differences among males and females.

*(4) In a similar vein as the above, the authors appear to use mice of different genotypes (however the exact genotypes and breeding strategy are not described) for their circuit manipulation studies without first validating that baseline behavioral expression, habituation, stress responses are not different. Therefore, it is unclear how to interpret the behavioral effects of circuit manipulation. For example in 7H, what would the VGLUT2-Cre mouse with control virus look like over time? Time is a confound for these behaviors, as mice often habituate to the task, and this varies from genotype to genotype. In Fig 8H, it looks like there may be some baseline differences between genotypes- what is normal food consumption like in these mice compared to each other? Do Cre+ mice just locomote and/or eat less? This issue exists across the figures and is related to issues of statistics, potential genotype differences, and other experimental design issues as described, as well as the question about the possibility of a general locomotor difference (vs only stress-induced). In addition, the authors use a control virus for the control groups in VGAT-Cre manipulation studies but do not explain the reasoning for the difference in approach.*

Thank you for highlighting the need for greater clarity about the breeding strategies used and for these related questions. We address the breeding strategy and then move to address the additional concerns raised. We have added details to the methods section to address this point. For VGLUT2-Cre mice we use litter mates controls from Cre/WT x WT/WT cross. The VGLUT2-Cre line (RRID:IMSR\_JAX:028863) (Vong L, et al. 2011) used here been used in many other reports. We are not aware of any reports indicating a phenotype associated with the addition of the IRES-Cre to the Slc17a6 loci and there is no expected impact of expression of VGLUT2. Also, we see in many of the experiments here that the baseline (Figures 4, 5, and 7) behaviors are not different between the Cre+ and Cre- mice. For VGAT-Cre mice we used a different breeding strategy that allowed us to achieve greater control of the composition of litters and more efficient cohorts cohort. A Cre/Cre x WT/WT cross yielded all Cre/WT litters. The AAV injected, Chr2eYFP or eYFP, allowed us to balance the cohort.

Regarding Figure 7H, which shows time immobile on the second day of a swim test, data from the Cre- mice demonstrate the natural course of progression during the second day of the test. The control mice in the VGAT-Cre cohort (Figure 7I) have similar trend. The change in behavior during the stimulation period in the Cre+ mice is caused by the activation of SUMVGLUT2+::POA neurons. The behavioral shift largely, but not completely, returns to baseline when the photostimulation stops. We have no reason to believe a VGLUT2-Cre+ mouse injected with control AAV to express eYFP would be different from WT littermate injected with AAV expressing Chr2eYFP in a Cre dependent manner.

Turning to concerns related to 8H, which shows data from fasted mice quantify time spent interacting with food pellet immediately after presentation of a chow pellet, we found no significant difference between the control and Cre+ mice. We unaware of any evidence indicating that the two groups should have a different baseline since the Cre insertion is not expected to alter gene expression and we are unaware of reports of a phenotype relating to feeding and the presence of the transgene in this mouse line. Even if there were a small baseline shift this would not explain the large abrupt shift induced by the photostimulation. As noted above, we saw shifts in behavior abruptly induced by the initiation of photostimulation when compared to baseline in multiple experiments. This shift would not be explained by a hypothetical difference in the baseline behaviors of litter mates.

*(5) The statistics used throughout are inappropriate. The authors use serial Mann-Whitney U tests without a description of data distributions within and across groups.*

*Further, they do not use any overall F tests even though most of the data are presented with more than two bars on the same graph. Stats should be employed according to how the data are presented together on a graph. For example, stats for pre-stim, stim, and post-stim behavior X between Cre+ and Cre- groups should employ something like a two-way repeated measures ANOVA, with post-hoc comparisons following up on those effects and interactions. There are many instances in which one group changes over time or there could be overall main effects of genotype. Not only is serially using Mann-Whitney tests within the same panel misleading and statistically inaccurate, but it cherry-picks the comparisons to be made to avoid more complex results. It is difficult to comprehend the effects of the manipulations presented without more careful consideration of the appropriate options for statistical analysis.*

We thank the reviewer for pointing this out and suggesting alternative analyses, we agree with the assessment on this topic. Therefore, we have extensively revised the statistical approach to our data using the suggested approach. Reviewer 1 also made a similar comment, and we would like to point to our reply to reviewer 1's second point in regard to what we changed and added to the new statistical analyses. Further, we have added a full table detailing the statistical values for each figure to the paper.

*Conceptual:*

*(6) What does the signal look like at the terminals in the POA? Any suggestion from the data that the projection to the POA is important?*

This is an interesting question that we will pursue in future investigations into the roles of the POA. We used the projection to the POA from SuM to identify a subpopulation in SuM and we were surprised to find the extensive arborization of these neurons to many areas associated with threat responses. We focused on the cell bodies as “hubs” with many “spokes”. Extensive studies are needed to understand the roles of individual projections and their targets. There is also the hypothetical technical challenge of manipulating one projection without activating retrograde propagation of action potentials to the soma. At the current time we have no specific insights into the roles of the isolated projection to POA. Interpretation of experiments activating only “spoke” of the hub would be challenging. Simple terminal stimulation experiments are challenged by the need to separate POA projections from activation of passing fibers targeting more anterior structures of the accumbens and septum.

*(7) Is this distinguishing active coping behavior without a locomotor phenotype? For example, Fig. 5I and other figure panels show a distance effect of stimulation (but see issues raised about the genotype of comparison groups). In addition, locomotor behavior is not included for many behaviors, so it is hard to completely buy the interpretation presented.*

We agree with the reviewer and thank them for highlighting this fundamental challenge in studies examining active coping behaviors in rodents, which requires movement. Additionally, actively responding to threatening stressors would include increased locomotor activity. Separation of movement alone from active coping can be challenging. Because of these concerns we undertook experiments using diverse behavioral paradigms to examine the elicited behaviors and the recruitment of SuMVGLUT2+::POA neurons to stressors. We conducted experiments to directly examine behaviors evoked by photoactivation of SuMVGLUT2+::POA. In these experiments we observed a diversity of behaviors including increased locomotion and jumping but also treading/digging (Figure 4). These are behaviors elicited in mice by threatening and noxious stimuli. An increase of running or only jumping could signify a specific locomotor effect, but this is not what was observed. Based on these



behaviors, we expected to find evidence of increase movement in open field (Figure 5G-I) and light dark choice (Figure 5J-L) assays. For many of the assays, reporting distance traveled is not practical. An important set of experiments that argues against a generic increase in locomotion is the operant behavior experiments, which require the animal to engage in a learned behavior while receiving photostimulation of SuMVGLUT2::POA neurons (Figure 6). This is particularly true for testing using a progressive ratio when the time of ongoing photostimulation is longer, yet animals actively and selectively engage the active port (Figure 6G-H). Further, we saw a shift in behavioral strategy induce by photoactivation in forced swim test (Figure 7H). Thus, activation of SUMVGLUT2::POA neurons elicited a range of behaviors that included swimming, jumping, treading, and learned response, not just increased movement. Together these data strongly argue that SuMVGLUT2::POA neurons do not only promote increased locomotor behavior. We interpret these data together with the data from fiber photometry studies to show SuMVGLUT2::POA neurons are recruited during acute stressors, contribute to aversive affective component of stress, and promote active behaviors without constraining the behavioral pattern.

Regarding genotype, we address this in comments above as well but believe that clarifying the use of litter mates, the extensive use of the VGLUT2-Cre line by multiple groups, and experimental design allowing for comparison to baseline, stimulation evoked, and post stimulation behaviors within and across genotypes mitigate possible concerns relating to the genotype.

*(8) What is the role of GABA neurons in the SuM and how does this relate to their function and interaction with glutamate neurons? In Supp 8, GABA neuron activation also modulates locomotion and in Fig 7 there is an effect on immobility, so this seems pretty important for the overall interpretation and should probably be mentioned in the abstract.*

Thank you for noting these interesting findings. We added text to highlight these findings to the abstract. Possible roles of GABAergic neurons in SuM extend beyond the scope of the current study particularly since SuM neurons have been shown to release both GABA and glutamate (Li Y, Bao H, Luo Y, et al. 2020, Root DH, Zhang S, Barker DJ et al. 2018). GABAergic neurons regulate dentate gyrus (Ajibola MI, Wu JW, Abdulmajeed WI, Lien CC 2021), REM sleep (Billwiller F, Renouard L, Clement O, Fort P, Luppi PH 2017), and novelty processing (Chen S, He L, Huang AJY, Boehringer R et al. 2020). The population of exclusively GABAergic vs dual neurotransmitter neurons in SuM requires further dissection to be understood. How they may relate to SUMVGLUT2::POA neurons require further investigation.

*Questions about figure presentation:*

*(9) In Fig 3, why are heat maps shown as a single animal for the first couple and a group average for the others?*

Thank you for highlighting this point for further clarification. We modified the labels in the figure to help make clear which figures are from one animal across multiple trials and those that are from multiple animals. In the ambush assay each animal one had one trial, to avoid habituation to the mock predator. Accordingly, we do not have multiple trials for each animal in this test. In contrast, the dunk assay (10 trial/animal) and the shock (5 trials/animal) had multiple trials for each animal. We present data from a representative animal when there are multiple trials per animal and the aggregate data.

*Why is the temporal resolution for J and K different even though the time scale shown is the same?*

Thank you for noticing this error carried forward from a prior draft of the figure so we could correct it. We replaced the image in 3J with a more correctly scaled heatmap.

*What is the evidence that these signal changes are not due to movement per se?*

Thank you for the question. There are two points of evidence. First, all the 465 nm excitation (Ca<sup>2+</sup> dependent) data was collected in interleaved fashion with 415 nm (isosbestic) excitation data. The isosbestic signal is derived from GCaMP emission but is independent of Ca<sup>2+</sup> binding (Martianova E, Aronson S, Proulx CD. 2019). This approach, time-division multiplexing, can correct calcium-dependent for changes in signal most often due to mechanical change. The second piece of evidence is experimental. Using multiple cohorts of mice, we examined if the change in Ca<sup>2+</sup> signal was correlated with movement. We used the threshold of velocity of movement seen following the ambush. We found no correlation between high velocity movements and Ca<sup>2+</sup> signal (Figure 3K) including cross correlational analysis (Supplemental figure 5). Based on these points together we conclude the change in the Ca<sup>2+</sup> signal in SUMVGLUT2<sup>+</sup>::POA neurons is not due to movement induced mechanical changes and we find no correlation to movement unless a stressor is present, i.e. mock predator ambush or forced swim. Further, the stressors evoke very different locomotor responses fleeing, jumping, or swimming.

*(10) In Fig 4, the authors carefully code various behaviors in mice. While they pick a few and show them as bars, they do not show the distribution of behaviors in Cre- vs Cre+ mice before manipulation (to show they have similar behaviors) or how these behaviors shift categories in each group with stimulation. Which behaviors in each group are shifting to others across the stim and post-stim periods compared to pre-stim?*

This is an important point. We selected behaviors to highlight in Figure 4 C-E because these behaviors are exhibited in response to stress (De Boer & Koolhaas, 2003; van Erp et al., 1994). For the highlighted behaviors, jumping, treading/digging, grooming, we show baseline (pre photostimulation), stimulation, and post stimulation for Cre<sup>+</sup> and Cre<sup>-</sup> mice with the values for each animal plotted. We show all nine behaviors as a heat map in Figure 4B. The panels show changes that may occur as a function of time and show changes induced by photostimulation.

The heatmaps demonstrate that photostimulation of SUMVGLUT2<sup>+</sup>::POA neurons causes a suppression of walking, grooming, and immobile behaviors with an increase in jumping, digging/treading, and rapid locomotion. After stimulation stops, there is an increase in grooming and time immobile. The control mice show a range of behaviors with no shifts noted with the onset or termination of photostimulation.

*Of note, issues of statistics, genotype, and SABV are important here. For example, the hint that treading/digging may have a slightly different pre-stim basal expression, it seems important to first evaluate strain and sex differences before interpreting these data.*

We examined the effects of sex as a biological variable in the experiments reported in the manuscript and found no differences among males and females in any of the experiments where we had enough animals in each sex (minimum of 5 mice) for meaningful comparisons. We did this by comparing means and SEM of males and females within each group (e.g. Cre<sup>+</sup> males vs Cre<sup>+</sup> female, Cre<sup>-</sup> males vs Cre<sup>-</sup> females) and then conducted a t-test to see if there was a difference. For figures that show time as a variable (e.g Figure 6C-E), we compared males and females with time x sex as main factors and compared them (including multiple comparisons if needed). We found no significant main effects or interactions between males and females. Because of this, and to maximize statistical power, we decided to move forward

to keep males and females together in all the analyses presented in the manuscript. It is worth noting also that the core of the experimental design employed is a change in behavior caused by photostimulation. The mice are also the same strain with only difference being the modification to add an IRES and sequence for Cre behind the coding sequence of the Slc17A6 (VGLUT2) gene.

*(11) Why do the authors use 10 Hz stimulation primarily? is this a physiologically relevant stim frequency? They show that they get effects with 1 Hz, which can be quite different in terms of plasticity compared to 10 Hz.*

Thank you for the raising this important question. Because tests like open field and forced swim are subject to habituation and cannot be run multiple times per animal a test frequency was needed to use across multiple experiments for consistency. The frequency of 10Hz was selected because it falls within the rate of reported firing rates for SuM neurons (Farrel et al., 2021; Pedersen et al., 2017) and based on the robust but sub maximal effects seen in the real-time place preference assays. Identification of the native firing rates during stress response would be ideal but gathering this data for the identified population remains a daunting task.

*(12) In Fig 5A-F, it is unclear whether locomotion differences are playing a role. Entrances (which are low for both groups) are shown but distance traveled or velocity are not.*

*In B, there is no color in the lower left panel. where are these mice spending their time? How is the entirety of the upper left panel brighter than the lower left? If the heat map is based on time distribution during the session, there should be more color in between blue and red in the lower left when you start to lose the red hot spots in the upper left, for example. That is, the mice have to be somewhere in apparatus. If the heat map is based on distance, it would seem the Cre- mice move less during the stim.*

We appreciate the opportunity to address this question, and the attention to detail the reviewer applied to our paper. In the real time place preference test (RTPP) stimulation would only be provided while the animal was on the stimulation side. Mice quickly leave the stimulation side of the arena, as seen in the supplemental video, particularly at the higher frequencies. Thus, the time stimulation is applied is quite low. The mice often retreat to a corner from entering the stimulation side during trials using higher frequency stimulation. Changing locomotor activity along could drive changes in the number entrances but we did not find this. In regard to the heat map, the color scale is dynamically set for each of the paired examples that are pulled from a single trial. To maximize the visibility between the paired examples the color scale does not transfer between the trials. As a result, in the example for 10 Hz the mouse spent a larger amount of time in the in the area corresponding to the lower right corner of the image and the maximum value of the color scale is assigned to that region. As seen in the supplemental video, mice often retreated to the corner of the non-stimulation side after entering the stimulation side. The control animal did not spend a concentrated amount of time in any one region, thus there is a lack of warmer colors. In contrast the baseline condition both Cre+ and Cre- mice spent time in areas disturbed on both sides of arena, as expected. As a result, the maximum value in the heat map is lower and more area are coded in warmer colors allowing for easier visual comparison between the pair. Using the scale for the 10 Hz pair across all leads to mostly dark images. We considered ways to optimized visualization across and within pairs and focused on the within pair comparison for visualization.

*(13) By starting with 1 hz, are the experimenters inducing LTD in the circuit? what would happen if you stop stimming after the first epoch? Would the behavioral effect continue? What does the heat map for the 1 hz stim look like?*

*Relatedly, it is a lot of consistent stimulation over time and you likely would get glutamate depletion without a break in the stim for that long.*

Thank you for the opportunity to add clarity around this point regarding the trials in RTPP testing. Importantly, the trials were not carried out in order of increasing frequency of stimulation, as plotted. Rather, the order of trials was, to the extent possible with the number of mice, counterbalanced across the five conditions. Thus, possible contribution of effects of one trial on the next were minimized by altering the order of the trials.

We have added a heat map for the 1 Hz condition to figure 5B.

For experiments on RTPP the average stimulation time at 10Hz was less than 10 seconds per event. As a result, the data are unlikely to be affected by possible depletion of synaptic glutamate. For experiments using sustained stimulation (open field or light dark choice assays) we have no clear data to address if this might be a factor where 10Hz stimulation was applied for the entire trial.

*(14) In Fig 6, the authors show that the Cre- mice just don't do the task, so it is unclear what the utility of the rest of the figure is (such as the PR part). Relatedly, the pause is dependent on the activation, so isn't C just the same as D? In G and H, why is a subset of Cre+ mice shown?*

*Why not all mice, including Cre- mice?*

Thank you for the opportunity to improve the clarity of this section. A central aspect of the experiments in Figure 6 is the aversiveness of SUMVGLUT2+::POA neuron photostimulation, as shown in Figure 5B-F. The aversion to photostimulation drives task performance in the negative reinforcer paradigm. The mice perform a task (active port activation) to terminate the negative reinforcer (photostimulation of SuMVGLUT2+::POA neurons). Accordingly, control mice are not expected to perform the task because SuMVGLUT2+::POA neurons are not activated and, thus the mice are not motivated to perform the task.

A central point we aim to convey in this figure is that while SuMVGLUT2+::POA neurons are being stimulated, mice perform the operant task. They selectively activated the active port (Supplemental Figure 7). As expected, control mice activate the active port at a low level in the process of exploring the arena. This diminishes on subsequent trials as mice habituate to the arena (Figure 6D). The data in Figures 6 C and D are related but can be divergent. Each pause in stimulation requires a port activation of a FR1 test but the number of port activations can exceed the pauses, which are 10 seconds long, if the animal continues to activate the port. Comparing data in Figures 6 C and D reveals that mice generally activated the port two to three times for each pause earned with a trend towards greater efficiency on day 4 with more rewards and fewer activations.

The purpose of the progressive ratio test is to examine if photostimulation of SuMVGLUT2+::POA continues to drive behavior as the effort required to terminate the negative stimuli increases. As seen in Figures 6 G and H, the stimulation of SuMVGLUT2+::POA neurons remains highly motivating. In the 20-minute trial we did not find a break point even as the number of port activations required to pause the stimulation exceed 50. We do not show the Cre- mice in Figure 6G and H because they did not perform the task, as seen in Figure 6F. For technical reasons in early trials, we have fully time stamped data for rewards and port activations from a subset of the Cre+ mice. Of note, this contains both the highest and lowest performing mice from the entire data set.

Taken together, we interpret the results of the operant behavioral testing as demonstrating that SuMVGLUT2+::POA neuron activation is aversive, can drive performance of an operant

tasks (as opposed to fixed escape behaviors), and is highly motivating.

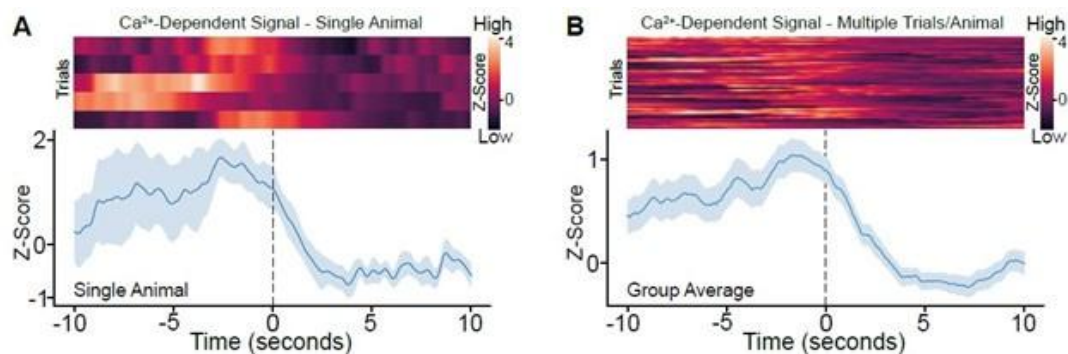
(15) In Fig 7, what does the GCaMP signal look like if aligned to the onset of immobility? It looks like since the hindpaw swimming is short and seems to precede immobility, and the increase in the signal is ramping up at the onset of hindpaw swimming, it may be that the calcium signal is aligned with the onset of immobility.

What does it look like for swimming onset?

In I, what is the temporal resolution for the decrease in immobility? Does it start prior to the termination of the stim, or does it require some elapsed time after the termination, etc?

Thank for the opportunity to addresses these points and improve that clarity of our interpretation of the data. Regarding aligning the Ca<sup>2+</sup> signal from fiber photometry recordings to swimming onset and offset, it is important to note that the swimming bouts are not the same length. As a result, in the time prior to alignment to offset of behaviors animals will have been swimming for different lengths of time. In Figure 7 C, we use the behavioral heat map to convey the behavioral average. Below we show the Ca<sup>2+</sup> dependent signal aligned at the offset of hindpaw swim for an individual mouse (A) and for the total cohort (B). This alignment shows that the Ca<sup>2+</sup> dependent signal declines corresponding to the termination of hindpaw swimming. Because these bouts last less than the total the widow shown, the data is largely included in Figure 7 C and D, which is aligned to onset. Due to the nuance of the difference is the alignment and the partial redundancy, we elected to include the requested alignment to swimming offset in the reply rather in primary figure.

#### Author response image 1.



Turning to the question regarding swimming onset, the animals started swimming immediately when placed in the water and maintained swimming and climbing behaviors until shifting behaviors as illustrated in Figure 7A and B. During this time the Ca<sup>2+</sup>-dependent signal was elevated but there is only one trial per animal. This question can perhaps be better addressed in the dunk assay presented in Figure 3C, F and G and Supplemental Figure 4 H and I. Here swimming started with each dunk and the Ca<sup>2+</sup> signal increased.

Regarding the question for about figure 7I. We scored for entire periods (2 mins) in aggerate. We noted in videos of the behavior test that there was an abrupt decrease in immobility tightly corresponding to the end of stimulation. In a few animals this shift occurred approximately 15-20s before the end of stimulation. This may relate to the depletion of neurotransmitter as suggested by the reviewer.



### Reviewer 3

#### Major points

*(1) Results in Figure 1 suggested that SuM-Vglu2::POA projected not only POA but also to the diverse brain regions. We can think of two models which account for this. One is that homogeneous populations of neurons in SuM-Vglu2::POA have collaterals and innervated all the efferent targets shown in Figure 1. Another is to think of distinct subpopulations of neurons projecting subsets of efferent targets shown in Figure 1 as well as POA. It is suggested to address this by combining approaches taken in experiments for Figure 1 and Supplemental Figure 2.*

Thank you for raising this interesting point. We have attempted combining retroAAV injections into multiple areas that receive projections from SUMVGLUT2::POA neurons. However, we have found the results unsatisfactory for separating the two models proposed. Using eYFP and tdTomato expressing we saw some overlapping expressing in SuM. We are not able to conclude if this indicates separate populations or partial labeling of a homogenous populations. A third option seems possible as well. There could be a mix of neurons projecting to different combinations of downstream targets. This seems particularly difficult to address using fluorophores. We are preparing to apply additional methodologies to this question, but it extends beyond the scope of this manuscript.

*(2) Since the authors drew a hypothetical model in which the diverse brain regions mediate the effect of SuM-Vglu2::POA activation in behavioral alterations at least in part, examination of the concurrent activation of those brain regions upon photoactivation of SuM-Vglu2::POA. This must help the readers to understand which neural circuits act upon the induction of active coping behavior under stress.*

Thank you for raising this important point. We agree that activating glutamatergic neurons should lead to activation of post synaptic neurons in the target regions. Delineating this in vivo is less straight forward. Doing so requires much greater knowledge of post synaptic partners of SUMVGLUT2::POA neurons. There are a number of issues that would need to be accounted for. Undertaking two color photo stimulation plus fiber photometry is possible but not a technical triviality. Further, it is possible that we would measure Ca<sup>2+</sup> signals in neurons that have no relevant input or that local circuits in a region may shape the signal. We would also lack temporal resolution to identify mono-postsynaptic vs polysynaptic connections. Thus, we would struggle to know if the change in signal was due to the excitatory input from SuM or from a second region. At present, we remain unclear on how to pursue this question experimentally in a manner that is likely to generate clearly interpretable results.

*(3) In Figure 4, "active coping behaviors" must be called "behaviors relevant to the active behaviors" or "active coping-like behaviors", since those behaviors were in the absence of stressors to cope with.*

Thank you for the suggestion on how to clarify our terminology. We have adopted the active coping-like term.

*(4) For the Dunk test, it is suggested to describe the results and methods more in detail, since the readers would be new to it. In particular, the mice could change their behavior between dunks under this test, although they still showed immobility across trials as in Supplemental Figure 4I. Since neural activity during the test was summarized across trials as in Figure 3, it is critical to examine whether the behavior changes according to time.*

Thank you for identifying this opportunity to improve our manuscript. We have expanded and added a detailed description of the dunk test in the methods section.

As for Supplemental Figure 4I, we apologize for the confusion because the purpose of this figure is to show that mice remained mobile for the entire 30-second dunk trial. This did not appreciably change over the 10 trials. We have revised this figure to plot both immobile and mobile time to achieve greater clarity on this point.

*Minor points*

*Typos*

*In Figure 1, please add a serotype of AAVs to make it compatible with other figures and their legends.*

*In the main text and Figure 2K, the authors used MHb/LHb and mHb/lHb in a mixed fashion. Please make them unified.*

*In the figure legend of Figure 6, change "SuMVGLUT2+::POA neurons drive" to "SuMVGLUT2+::POA neurons " in the title.*

*In line 86, please change "Retro-AAV2-Nuc-flox(mCherry)-eGFP" to "AAV5-Nuc-flox(mCherry)eGFP".*

*In line 80, please change "Positive controls" to "As positive controls, ".*

Thank you for taking the time and making the effort to identify and call these out. We have corrected them.